# GRAVITY MODELLING OF THE CRUSTAL STRUCTURE BELOW BAVALI SHEAR ZONE AND ADJACENT MAJOR PLUTONS OF NORTHERN KERALA

THESIS SUBMITTED TO THE

**COCHIN UNIVERSITY OF SCIENCE AND TECHNOLOGY**

IN PARTIAL FULFILMENT OF THE REQUIREMENTS

FOR THE DEGREE OF

**DOCTOR OF PHILOSOPHY**

IN THE FACULTY OF MARINE SCIENCE

BY

**P. JOHN KURIAN**

**DEPARTMENT OF MARINE GEOLOGY AND GEOPHYSICS**
**SCHOOL OF MARINE SCIENCES**
**COCHIN UNIVERSITY OF SCIENCE AND TECHNOLOGY**
**LAKESIDE CAMPUS, COCHIN – 682 016**

**MAY 2000**

## CERTIFICATE

I certify that this thesis, "**Gravity modelling of the crustal structure below Bavali shear zone and adjacent major plutons of Northern Kerala**" has been prepared by P. John Kurian under my supervision and guidance in partial fulfilment of the requirements for the degree of Doctor of Philosophy and no part thereof has been submitted for any other degree.

M.S.B.R. Krishna

Cochn – 16
May 15, 2000

M. Radhakrishna
(Research Supervisor)
Dept. of Marine Geology and Geophysics
School of Marine Sciences
Cochin University of Science and Technology
Cochin – 682 016

# CONTENTS

## Chapter 3 – Petrophysical Properties of Major Rock Types in the Area



## Chapter 4 – Data Acquisition and Reduction

# LIST OF FIGURES

Fig. 4.1. Map showing the distribution of permanent gravity bases established in the present study for the purpose of gravity surveys in northern Kerala. The base station value at Vallathol Nagar RS established by Singh et al.(1985) has been carried forward for this purpose. Numbers refer to the serial number in sketches shown in Fig 4.2 to Fig 4.8.

Fig. 4.2. Sketches showing location of six permanent base stations (nos. 1-6). Abbreviations and symbols used are shown in Fig .4.8.

Fig. 4.3. Sketches showing location of six permanent base stations (nos. 7-12). Abbreviations and symbols used are shown in Fig .4.8.

Fig. 4.4. Sketches showing location of six permanent base stations (nos. 13-18). Abbreviations and symbols used are shown in Fig .4.8.

Fig. 4.5. Sketches showing location of six permanent base stations (nos. 19-24). Abbreviations and symbols used are shown in Fig .4.8.

Fig. 4.6. Sketches showing location of six permanent base stations (nos. 25-30). Abbreviations and symbols used are shown in Fig .4.8.

Fig. 4.7. Sketches showing location of six permanent base stations (nos. 31-36). Abbreviations and symbols used are shown in Fig .4.8.

Fig. 4.8. Sketch showing location of one permanent base station(no. 37). Abbreviations and symbols used for all stations are shown in the legend.

Fig. 4.9. Distribution of gravity stations utilized in the present study. The NGRI stations are from Qureshy et al.(1981) and the HIG, SOI and ONGC data are from Woollard et al.(1969).

Fig. 4.10. Histograms showing the number of base ties against dynamic drift rate for (a) L & R gravimeter and (b) W Sodin gravimeter.

Fig. 5.1. Elevation map of the northern Kerala region based on bench mark and spot height data from the Survey of India topographic maps(1:50,000 scale) and altimeter measurements along gravity traverses. Contour interval is 100 meters.

Fig. 5.2. Free-air anomaly map of the Bavali shear zone and adjoining regions. Contour interval is 10 mGal. Though the original data permits a 5 mGal contour interval, 10 mGal contour interval is chosen to avoid overcrowding especially along steep gradients.

Fig. 5.3. Bouguer anomaly map of the Bavali shear zone and adjoining regions. Contour interval is 5 mGal. Lines AA' through FF' represent profiles selected for 2-d modelling.

Fig. 5.4. The contour maps of average values for 1/8° x 1/8° grid areas of the study area.

Fig. 5.5. Plot showing the 1/8°x1/8° averaged gravity anomaly values against corresponding elevation values in the study area. The best fit lines with equations are also shown.

Fig. 5.6. The contour maps of average values for 1/4° x 1/4° grid areas of the study area.

Fig. 5.7. Plot showing the 1/4°x1/4° averaged gravity anomaly values against corresponding elevation values in the study area. The best fit lines with equations are also shown.

Fig. 5.8. Plot showing the 1/2°x1/2° averaged gravity anomaly values against corresponding elevation values in the study area. The best fit lines with equations are also shown.

Fig. 5.9. Comparison of average Bouguer anomaly Vs. elevation with other parts of the Indian peninsula for 1/2°x1/2° areas.

Fig. 6.1(a). Nature of the gravity field and elevation along four profiles AA' through DD' in the region (See Fig. 2.2 and Fig. 5.3 for their location). Details on the Bavali shear and surface geology are adopted from Fig. 2.2 as given in Fig. 6.1 (b)

Fig. 6.1(b). Nature of the gravity field and elevation along two profiles EE' and FF' in the region. Other details are same as in Fig. 6.1 (a).

Fig. 6.2(a). The crustal thickness map of Subba Rao (1988) pertaining to the study region.

(b). 1/4° X1/4° average Bouguer anomaly map in the study region

(c). Crustal thickness map obtained in the present study based on (b). The details of the procedure for crustal thickness estimation is outlined in the text.

Fig. 6.3. Moho configuration estimated along six gravity profiles based on1/4°X1/4° average Bouguer anomalies. Details on the geology are adopted from Fig. 2.2. Thick arrow shown on each profile indicates the location of the Bavali shear zone (Since the Moho rise observed is around 2km in all the profiles, the Moho configuration

shown here is vertically exaggerated for the purpose of correlation with surface features).

Fig. 6.4. Interpreted crustal structure along profile AA'. Details on geology and Bavali shear zone are adopted from Fig. 2.2. Other details are discussed in the text.

Fig. 6.5. Interpreted crustal structure along BB'

Fig. 6.6. Interpreted crustal structure along CC'

Fig. 6.7. Interpreted crustal structure along DD'

Fig. 6.8. Interpreted crustal structure along EE'

Fig. 6.9. Interpreted crustal structure along FF'

Fig. 6.10. Interpreted crustal thickness (alternative model) along profile AA'. see text for more details.

Fig. 6.11. Interpreted crustal thickness (alternative model) along profile BB'. see text for more details.

Fig. 7.1. Detailed geological map of the Perinthatta anorthosite and surrounding regions.

Fig. 7.2. Bouguer anomaly map of the Perinthatta anorthosite and adjacent regions. The dashed line and the inside numbers indicate lithological boundaries as shown in the legend. The location of six profiles AA' through FF' considered for regional-residual separation are also shown in the map.

Fig. 7.3. Map showing the six profiles AA' through FF' considered for regional-residual separation. The regional gravity field for these profiles were obtained by using both graphical and least-square techniques. The dashed line indicate the least-square regional while the dotted line indicate the graphical regional. (see section 7.3 for details). Symbols for the rock types are same as those in Fig. 7.1.

Fig. 7.4. Residual gravity anomaly map of the Perinthatta anorthosite region. The dashed line shows the surface exposure of the pluton. The profiles II' to KK' were considered for gravity modeling.

Fig. 7.5 . Gravity models showing the structure of Perinthatta anorthosite along three selected profiles. Location of the profiles are shown in Fig. 7.4. 1. Anorthosite 2.Charnockite 3.High density cylindrical body 4.Pyroxene granulate.

Fig. 7.6. Schematic diagram showing a plausible model of massif type anorthosite genesis (after Ashwal, 1993).

Fig. 8.1. Geological map of the region around Kalpatta granite (modified after GSI, 1995; Kumar et al. , 1998)

Fig. 8.2. Foliation map of the Kalpatta granite region (after Kumar et al. 1998). The dotted line indicate the outline of the granite body.

Fig. 8.3. Bouguer anomaly map of the Kalpatta granite and the adjoining regions (contour interval is 2 mGal). Solid circles indicate the locations of gravity observations. The small dotted lines indicate the surface exposure of the Kalpatta and Ambalavayal granite bodies. The location of the Bavali shear zone is also shown on the map. The location of the 10 approximately north oriented profiles (N1-N1' through N10-N10') and 10 east oriented profiles (E1-E1' through E10-E10') used for the preparation of residual anomaly map of the Kalpatta granite are shown.

Fig. 8.4(a). Ten north oriented profiles selected for regional- residual separation. Graphical smoothing method constrained by the surface geology was used to draw the regional. Symbols of rock types are same as those in Fig. 8.1.

Fig. 8.4(b). Ten east oriented profiles selected for regional- residual separation. Graphical smoothing method constrained by the surface geology was used to draw the regional. Symbols of rock types are same as those in Fig. 8.1.

Fig 8.5. Residual anomaly map of Kalpatta granite. The lines AA' to CC' indicate the profiles selected for 2-dimensional modeling.

Fig 8.6. Two-dimensional gravity models of the Kalpatta granite body along profiles shown in Fig. 8.5.

Fig 8.7. Three-dimensional depth configuration of the Kalpatta granite body. The maximum depth obtained is about 6.5 km. The surface exposure of the granite body is shown as thick dashed line.

Fig. 8.8. Cross-section of the 3-D depth model along X-X' (location shown in Fig. 8.7).

## LIST OF TABLES

# *Chapter I*

# Introduction

## 1.1 General Introduction

Geophysical methods play an important role in deciphering the subsurface geology and related problems. These methods are best adopted for the study of regional geology, the crustal structure and nature of large scale geologic or tectonic features, besides prospecting for natural resources and in problems related to engineering geology. The gravity method, one of the foremost geophysical tools, is based on the measurement of variations in the gravitational field on the surface of the earth. The measured variations are interpreted in terms of plausible subsurface mass distributions. The gravity field observed at any place on the earth is due to the cumulative effect of all the masses lying beneath. The free air and Bouguer anomaly maps in correlation with the surface geology could be used to infer the presence of anomalous masses in the crust, their depth and horizontal extent. Since the Bouguer anomaly bears a relationship to the crustal geology, topography as well as crustal composition, it is very useful for the study of geologic structures, if the density configuration can be well constrained.

The South Indian shield is regarded as a crustal unit made up essentially of Archaean continental nuclei and Proterozoic mobile belts represented respectively by granite-gneiss-greenstone terrain in north and the high grade granulite terrain south of it. The southern granulilte terrain (SGT) is dissected by several shear belts and is affected by retrogressive metamorphism (Raith et al., 1983) followed by Pan-African granulite facies metamorphism at several

locations (Bartlett et al., 1995). A number of agencies such as NGRI, SOI, GSI, ONGC and CESS have conducted regional gravity surveys in the southern Indian shield. Many individual workers who analyzed and interpreted these data made significant contributions in understanding the nature of the crust, crustal configuration and subsurface mass heterogeneities in different parts of the southern Indian shield (Sankar Narayan et al., 1963; Qureshi, 1971; Kailasam, 1975; Krishna Brahmam and Kanungo, 1976; Subrahmanyam, 1978; Subrahmanyam and Verma, 1980; Subrahmanyam, 1983; Singh et al., 1985; Harinarayan and Subrahmanyam, 1986; Mishra, 1988; Krishna Brahmam, 1993; Mishra and Rao, 1993; Mahadevan, 1994; among others). Other geophysical works of great significance in understanding the crustal structure in this region include the Kavali-Udipi DSS study by Kaila and Bhatia (1981) and the aeromagnetic data analysis by Reddi et al. (1988) and seismic tomography data by Rai et al. (1993). The importance of transect studies along selected corridors in the deep continental crustal investigations in this region have been highlighted by a few workers (Mahadevan, 1993; Radhakrishna and Ramakrishnan, 1993). The region of northern Kerala is characterized by the presence of a major lineament called Bavali lineament trending WNW-ESE and located close to the gneiss-granulite transition zone. The Bavali shear zone along the lineament and the adjoining Precambrian lower crustal segments provide a unique assemblage of several plutonic and metamorphic rocks and a variety of structural features.

## 1.2 Objectives

Though some parts of northern Kerala were covered in the earlier gravity as well as other geophysical surveys, the data acquired were mostly of regional interest and not sufficient to make any detailed or meaningful geological interpretation of more localized features. The primary aim of the present study is to acquire a large amount of gravity data, to prepare gravity maps and interpret the data in terms of crustal structure below the Bavali shear zone and adjacent regions of northern Kerala. More precise objectives focussing various geological problems in the area have been presented at the end of chapter II after synthesizing the geology of the area and previous gravity works.

## 1. 3 Study Area

The region selected for this study covers an area of 15,000 sq. km between Lat. 11° 55' -- 12° 30' N and Long. 75° E -- 76° 30' E (Fig. 1.1). The region is characterized by a major lineament, called the Bavali lineament, trending WNW-ESE. It runs along the Wynad schist belt, which is located in the southern high grade terrain close to the gneiss-granulite transition zone of the southern Indian shield. Several minor to large igneous plutons such as syenite, granite, anorthosite and gabbro are spatially associated with the Bavali shear zone having a width of 10km and length of 100km between Mananthavady and Payyannur.

## 1.4 Methodology

A detailed geophysical work of this dimension involves field data collection, laboratory measurements and processing and interpretation of the data. Various methods and techniques utilized in the present study are briefly summarized below:

- Establishment of a good network of permanent gravity base stations for use in gravity surveys in the region. These base stations would also be useful for any future gravity study in the region.
- Acquisition of intermediate gravity stations almost uniformly spaced covering all available roads in the region.
- Collection of good number of rock samples for rock density and susceptibility measurements in the laboratory.
- Preparation of gravity maps and qualitative analysis to infer various subsurface mass anomalies in the region.
- Interpretation of gravity data in terms of 2-dimensional and 3-dimensional crustal models and their tectonic significance.

Detailed methodology including the descriptions of equipments/ procedures adopted are given in the concerned chapters

## 1.5 Scope of the Present Study

In the present study, a large amount of gravity data has been generated over the region ensuring as uniform a coverage as permitted by factors of accessibility. The data have been analyzed and interpreted in terms of crustal structure below the Bavali shear zone. Based on the methodology given above, for the sake of convenience, the thesis is divided into nine chapters.

The chapter I gives a general introduction to the geophysical studies in the southern Indian shield. The study area, its importance and methodology adopted have been briefly outlined in this chapter.

Chapter II describes the regional geology of the Bavali shear zone and the adjoining areas highlighting the various geologic events including the emplacement of igneous plutons in the region. The structure and tectonics of the shear zone is discussed in the light of the regional geological setting of the southern Indian shield. The updated geologic map presented in this chapter incorporating the details from recently published maps would be useful in the interpretation of the gravity data. A review of previous geophysical works in the study area has been made to identify important geological problems that need gravity work.

Chapter III describes the density and susceptibility measurements of all rock types present in the study area. Enough representative rock samples were

collected so as to assign an average value to each unit. An attempt was made to correlate the physical property measurements with mineralogical and geochemical data wherever possible in order to explain the variations in terms of mineralogy of the rock samples. The density values of the surface rocks of the area would help during qualitative analysis of gravity maps, i.e., whether the anomalies are resulting from lateral changes in surface rocks and their subsurface extension, or from deep-seated mass distribution, or from a combination of both.

Chapter IV gives an account of the previous gravity data and the methodology adopted in data acquisition and reduction. Since, available gravity data in the region is very sparse and completely devoid of permanent base stations accurate enough for the present purpose, thirty six base stations at permanent locations were established covering the whole area. A total of around 850 gravity observations have been made at an average station spacing of 1km along all possible roads in the region. Elevation data have been collected simultaneously with the gravity survey using an altimeter. The various reduction procedures adopted for making appropriate corrections to raw gravity data to obtain free-air anomaly, Bouguer anomaly and elevation data for the study region have been discussed. A brief summary of different regional – residual separation technique and the method adopted in the present study are discussed.

The correlation of the gravity field with the surface geology and the relationship of average gravity field versus elevation have been discussed in chapter V. By studying the relationship of gravity anomalies to elevation, some broad information on crustal configuration can be obtained relating to the tectonics of the region. The free-air anomaly, Bouguer anomaly and elevation maps prepared for the region and their correlation with the major structural features of the area are studied. Bouguer anomaly is known to have a strong negative correlation with elevation whereas free-air anomaly has a positive correlation with elevation. In order to understand the geological effects of the underlying masses at various depths on the gravity field, 1/8°X 1/8° and 1/4° X 1/4° average maps and their relation with average elevation are discussed in this chapter.

The interpretation and tectonic significance of these derived models along profiles traversing different parts of Bavali shear zone are discussed in chapter VI. Quantitative interpretation of Bouguer anomalies along selected profiles cutting across the Bavali shear zone have been made to delineate subsurface configuration of the shear zone. The models thus interpreted suggest that the shear zone is characterized by variations in the thickness of upper and lower crust on either side. The crustal thickness variations and presence of high density material have been discussed in terms of their geological implications.

Chapter VII deals with the gravity interpretation of Perinthatta anorthosite in view of its peculiar gravity signature on the gravity map. Gravity investigations over anorthosite massif have been a subject of interest to many researchers and have provided valuable constraints on their tectono-magmatic setting. The Perinthatta anorthosite is one among the series of mafic to felsic intrusives associated with Bavali shear zone. It is emplaced in high grade metamorphic rocks comprising charnockites and pyroxene granulites. A detailed analysis of the gravity field over Perinthatta anorthosite and adjacent regions was carried out in order to decipher the nature and subsurface extent of the pluton. Since the gravity field over Perinthatta anorthosite body does not conspicuously show any anomaly, regional residual separation was attempted in order to isolate the gravity field of the anorthosite body from the rest of the features. A comparison with the exposed part of the anorthosite body with the residual anomaly map suggests subsurface extension of this pluton covering a much wider area, though the pluton may not have deep extensions. Gravity modeling along selected profiles cutting the anorthosite body is attempted. The tectono-magmatic implications of these gravity models in terms of structure of anorthosite are discussed.

Chapter VIII deals with the detailed gravity analysis of the Kalpatta granite. The Kalpatta and Ambalavayal granites form a major intrusive structures on the south-eastern part of the Bavali shear zone. The Kalpatta granite falls within the widespread Wynad gravity low and its shape and subsurface extension are

important in understanding the Wynad gravity low. Detailed gravity map prepared for this region suggests three-dimensional nature of these bodies. The gravity anomalies over Kalpatta granite show approximately oval shape with a negative gravity anomaly centered over the body. Based on the regional residual separation, a residual anomaly map was prepared in order to arrive at a three-dimensional model for the Kalpatta granite. The model indicates that the granite body has smooth arcuate contacts with an inward dipping surface increasing towards center to a maximum depth of 6.5km. The tectonic significance of this model has been discussed in detail in this chapter.

Chapter IX presents the summary and conclusions of the gravity interpretation of Bavali shear zone and the adjacent regions.

*Chapter II*

# Geology of The Area

## 2.1 Introduction

The southern Indian shield is regarded as a crustal unit made up, essentially, of Archaean continental nuclei and Proterozoic mobile belts which are represented respectively by the granite-greenstone terrains of Karnataka and the high grade granulite terrain further south. Fermor(1936) first identified a boundary to separate charnockitic and non-charnockitic (gneiss-schist) terrains in the shield popularly known as 'Fermor line'. Later works revealed that there exists a narrow transition zone along which the low-grade gneiss-granite-greenstone rocks transform to high-grade granulite facies rocks (Radhakrishna et al.,1990; Naqvi and Rogers, 1987). The various thermotectonic events operated in the evolution of different tectonic units of the shield have left their imprint in terms of deep crustal structure. The Southern Granulite Terrain (SGT) south of the transition zone is traversed by a set of prominent faults or shears (Katz, 1978). Landsat imagery study in this region by Drury and Holt (1980) revealed the regional nature of these shear zones. Some of the prominent shear zones in the SGT include Bavali shear zone, Moyar-Bhavani shear system, Palghat-Cauvery shear zone and Achankovil shear zone (Fig. 2.1). A dextral sense of shear was proposed for most of the shears. Many of these shear zones contain recrystallized cataclastic rocks, foliation and lineation parallel to the shears (Drury et al., 1984). The region of northern Kerala is characterized by one such shear/fault zone trending WNW-ESE named after Bavali river (Nair et al.,1976). The Bavali shear zone is considered by some workers as the western

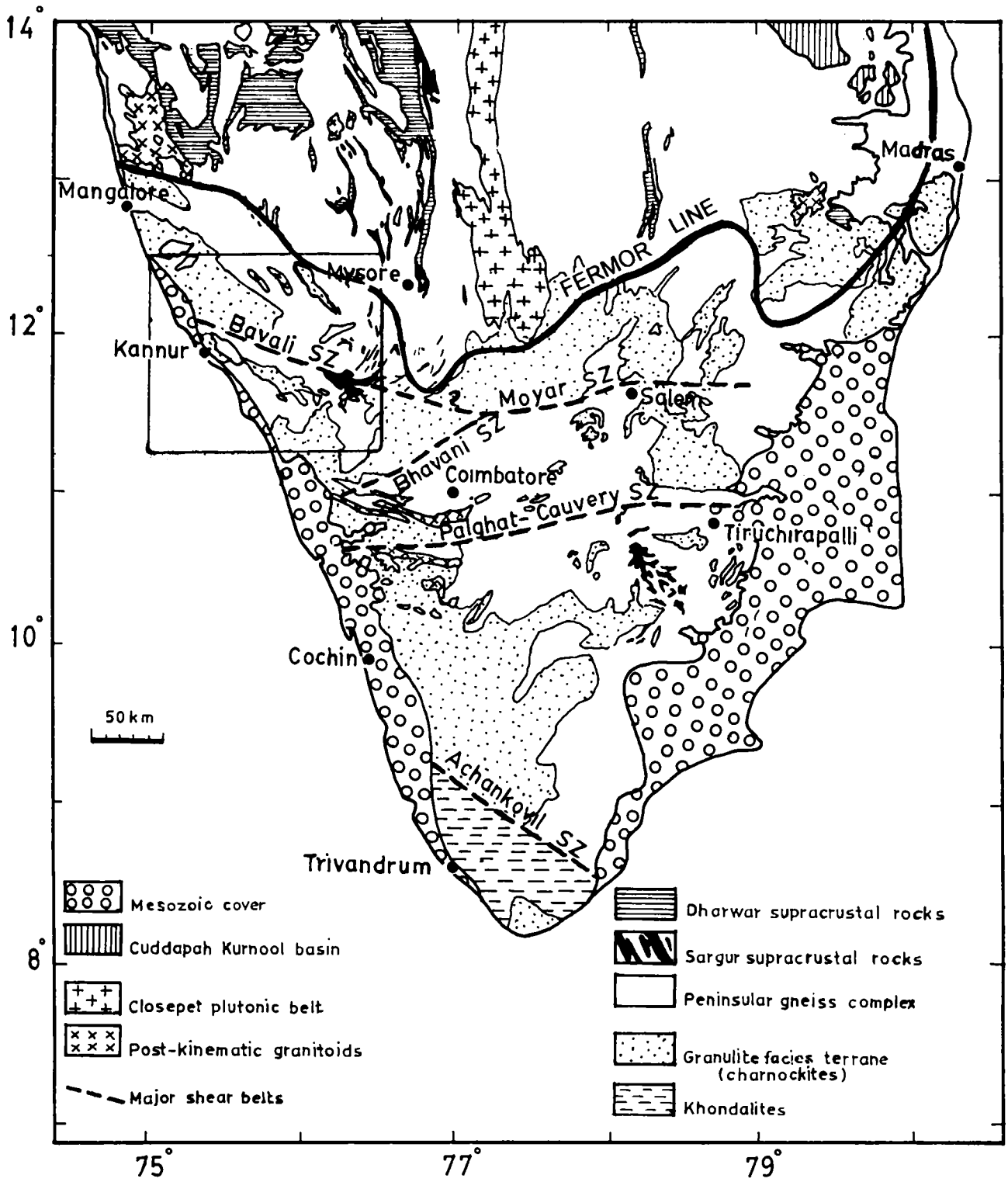


Fig 2.1. Geological map of Southern Peninsular India showing major shear zones (modified after Raith et al., 1983 ). The thick line popularly known as 'Fermor line'(Fermor,1936) delimits the northern boundary for charnockites. The area marked by the rectangle indicates the present study area.

extension of the Moyar shear which in turn is a part of the Moyar-Bhavani shear system of Tamil Nadu.

The Bavali shear zone and the adjoining Precambrian lower crustal segments provide a unique assemblage of several plutonic and metamorphic rocks and a variety of major structural features. Thus, a proper geological and geophysical study of the Bavali shear zone and the associated intrusives can provide significant information on the deep crustal, tectonic, metamorphic and magmatic processes in the southern granulite terrain. A detailed account of the geology of the Bavali shear zone and the adjoining areas is presented below.

## 2.2 Geology of the Area

The geological set-up of the Bavali shear zone and the adjoining areas has been discussed by Nambiar et al. (1985) based on the landsat imagery data. A revised geological map of the area compiled from Nambiar (1987) and GSI (1995) is given in Fig 2.2. As can be seen from the map, the charnockite rocks and their retrograded products constitute the predominant rock types in the region. The Wynad schist belt is represented as enclaves of schistose rocks within the gneissic rocks. Geology of the area at many places is obscured by the presence of thick cover of laterite / soil/ vegetation. Based on the petrological data, Nambiar et al. (1992) divided the northern Kerala region into four broad provinces consisting of (1) schist and gneiss province covering the northern part of Kasaragod district, (2) northern charnockite province

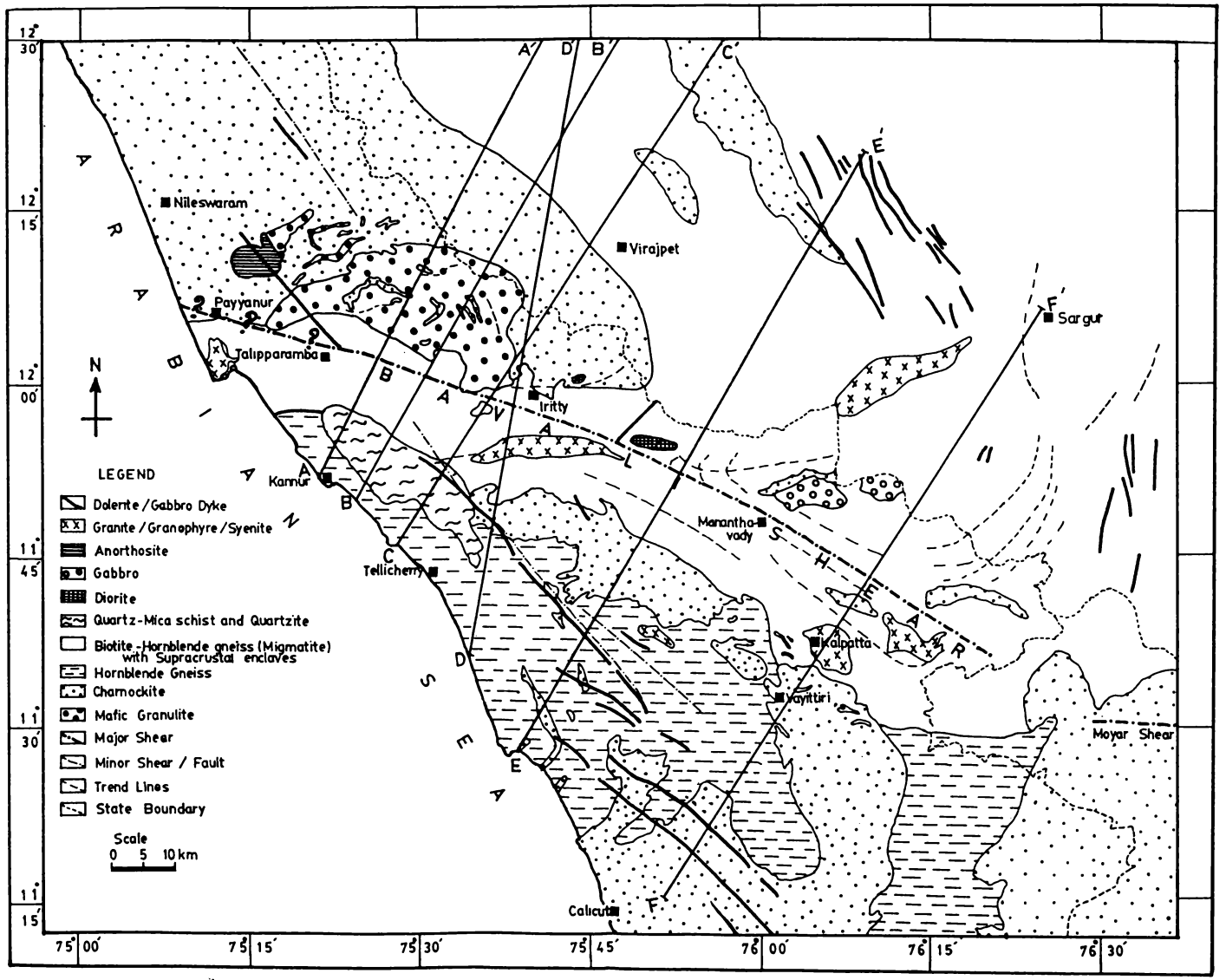


Fig. 2.2. Geological map of the Bavali shear zone and the adjoining regions (modified after Nambiar,1987 and GSI, 1995 ). Thick lines AA′ through FF′ show the location of the regional gravity profiles considered for modeling the crustal structure.

covering parts of Kasaragod and Kannur districts, (3) schist province of Wynad with schistose associated rocks of the Wynad – Kannur area, and (4) southern charnockite province covering Calicut- Wynad-Malappuram districts.

The area of present investigation covers parts of these major provinces and certain salient geological features of the provinces pertaining to the study area are given below.

### 2.2.1 Schist-Gneiss Province

The schist-gneiss complex of the Wynad –Kannur area extends for about 150 km in a WNW-ESE direction with an approximate width of about 10-20 km. It is characterized by the presence of small isolated patches of schists in the gneissic country rock. Equivalence of Sargurs and Dharwars of Karnataka are identified among the metapelite- metavolcanic sequence of the area (Nair et al., 1976). The most conspicuous feature of this province is the NW-SE Bavali fault running over 100 km through the middle of the area (Nair et al., 1976). Nambiar et al. (1982) described the deformed pillow structure from the meta ultramafics. Several igneous plutons of acidic and basic in composition have been found to be emplaced within or close to the gneisses and schists. The gabbro-granophyre complex of Ezhimala, gabbro-diorite bodies near Kartikulam and Tolpetti and the granite plutons of Peralimala, Ambalavayal and Kalpatta are some of the major plutons in this region. A detailed description of the plutons is given in section 2.3.

A smaller basin of younger metasediments called the Vengad basin occurs to the south of the western end of Wynad schist belt. This lensoid shaped Vengad basin occupies nearly 300 sq.km in Kannur district and is considered as equivalent to Proterozoic basin of Dharwars of Karnataka. This formation, overlying the gneisses and charnockites, consists of schists and quartzites with conglomerates at the base.

### 2.2.2 Charnockite Provinces

The charnockite provinces are located in the north as well as the southern part of Wynad schist belt. While charnockites in the northern part are coarse grained and mostly massive and felsic, in the southern part, they are medium grained, banded charnockites of intermediate composition.

#### 2.2.2.1 Northern Charnockite Province

The charnockites of the northern province of Kasargode-Kannur districts are characterized by the presence of blue quartz and greyish green feldspar. These rocks are dark, bluish grey massive and coarse grained. However, some are of medium grain size, while few others have a very coarse texture. Retrogression of charnockites to gneisses with hydrous mineral assemblages are common in the area. A massif type anorthosite body near Perinthatta is situated within the charnockite province (Vidyadharan et al., 1977).

#### 2.2.2.2 Southern Charnockite Province

The southern charnockite province of the Calicut-Malappuram-S.Wynad district is dominated by the dark grey coloured orthopyroxene – bearing intermediate to acid granulites and has a slightly different petrological association from that of the northern charnockite province. In several places, intrusive veins of granitic rocks, cut across these formations causing retrogression in the host charnockite. The rocks along the retrogressed areas are lighter in colour and are mostly devoid of orthopyroxene.

## 2.3 Description of Major Plutons in the Region

The emplacement history and structural association of some of the major plutons vis-a-vis the schist belt and the Bavali fault has an important relevance in understanding the evolution of the shear zone. Generally these plutons are E-W or NW-SE elongated elliptical bodies showing sharp contacts with the country rocks and show spatial association with the Bavali lineament (Fig 2.3). A brief account of geology and structure of the important igneous plutons of the region are given below.

### 2.3.1 Ezhimala Igneous Complex

The gabbro, granite and granophyre rocks of Ezhimala emplaced in the Precambrian migmatitic gneisses together constitute the Ezhimala Igneous complex. This pluton, exposed near Ezhimala of Kannur district is in the WNW

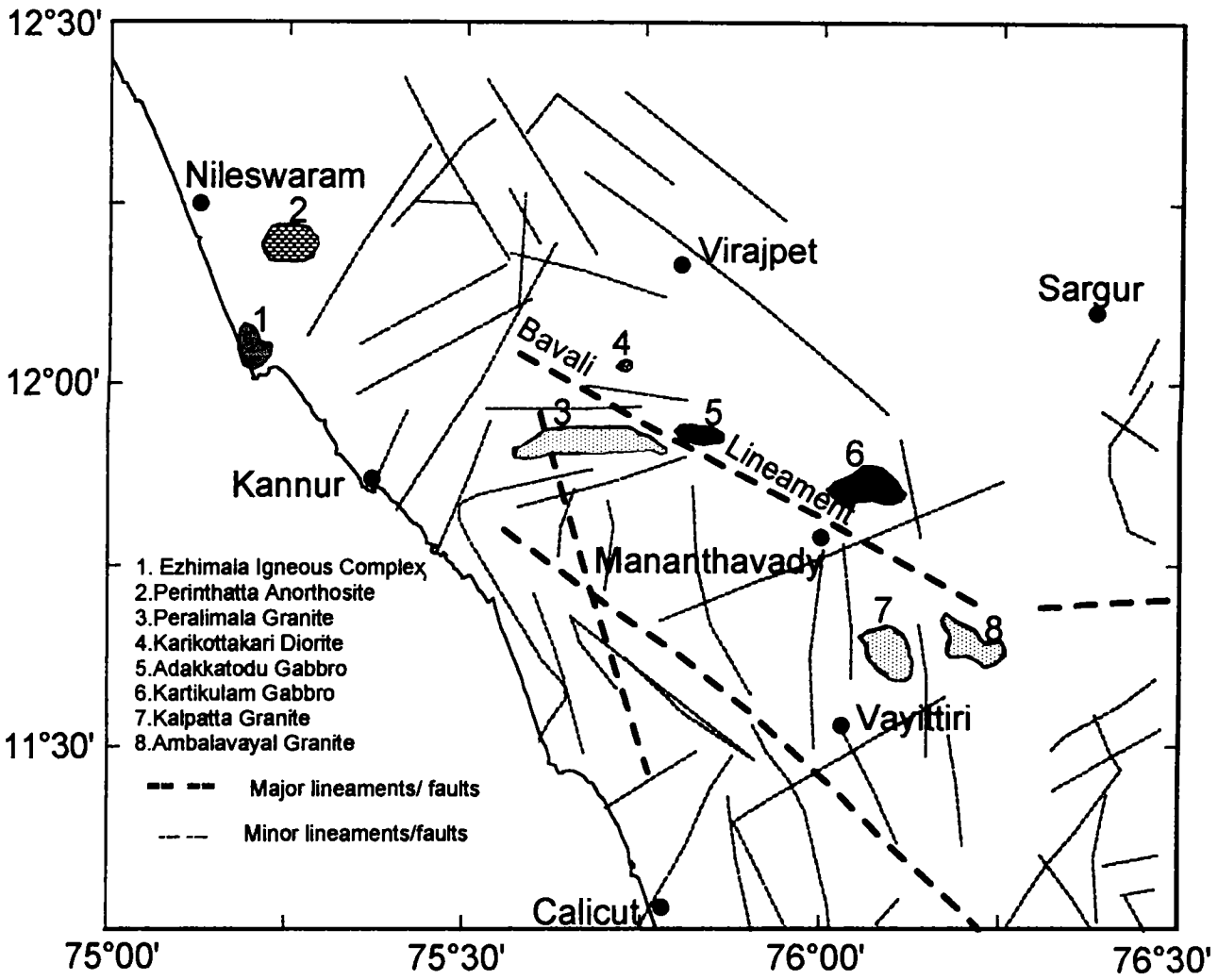


Fig 2.3. Map showing major/ minor lineaments (after Varadarajan and Balakrishnan, 1980) and the major plutons in the study area

end of Bavali lineament. It is elongated in a NNW-SSE direction and has a maximum exposure length of 6 km with a width of 3 km. The pluton is hosted by gneisses with enclaves of sillimanite-kyanite schists. The exposed part of the pluton contains gabbro, often grading into leucogabbro in the east and south. It appears that granite has cut through the gabbro. Rb-Sr isochron age of 678 Ma has been reported by Nair and Vidyadharan(1982) for the granite and granophyres.

### 2.3.2 Kalpatta Granite

The granite intrusion falling near Kalpatta region of Wynad district is an elliptical stock covering an area of about 50 sq.km. The first scientific account on the occurrence of Kalpatta granite was made by the Geological Survey of India(Nair et.al., 1976). Nair et al. (1983) conducted a preliminary study on the petrochemistry of the granite. This homogeneous massive rock of light grey color, exhibiting sharp contacts with the country rock is falling in the high grade-low grade transition zone of the Wynad schist belt. It is medium to coarse grained grey biotite granite and emplaced within the biotite-hornblende gneisses and charnockites.

### 2.3.3 Peralimala Granite

Peralimala pluton has been termed by various authors as granite(Nair and Vidyadharan, 1982), alkali granite(Nair and Santosh, 1984) and syenite

(Ravindrakumar and Sinha-Roy, 1985). This E-W elongated pluton covering an area of about 60 sq.km with a length of about 20 km and average width of about 4 km is exposed in the western part of Wynad schist belt and borders the major fault zone of Bavali lineament in the northern side . The pluton is intrusive into migmatitic gneisses containing several scattered patches of metasediments and mafic rocks. The rock is medium grained and generally grey in color often with pink K-feldspar. At some places foliation has developed due to the preferred orientation of hornblende. Geochronological data indicate an age of ca.750±40 Ma for the pluton (Santosh et.al., 1989).

### 2.3.4 Ambalavayal Granite

The granite body exposed in the Ambalavayal region of Wynad district belongs to the late Precambrian-early Paleozoic anorogenic magmatic regime (Nair and Santosh, 1984; Santosh and Nair, 1986). This pluton is intruded into the Precambrian gneisses and outcrops as an E-W elongated elliptical pluton covering an area of about 25 sq.km. On a regional scale, the granite is emplaced at the intersection of Bavali and Moyar shear zones.

The granite is pink medium grained and shows general hypidiomorphic granular texture with quartz, perthic K-feldspar and plagioclase as dominant constituents. Hornblende, riebeckite, biotite and sphene are the principal accessories in this rock. Plagioclase is dominantly albitic. The Ambalavayal

granite shows well developed foliation due to the preferred orientation of hornblende and / or biotite.

Geochemical characters denote an alkaline nature while tectonic aspects suggest probable anorogenic affiliation. The 595 Ma age of the intrusive (Santosh et al.,1986) is co-relatable with the Pan-African thermo-tectonic regime.

### 2.3.5 Perinthatta Anorthosite

The Perinthatta anorthosite located in the NW end of the Bavali shear zone, is the only major anorthosite occurrence in the region. The anorthosite is emplaced within the high grade metamorphic rocks and is surrounded mainly by charnockite and pyroxene granulite. This massif type pluton presumably of late Proterozoic age was first reported by Vidyadharan et al.(1977). The surface exposure of the pluton suggests a minimum areal extent of 60 sq.km. However, the exact extent of the pluton is uncertain, since the area is covered by laterites and coastal sedimentaries. Petrographic and geochemical details of the rock were presented by Nambiar et al. (1982), Ravindrakumar (1986) and Nambiar et al. (1997). Petrographically the pluton is made up of anorthosite (with more than 90% plagioclase) and mafic variants like dioritic anorthosite and anorthositic diorite and rare occurrence of Fe-Ti oxide rich rocks (Nambiar et al. 1997).

### 2.3.6 Adakkathodu Gabbro

The Adakkathodu gabbro occurs east of the Peralimala hill range of Kannur district. This gabbro is referred by Nair et al.(1976) as a melagabbro massif. Preliminary study of the mineralogy and petrochemistry was presented by Ravindrakumar(1986) and Nambiar (1987) gave an account of the field relations and petrography of the pluton. The intrusive with an areal extent of about 20 sq.km. is elongated in an E-W direction. It is medium to coarse grained massive rock with a dark grey color. The pluton is bordered on the north by an E-W shear marked by the straight course of Chinkanni-puzha stream. It is emplaced within the gneisses which shows regional E-W strike with steep to vertical dips and the pluton has its long axis parallel to the regional foliation.

### 2.3.7 Kartikulam Gabbro

The gabbro exposed in Kartikulam near Mananthavady of Wynad district in the northern part of the Bavali lineament is a dark colored and medium grained rock. At some places coarse grained anorthosite patches are observed and they are similar to Perinthatta anorthosite. The essential minerals of the rock include plagioclase feldspar and clinopyroxene.

### 2.3.8 Karikkottakkari Diorite

The grey colored medium grained diorite is exposed in the Karikkottakkari near Iritty. The pluton with an areal extent of about 6 sq.km. has intruded into

the garnet-biotite gneisses and charnockites. At some locations foliations have developed. The essential minerals of this pluton include plagioclase feldspar and clinopyroxene. The mafic enclaves are frequent in the pluton.

## 2.4 Dykes

Dykes of northern Kerala mostly of late Phanerozoic age are fresh dolerites and subalkalic Fe-rich quartz tholeiites with strike extensions in NW-SE, NNW-SSE and NE-SW directions (Radhakrishna et al., 1986). However, a few dykes of Proterozoic age have also been noticed in the region and they appear to have a variety of strike directions. The K-Ar age data of NW-SE trending dolerites range from 99-129 Ma (Radhakrishna and Mathew, 1995). Based on geochemical and palaeomagnetic correlations, presence of excess Ar is suspected in these dykes. Majority of the dykes are considered to be coeval with 69-70 Ma central Kerala dolerites.

## 2.5 Structure

One important feature of the South Indian granulite terrain is the presence of several Proterozoic shear zones. These shear zones dissect the granulite terrain into several blocks and expose different crustal levels . The Bavali shear is one among these shear zones and is considered to be the western extension of the Moyar shear zone which is a part of the Moyar-Bhavani shear system of Tamil Nadu. It trends in a WNW direction and the displacement of Biligirirangan

hills and Nilgiri massif has been inferred due to the dextral sense of the shear (Drury and Holt, 1980). The trend lines in Fig 2.2 show a swing near the shear zones from roughly N-S through NE-SW to roughly E-W . This swing in trend lines was earlier attributed to the dextral movement along the Moyar shear. Later Naha and Srinivasan (1996) argued that the Moyar shear is characterized by a predominantly dip-slip transport. According to them, such a movement on a sub-vertical plane striking EW could in no way rotate the northerly trends to EW and this veering of the trends is an inherent feature of the superposed fold system.

The Wynad schist is exposed all along the length of the Bavali shear. Discrete zones of mylonite and pseudotachylite veins are seen along the shear. Sheared biotite-gneiss is the major rock in the shear zone. The gneiss and mylonite zones are extremely deformed due to several phases of deformation. In the field, at least, three folding episodes have been identified and distinguished as $F_1$, $F_2$ and $F_3$, the three generations of folds, where $F_1$ is the oldest and $F_3$ is the youngest (Soney, 2000).

In addition to the Bavali lineament, a number of other lineaments have been identified in the region by previous workers (Varadarajan and Balakrishnan, 1980; Nair, 1990). The major and minor lineaments/ faults in the study region are shown in Fig.2.3. Though the surface criteria set for the identification of shear zones/ faults are not observed in all these lineaments of the region, many

of these are associated with features like straight drainage course, vegetation pattern, topographic alignments etc and in few cases these coincide with established fault zones.

## 2.6 Geochronology

Acidic and alkaline intrusives which lie within or close to the shear zone range in age from 550-750 Ma. Rb-Sr isochron age of 678 Ma is reported by Nair and Vidyadharan (1982) for Ezhimala pluton and an age of 750 Ma for Peralimala pluton by Santosh et al.(1989). U-Pb Zircon age of 765 Ma is reported for Kalpatta granite by Odom (1982) while Santosh et al.(1986) suggested an age of 595 Ma for Ambalavayal granite by Rb-Sr method. For charnockites and gneisses of the area, no geochronological data is available. Similar rocks in the adjoining areas indicate an age of nearly 2.6 Ga for charnockites (Crawford,1969; Spooner and Fairbairn, 1970; Venkatasubramanian, 1975; Odom, 1982).

## 2.7 Previous Geophysical Work

Though some detailed geophysical investigations were made north of the present study area in the Dharwar greenstone-gneiss-granite terrain (Naqvi, 1973; Subrahmanyam, 1978; Subrahmanyam and Verma, 1982), previous geophysical studies in the study region were mostly of regional and qualitative in nature. Qureshy et al.(1969) and Krishna Brahmam and Kanungo (1976)

inferred the gravity low in the Mananthavady-Gudalur region as due to granite beneath the Dharwar schists. Qualitative analysis of the total intensity aeromagnetic anomaly map in parts of Kerala-Karnataka-TamilNadu regions has been made by Ramachandran (1985). The map covers part of the study region upto 12°N . He identified various magnetic units based on differences in magnetic intensity, gradient, relief and contour pattern. Some major magnetic anomaly trends and the boundary of the magnetic units pertaining to the study region are shown in figure 2.4. While the southern magnetic unit comprises of Wynad, Nilambur and coastal tract from Kannur to Calicut underlain by charnockites, gneisses and igneous intrusives, the northern magnetic unit include the Gundlupet-Mananthavady tract underlain predominantly by high-grade gneisses with enclaves of Sargur group of rocks and granites. The same aeromagnetic map has been utilized by Reddi et al. (1988) to study the crustal structure beneath the granulite terrain of TamilNadu-Kerala. Their qualitative analysis indicate increase in crustal thickness towards north and east with several independent crustal blocks involved in vertical movements.

Based on the above investigations and a comprehensive review of the geology of the area, certain salient geological problems that need detailed geophysical investigation are given below.

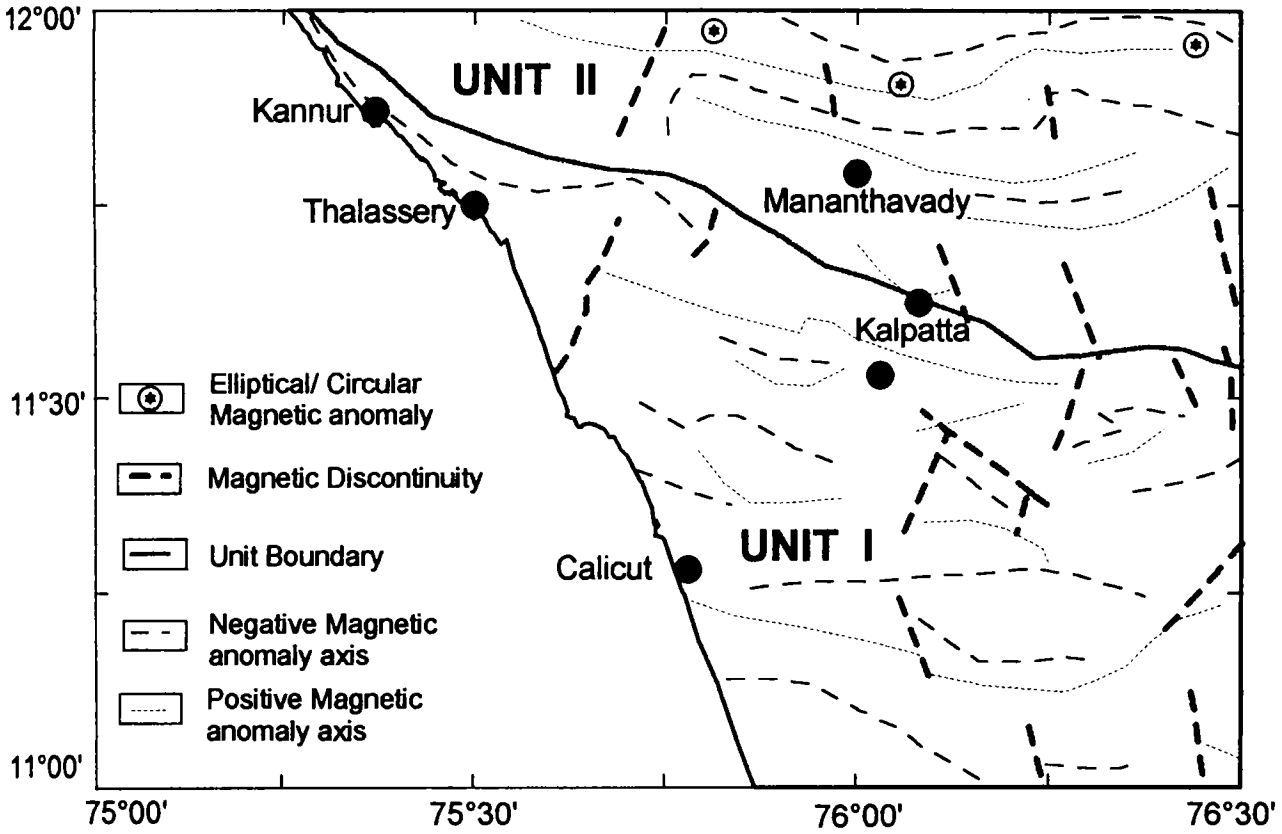


Fig 2.4. Interpreted aeromagnetic anomaly map showing major anomaly trends and magnetic units in the study area. (modified and redrawn after Ramachandran, 1985)

## 2.8 Geological Problems – A Gravity Approach.

The significant geological problems of the area include the nature and evolution of different metamorphic provinces, various acid and basic igneous plutons as well as major structural features and the inter-relationship of the above three (metamorphism, magmatism and tectonism) with the subsurface geology and crustal configuration. These can be studied to a great extent by detailed gravity analysis. The specific geological problems as identified after the preliminary study on the geology and the existing gravity data are:

- Subsurface nature of the Bavali shear and fault zone and crustal thickness variations in different provinces
- Shape and subsurface extension of Perinthatta anorthosite body, especially to see the nature of feeder pipes if present, to check the presence or absence of any large quantity of mafic units beneath it.
- Form, structure and subsurface geometry of the Kalpatta granite pluton and its tectonic significance.
- Tectonomagmatic history of the granulite terrain and major plutons in relation to the shear zone based on crustal configuration .

Since the gravity field reflects subsurface mass anomalies due to significant variations in crustal densities, these problems can be addressed by analysis of gravity field. In the present study, gravity field is analyzed by acquiring closely spaced gravity observations and the study oriented towards

understanding certain salient geological problems taking into account the availability of good and reasonably spaced roads in the area, along with geological criteria. The methodology adopted in data acquisition and results of the gravity investigations have been summarized in chapters IV to VIII.

*Chapter III*

# Petrophysical Properties of Major Rock Types in the Area

## 3.1 Introduction

For any geological interpretation of the potential field data, it is necessary to estimate physical properties of various rock types in the area. The determination of density and susceptibility values of rocks exposed in an area would help the gravity and magnetic interpretation in deciphering whether the anomalies result from the lateral distribution of surface rocks and their subsurface extension or from deep-seated mass distribution or from a combination of both.

A wide variety of igneous and metamorphic rocks are reported from the area for the present study. Many of the rocks have not been studied in detail for their mineralogical and chemical variations nor for their petrophysical properties. Quite interestingly, as discussed in the previous chapter, the regional gravity or aeromagnetic data over the area shows several gravity / magnetic highs and lows. Many earlier workers have speculated concealed / unmapped litho-units with extremely high density or high magnetic susceptibility to account for such anomalies. It is imperative to have data on the density and magnetic susceptibility of the rocks of the area for several attributes of the present work, like:

- for a better understanding of the aeromagnetic expressions, presented in chapter II, for the region;

- to make an attempt, if possible, to group the rocks in terms of their density and magnetic susceptibility, in conjunction with other petrographic data; and
- to check the presence of rock belts with high susceptibility that are significant in identifying marker units.

In the present study, the density and susceptibility values have been estimated for dominant surface rock types, ie., charnockites, gneisses and various felsic and mafic igneous plutons in the Bavali shear zone and adjoining areas of northern Kerala. The densities and susceptibilities have been compared with the available mineralogical and geochemical data of samples from the major rock types in the area . Such comparison would be useful to study the effect of mineralogy and geochemistry on physical properties of surface rocks.

## 3.2 Factors Controlling Density and Susceptibility

The density of igneous and metamorphic rocks is very closely related to mineral composition. Many genetic processes generating the mineral composition will be reflected in the density of rocks (Henkel, 1976). For acid plutonic rocks, density is controlled by the amount of mafic minerals, while in basic rocks, the amount of plagioclase is determinative(Platou,1968; Henkel, 1970). Other possible factors are nature of mafics present, percentage of opaques or high density accessories, quartz : feldspar ratio of felsic rocks, massive vs foliated nature of rocks, degree and type of weathering of rocks etc. The magnetic properties are useful indicators of the geochemical and

petrological state of a rock (Lapointe et al., 1984). The magnetic properties depend essentially on the characteristics of a small group of magnetic carrier minerals that are universal constituents of all rocks. The magnetic minerals generally belong to the ternary system $FeO$-$Fe_2O_3$-$TiO_2$ which include magnetite, titanomagnetite, haematite, ilmenite and rutile. The magnetic susceptibility of a rock does not wholly depend on the amount of iron oxides present, but is mainly influenced by the quantity of iron oxides in ferrimagnetic minerals. The main ferrimagnetic mineral is magnetite apart from the members of the titanomagnetic series and pyrhotite.

## 3.3 Previous Work

Aravamadhu (1974) estimated susceptibilities of charnockite samples from the South Indian shield and observed a linear relationship between the magnetite content and susceptibility values. Densities and magnetic susceptibilities of Precambrian rocks from South Indian Shield have been estimated by Subrahmanyam and Verma(1981). Densities and magnetic susceptibilities of metamorphic rocks from South Indian Granulite terrain have been estimated by Ramachandran and Bosu (1991) and Ramachandran (1990) respectively. Ramachandran (1992) estimated petrophysical properties of granulite rocks in the southern Indian shield. Petrophysical properties of some dolerite dykes of Andhra Pradesh have been analyzed by Varaprasada Rao et al. (1978).

## 3.4 Sampling and Distribution

As can be seen from the detailed geological map (Fig. 2.2), charnockites and gneisses are the dominant rock types in the area. Apart from these rocks, a large number of plutonic igneous rocks such as granite, gabbro, anorthosite, and diorite are present in the region (Fig.2.3). Fresh samples of these rocks were collected mainly from quarries and outcrops in the study area. Samples of charnockite and gneiss were collected from the study region and also from the adjoining areas. Some samples of dolerite and granulite were also collected from the area. Igneous rocks were sampled from 125 locations and metamorphic rocks from 40 locations. In some places, more than one sample were collected so as to assess the variation of physical properties in the same location. Densities of 165 samples and susceptibilities of 205 samples were measured in the laboratory. All the rocks of the area being medium or coarse grained, identification of rock types was made based on megascopic features and the results are tabulated accordingly. The samples of major plutons include granites from Ezhimala, Peralimala , Ambalavayal and Kalpatta, gabbro from Ezhimala and Kartikulam, diorite from Karikottakari and Bavali and anorthosite from Perinthatta.

## 3.5 Measurements

### 3.5.1 Density

Density measurements made in the laboratory are based on the formula (Archimede's Principle),

$$\rho = \frac{W1}{(W1-W2)}$$

$\rho$ - density in gm/cc

W1 - weight of the samples in air (in gm.)

W2 - weight of the samples in water (in gm.)

Weight of the sample was determined using an electrical balance (having an accuracy of 1 mg.), first by weighing the sample in air and then by weighing the sample immersed in water. Weight of samples measured ranged from 60 to 95 grams in air. Since all samples measured were of either igneous or metamorphic rocks with negligible porosity, density measured closely approximates the field density.

### 3.5.2 Susceptibility

The susceptibility measurements were made in the laboratory using a Kappameter (K-2 magnetic susceptibility meter, EDA make, borrowed from Center for Exploration Geophysics (CEG), Osmania University, Hyderabad), which has an accuracy of $\pm$ 5% . The instrument has been calibrated using standard samples available and a calibration chart was prepared . The readings were reduced using this calibration chart. Samples of more than 1 kg in size

were selected for measurement and readings were taken along fresh and plane surfaces.

## 3.6 RESULTS

Density (in gm/cc) and susceptibility (in $10^{-6}$ cgs units) data for a total of eight rock types have been summarized in Table 3.1 and 3.2 respectively and histograms of these data for all rock types are shown in Fig. 3.1 and 3.2 respectively.

For some of the samples used in the present study, detailed geochemical analysis was carried out by Nambiar et al. (1999) and Soney (2000). The mafic percentage compiled from these works for the samples having density estimates are presented in Table 3.3. Since chemical composition can play a major role on density estimates, the values are analyzed in the light of available geochemical data. Since susceptibility is dependent on the ferrimagnetic minerals, an attempt is made to correlate susceptibility with mineral content. Granite and gabbro rocks are sampled from different locations and mineralogical data is also available for these samples. The density and susceptibility variations within granites and gabbros from different locations have been compared and explained in terms of variations in the mineralogical data. The density and susceptibility values obtained in this study were also compared with the values given in previous works like Subrahmanyam and Verma (1981), Ramachandran (1990), Ramachandran and Bosu (1991) and

**Table 3.1. Results of density measurements for the major rock types in the study area.**

| Sl. No. | Rock Type | No. of Samples | Mean (gm/cc) | S.D. | Range (gm/cc) |
|---|---|---|---|---|---|
| 1. | Granite | 63 | 2.67 | 0.0385 | 2.57 – 2.78 |
| | (a) Ezhimala | 22 | 2.69 | 0.0432 | 2.57 – 2.78 |
| | (b) Peralimala | 17 | 2.66 | 0.0300 | 2.61 – 2.71 |
| | (c) Ambalavayal | 18 | 2.67 | 0.0143 | 2.64 – 2.69 |
| | (d) Kalpatta | 6 | 2.67 | 0.00665 | 2.66-2.68 |
| 2. | Gabbro | 18 | 2.99 | 0.140 | 2.64 – 3.14 |
| | (a) Ezhimala | 11 | 2.95 | 0.1702 | 2.64 – 3.14 |
| | (b) Kartikulam | 7 | 3.04 | 0.0443 | 2.97 – 3.11 |
| 3. | Diorite | 7 | 2.75 | 0.0811 | 2.68 – 2.92 |
| | (a) Karikottakari | 4 | 2.79 | 0.0883 | 2.74 – 2.92 |
| | (b) Bavali | 3 | 2.69 | 0.0120 | 2.68 – 2.70 |
| 4. | Anorthosite | 13 | 2.77 | 0.0940 | 2.67 – 3.01 |
| 5. | Dolerite | 6 | 3.02 | 0.1231 | 2.87 – 3.21 |
| 6. | Granulite | 12 | 2.75 | 0.0928 | 2.64 – 2.98 |
| 7. | Charnockite | 14 | 2.76 | 0.0730 | 2.67 – 2.89 |
| 8. | Gneiss | 28 | 2.73 | 0.1061 | 2.64 – 3.15 |

**Table 3.2. Results of magnetic susceptibility measurements for the major rock types in the study area**

| Sl. No. | Rock Type | No. of Samples | Range ( $10^{-6}$ cgs units) | S.D. |
|---|---|---|---|---|
| 1. | Granite | 67 | 0 – 5000 | 1334 |
| | (a) Ezhimala | 29 | 520 – 5000 | 1360 |
| | (b) Peralimala | 18 | 0 – 3600 | 923 |
| | (c) Ambalavayal | 20 | 0 – 3300 | 798 |
| 2. | Gabbro | 34 | 100 – 6150 | 1450 |
| | (a) Ezhimala | 20 | 1300 – 6150 | 1314 |
| | (b) Kartikulam | 12 | 100 – 6000 | 1616 |
| | (c) Peralimala | 2 | 760 – 1450 | 345 |
| 3. | Diorite | 11 | 0 – 6800 | 2580 |
| | (a) Karikottakari | 7 | 390 – 6800 | 2825 |
| | (b) Bavali | 4 | 0 – 760 | 364 |
| 4. | Anorthosite | 26 | 0 - 4800 | 1969 |
| 5. | Dolerite | 8 | 75 – 4100 | 1748 |
| 6 | Granulite | 15 | 75 - 4700 | 1390 |
| 7 | Charnockite | 20 | 190 - 2600 | 874 |
| 8 | Gneiss | 24 | 50 - 2900 | 800 |

**Table 3.3:** Density and respective mafic percentage for some of the plutonic rock samples from the study area.

**GRANITE**

| Sample No. | Density (gm/cc) | Mafic content (%) |
|---|---|---|
| S83 | 2.71 | 1.3 |
| S77/A | 2.66 | 2.2 |
| S80/A | 2.62 | 1.5 |
| S81/A | 2.69 | 4.9 |
| S87/A | 2.67 | 4.9 |
| S74 | 2.64 | 2.1 |
| S24/1 | 2.71 | 6.2 |
| S25/1 | 2.73 | 12.9 |
| S45/B | 2.57 | 2.1 |
| S54/C | 2.75 | 13.5 |
| S90/A | 2.65 | 6.4 |
| S19/1 | 2.61 | 1.6 |
| S23/1 | 2.7 | 8.1 |
| S34/1 | 2.74 | 10.7 |
| S77/B | 2.67 | 3.6 |
| S116/A | 2.68 | 3.1 |
| S77/A | 2.66 | 3.7 |
| S124/A | 2.66 | 2.3 |
| S120 | 2.66 | 2.3 |
| S77/B | 2.67 | 2.9 |
| S125/B | 2.67 | 3.4 |
| S90/C | 2.65 | 2.3 |
| S81/A | 2.69 | 4.4 |

**GABBRO**

| Sample No. | Density (gm/cc) | Mafic content (%) |
|---|---|---|
| S48/A | 2.84 | 25.7 |
| S50/A | 2.97 | 39.7 |
| S52/A | 2.99 | 53.8 |
| S53/A | 2.98 | 39 |
| S127/A | 3.11 | 49.4 |
| S131 | 3.02 | 34.8 |
| S128/A | 3.06 | 39.1 |

**ANORTHOSITE**

| Sample No. | Density (gm/cc) | Mafic content (%) |
|---|---|---|
| S1/A | 3.01 | 49.2 |
| S2/A | 2.75 | 40.7 |
| S3/B | 2.7 | 3.3 |
| S12/F | 2.72 | 3.26 |
| S4/A | 2.69 | 2.6 |
| S11/C | 2.78 | 13.18 |
| S12/T | 2.72 | 10.88 |
| S12/L | 2.67 | 6.97 |
| S12/M | 2.76 | 5.91 |
| S21/1 | 2.71 | 31.73 |
| S11/C | 2.78 | 6.71 |

**DIORITE**

| Sample No. | Density (gm/cc) | Mafic content (%) |
|---|---|---|
| S62/B | 2.92 | 15.1 |
| S64/A | 2.74 | 8.7 |
| S57 | 2.74 | 6.4 |
| S61/A | 2.75 | 7.7 |

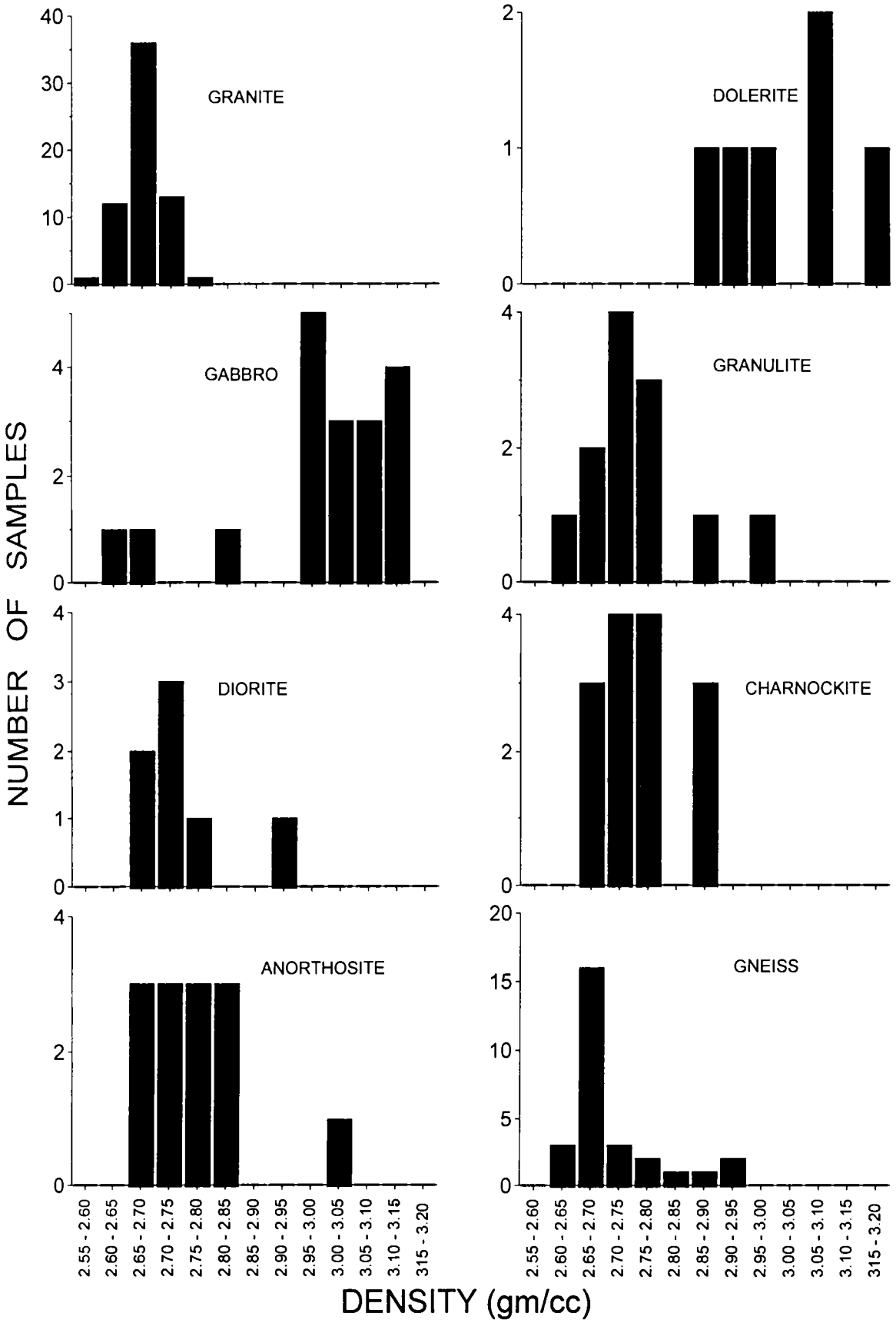


Fig 3.1.Histograms showing the frequency distribution of densities for themajor rocks in and around the Bavali shear zone of northern Kerala

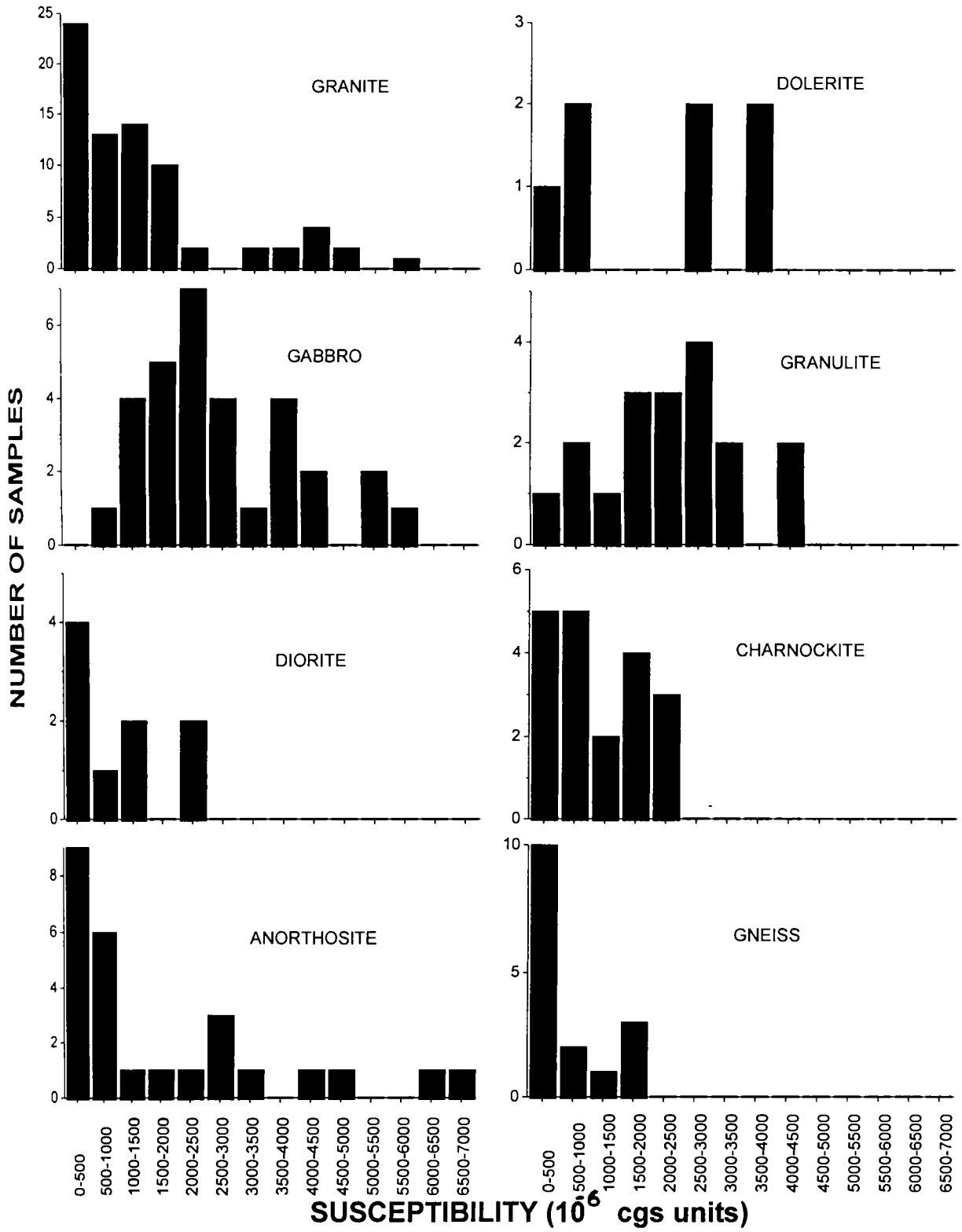


Fig 3.2. Histograms showing the frequency distribution of magnetic susceptibilities for the major rocks in and around the Bavali shear zone of northern Kerala

Ramachandran(1992) for the south Indian shield. The density and susceptibility data for each rock type is discussed in detail as given below.

### 3.6.1 Granites

The density estimates of sixty-three granite samples from Ezhimala, Peralimala, Ambalavayal and Kalpatta gave an average density of 2.67 gm/cc. The histogram (Fig 3.1) shows that the values are normally distributed and densities of most of the samples are around 2.65-2.70 gm/cc range. The variation in densities among samples for different areas has been analyzed in relation to mafic content of the rock. Ezhimala samples, in general, show higher average density than Ambalavayal, Kalpatta and Peralimala. This high density can be attributed to the presence of high mafic percentage in Ezhimala samples. Hornblende (3.02-3.45 gm/cc) is also comparatively more in Ezhimala samples. When compared to Peralimala samples, the mafic percentage is more in Ambalavayal samples and therefore they have higher density. Moreover, feldspar (2.56-2.63 gm/cc) content is less in Ambalavayal samples than in Peralimala. Peralimala granite is characterized by the highest felsic content among the four. The density variations in the granite samples confirm a linear relationship with modal mafic content as depicted in Fig 3.3. However, the figure shows for few samples with extremely low mafic content (less than 2.5 %) a wide range in densities (2.56 – 2.67 gm/cc). This may be probably due to varying quartz-feldspar ratio in the rocks, variation in the presence of high density opaques though such variations is minor or, possible error in precisely

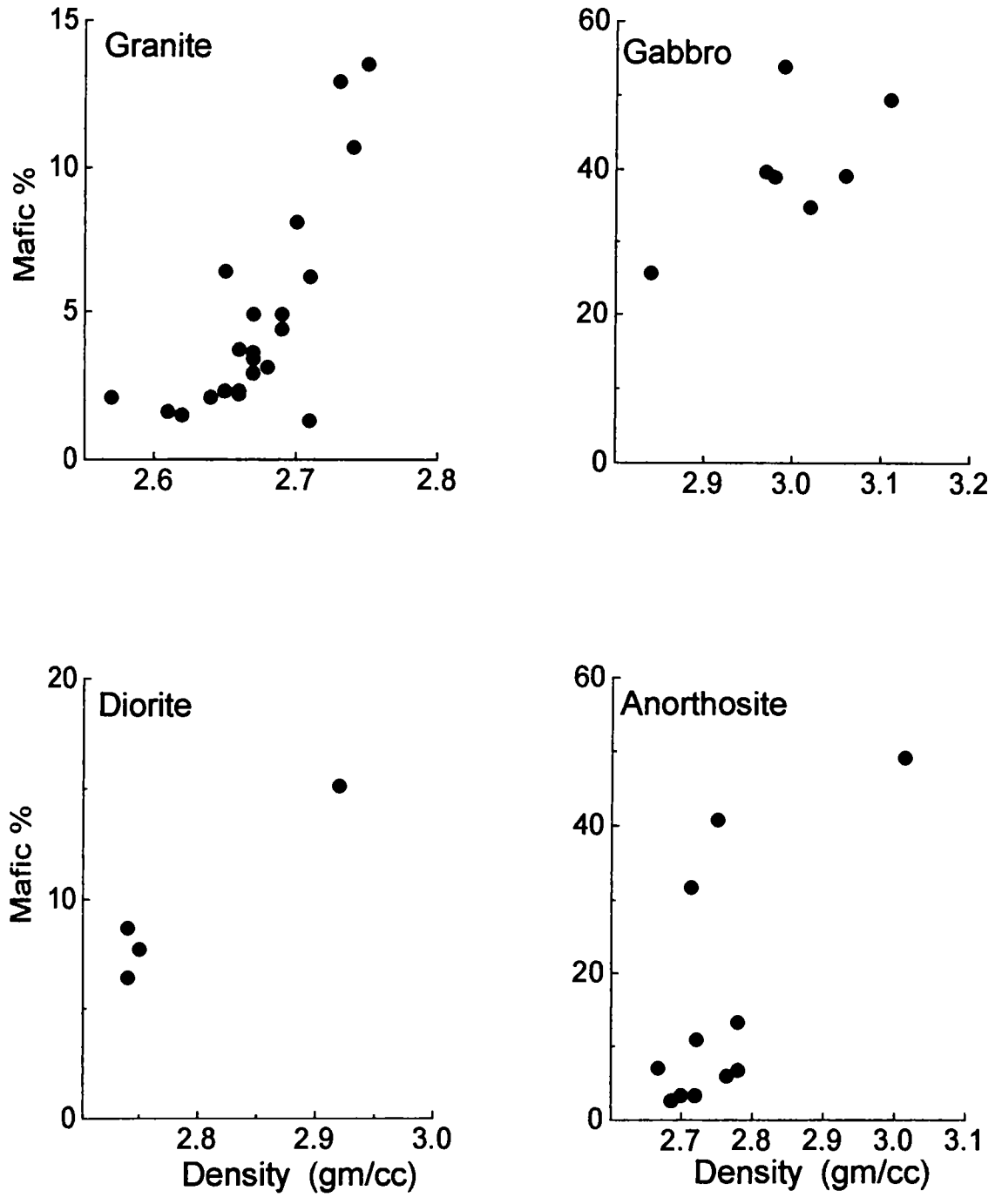


Fig 3.3. Binary plots showing the variation of density with modal mafic content in some of the plutonic rocks from the area.

estimating mafic percentage in highly felsic rocks. For example, the sample S45/B of Ezhimala granite shows extremely high quartz (34%) and also the least density. Some samples show anomalously high density values and their modal mineralogical data indicate that it can be generally attributed to the high mafic content in the samples.

Susceptibility values (in $10^{-6}$ cgs units) the sixty seven granite samples measured range from 0 to 5000. Twenty nine Ezhimala samples range in values from 520-5000, while eighteen Peralimala samples have a range of 0-3600 and twenty Ambalavayal samples have a range of 0-3300. The high iron oxide content of these granitic rocks may indicate a high magnetite content, which is highest in Ezhimala samples followed by Peralimala and Ambalavayal and the observed differences in susceptibility among samples can be explained due to such variation.

The wide range in density and magnetic susceptibility values shown by the granitic rocks of the area would probably be due to their diverse type of origin and environment as indicated in previous petrological works. Geochemical analysis of Ezhimala granite pluton by Sinha-Roy and Ravindrakumar (1986) indicate that the granite suite is a product of diapiric emplacement of magma generated at shallow depths, which is a constituent of important magmatic events in the Kerala region in late Proterozoic and early Palaeozoic times. Geochemical data of the Peralimala granite shows high content of alkalies suggesting possibly the existence of phlogopite - rich pockets in the mantle, from where the melt

equilibrated. According to Nair and Santosh (1984), this may indicate that the granite pluton is a manifestation of rift related alkaline magmatism. Kumar et al.(1998) studied the mineralogy and major and trace element geochemistry of Kalpatta granite and suggest that the variants are products of polyphase late magmatic crystallization. Petrochemical study of the Ambalavayal granite by Santosh (1986) indicates derivation of the granite from an alkali- enriched partial melt through quartz and alkali feldspar fractionation.

### 3.6.2 Gabbro

The density estimates of eighteen gabbro samples gave an average density of 2.99 gm/cc . Histogram of the data shows that majority of the values are between 2.95-3.15 gm/cc with a peak at 2.95-3.00 gm/cc class (Fig.3.1). Gabbro is sampled from two localities, i.e., from Kartikulam and Ezhimala. The density variations among these samples have been compared with mineralogical data. The amount of plagioclase present is the controlling factor of density in basic plutonic rocks. The high density of Kartikulam samples( average of 3.04 gm/cc) is due to high average mafic content. Ezhimala is characterized by the presence of leucogabbro variety and a few of these rocks sampled shows extremely low densities (2.64 to 2.68gm/cc) because of comparatively more feldspar (2.56-2.63 gm/cc) content in leucogabbro. The low density could also be partly due to the presence of granite veins occasionally seen in Ezhimala gabbro which may increase the felsic content. Density versus modal mafic

mineral percentage plot for gabbro samples shown in Fig 3.3 indicates the control of mafic content on density.

Magnetic susceptibility of thirty-two gabbro samples measured gave a range of 100 – 6150 out of which twenty Ezhimala samples have a range of 1300-6150 and twelve Kartikulam samples, range of 100-6000. Geochemical data indicate the presence of more iron oxides which may point to more magnetite content in Ezhimala samples than in Kartikulam. This is consistent with the high range of susceptibility in Ezhimala samples. However, a direct correlation between iron content and magnetite content may not exist, as much of the iron may be fixed in non-magnetic minerals like hornblende and biotite.

### 3.6.3 Diorite

Data of seven diorite samples measured indicate an average density of 2.75 gm/cc with a range of 2.68-2.92 gm/cc. Histogram of the data shows that, most of the values fall in the range 2.70-2.75 gm/cc. For a few samples where modal mafic mineral percentage is available, it is seen that the density is consistent with the mineralogy especially the mafic mineral percentage (Fig 3.3) . The high density value of 2.91 gm/cc shown in the figure is due to high mafic content in the sample. Eleven diorite samples give susceptibility in the range of 0 – 6800.

### 3.6.4 Anorthosite

The densities estimated for twenty six anorthosite samples gave an average of 2.77 gm/cc and show a range of 2.67-3.01 gm/cc with most of the samples ranging between 2.70-2.84 gm/cc. Anomalously high density is observed for a small number of the samples. The density variations observed in anorthosite samples are seen consistent with the minerological data, especially the mafic mineral percentage in them. Nambiar et al.(1997) classified the mafic variants associated with the Perinthatta anorthosite as dioritic anorthosite and anorthositic diorite and a small group of opaque-rich anorthositic rocks. A comparison of the petrographic details with the density data shows that the density values of 2.75±0.2 are essentially for anorthosites or its mafic variants and high density values are for opaque-rich rocks. For a few samples where modal mineralogy is available, this aspect is more clear. The variation of density with modal mafic mineral percentages of anorthositic rocks is depicted in Fig 3.3). The density estimate for anorthosite rocks by Subrahmanyam and Verma (1981) is much higher (2.85 gm/cc) than the present estimates because their samples were more gabbroic in composition.

For a total of twenty six anorthosite samples measured, the susceptibility values show a range of 0 – 4800. Histogram prepared on the data shows a large scatter which may be due to the varying percentage of magnetite content.

### 3.6.5 Dolerite

Dolerite dykes are sparse and only a few samples are collected from Perinthatta, Ezhimala and Peralimala . Six samples gave an average density of 3.02 gm/cc with a range of 2.87-3.21 gm/cc (cf. 3.03 gm/cc of Subrahmanyam and Verma, 1981).

The susceptibility measurements of eight samples gave a range of 75-4100. Histogram of the data shows large scatter in the value.

### 3.6.6 Granulite

Granulites are sampled mostly from the area north-west of Perinthatta anorthosite in the high grade charnockite region of northern Kerala. Twelve samples gave an average density of 2.75 gm/cc with a range of 2.64 - 2.98 gm/cc. Histogram of the data show a peak at 2.70 – 2.75 gm/cc range. Samples are mostly pyroxene granulites and some samples have higher densities because of high mafic content.

The susceptibility values measured for fifteen granulite samples gave a range in values from 75 – 4700. Histogram of the data show clustering between 1500 – 3500 range.

### 3.6.7 Charnockite

Charnockite samples are collected from all along the shear zone and around the associated intrusives. Fourteen samples collected gave an average density of 2.76 gm/cc with a range of 2.67-2.89 gm/cc. Histogram shows the peak at 2.70-2.80 range. The average density value obtained in the present study is in good agreement with the density estimate of 2.77 gm/cc made by Ramachandran and Bosu (1991) and Ramachandran (1992) for the charnockites of south Indian granulite terrain.

A total of twenty samples measured gave susceptibility over a range of 190 – 2600. Ramachandran (1990) classified the charnockites of Southern Granulite Terrain into two groups, group I characterized by low susceptibility values (6-200) and group II characterized by medium to high susceptibilities (200-4420). He attributed this variation to absence / presence of magnetite content and explained as due to changes in magnetic mineralogy during prograde and retrograde metamorphic process. The susceptibilities of samples in the study region fall mostly under group II and are consistent with the observation that retrogression is only locally noticed in the charnockite rocks in this region.

### 3.6.8 Gneiss

The samples of gneissic rocks have been collected from all along the shear zone and around the associated intrusives. A total of twenty eight samples measured gave a range of 2.64-2.94 gm/cc with an average density of 2.73

gm/cc. The histogram of data shows a peak at 2.65-2.70 gm/cc range with an affinity towards higher densities. The average density obtained in this study correlates well with the density estimates given by Ramachandran and Bosu (1991) for biotite and hornblende gneiss (2.72 gm/cc) in the south Indian granulite terrain.

Of the twenty four gneiss samples measured the susceptibility values range from 50 - 2900. Histogram shows that the most of the values are below 500.

## 3.7 Density vs. Magnetic Susceptibility (D-MS) Relationship

As the mineral composition of rocks are the chief factors in controlling both the density and susceptibility, some correlation is sometimes observed between the two. As mentioned earlier in section 3.2, abundance of mafic minerals and amount of plagioclase present in a rock are the primary factors which determine the density of the rock while the magnetite content of a rock is the primary controlling factor in the case of magnetic susceptibility. A roughly linear relationship has been observed between the magnetic susceptibility and magnetite content by Nagata (1961) for igneous rocks. Aravamadhu (1974) studied the magnetic properties of charnockites from south India and obtained a linear relationship for the variation of susceptibility with percentage by weight of magnetite. Henkel (1976) studied the correlation between density and magnetic susceptibility for Precambrian rocks from Northern Sweden and described, based

on these relations, the various geological processes which control these physical parameters. Subrahmanyam and Verma(1981) observed a linear relationship between density and log(K) for most of the rocks types they studied from southern Indian shield.

The D-MS scatter plots for each rock type are shown in Fig 3.4 (a) and Fig 3.4(b). The granites show a wide range in magnetic susceptibility though they have a limited range in density. There is a slight increase in magnetic susceptibility with increase in density. Most of the gabbro samples fall in a limited but high range compared to other rocks, in both density and susceptibility values. The plots cluster around 3.05 gm/cc and 2000 cgs units. The charnockites show wider range in density but a limited range in magnetic susceptibility and there is high susceptibilities even for samples with very low density. Compared with this, gneisses show a much wider range in magnetic susceptibility, though density wise they are much lighter compared to charnockites. Some of the gneisses are known to represent retrogressed charnockites and most of the charnockites are high-grade metamorphic equivalents of gneisses. The recrystallization behaviour in such transformations does not generally bring in change of density but magnetic susceptibility may increase just before it is converted to charnockite (as there is crystallization of iron oxide minerals during this stage) and it will decrease on retrogression. Dolerite samples though few in number, show a linear relation between density and magnetic susceptibility.

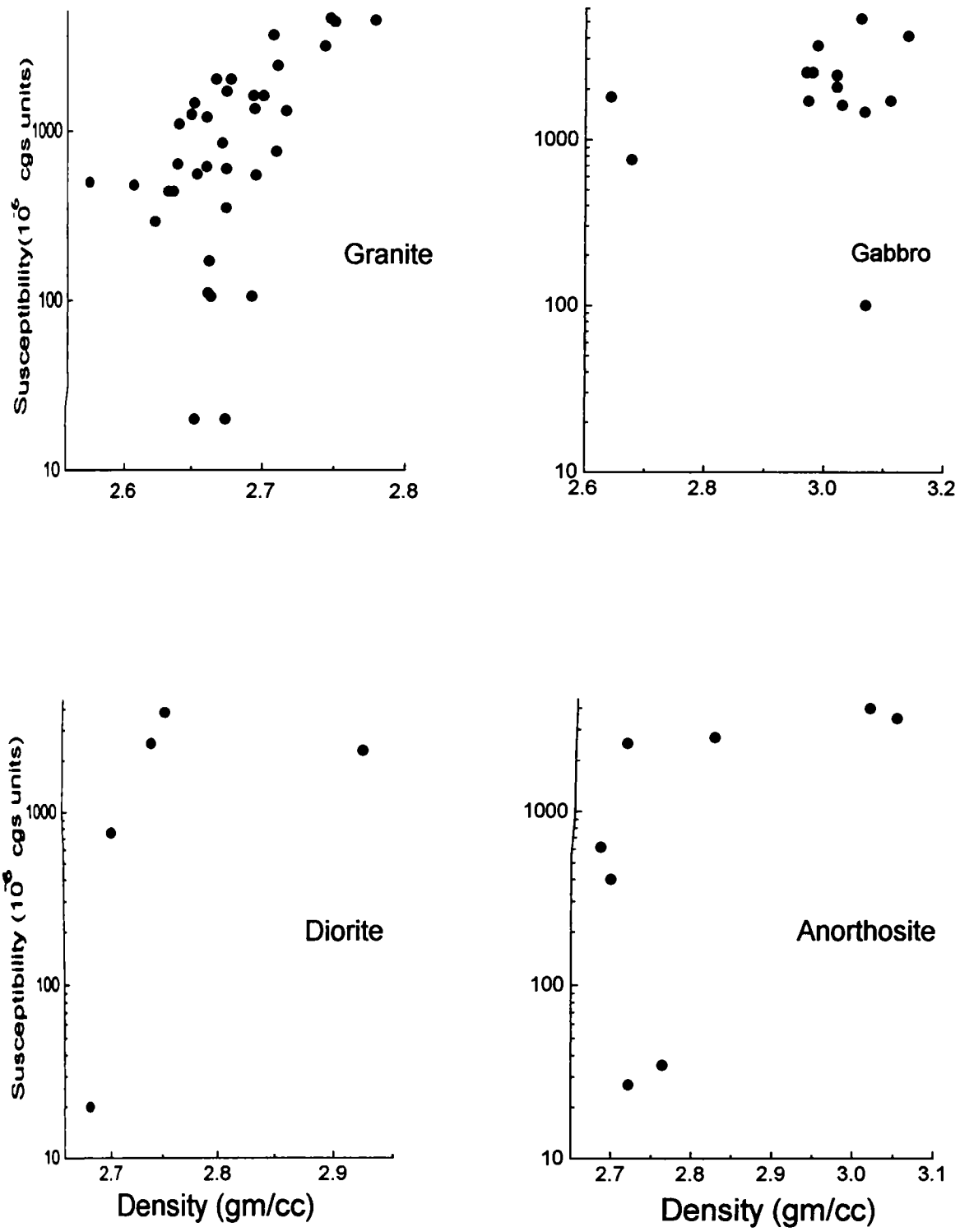


Fig 3.4(a): Plot of density vs. susceptibility for granite, gabbro, diorite and anorthosite rocks of the study area.

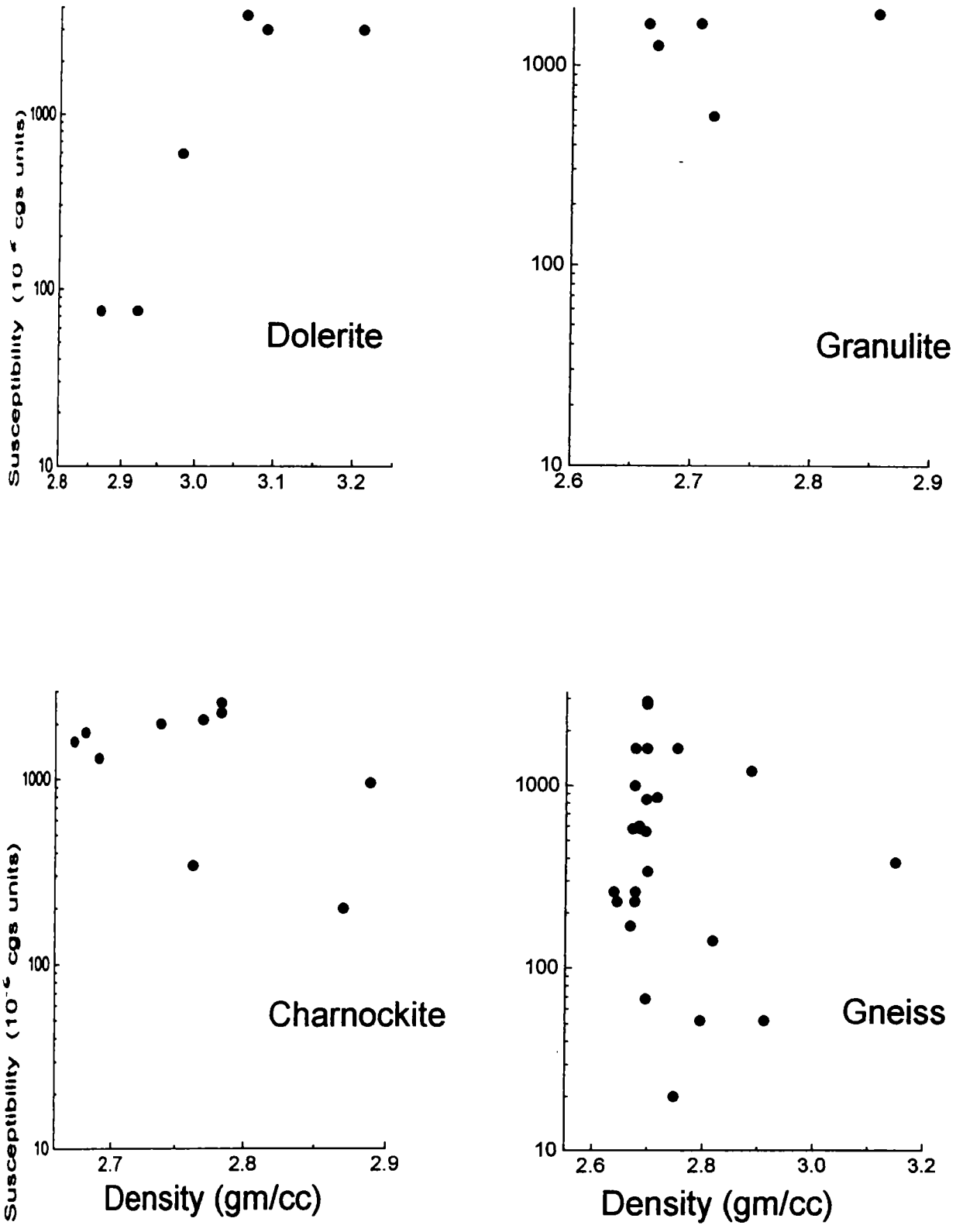


Fig 3.4(b). Plot of density vs. susceptibility for dolerite, granulite, charnockite and gneissic rocks of the study area

As may be seen from Figs 3.4 (a) and 3.4(b), the D-MS plots have wide range arising from a large standard deviation in the susceptibility values. For the purpose of comparison, the minimum area occupied by at least 60% of the values is considered as representing the D-MS field for each rock type. These fields are compared in Fig 3.5. The above figure confirms the lack of a definite linear relationship between density and magnetic susceptibility. While this problem needs detailed study in terms of more mineralogical and petrological data, a possible inference could be the lack of primary genetic consaguinity between the formations of the area.

## 3.8 Conclusions

Density and susceptibility measurements of nearly 200 samples of all the eight rock types of the study area have been carried out. The densities of dominant rocks of the area are 2.76 gm/cc for charnockite, 2.73 gm/cc for gneiss and 2.75 gm/cc for granulite. The densities for major plutonic rocks show averages of 2.67 gm/cc for granite, 2.99 gm/cc for gabbro, 2.75 gm/cc for diorite, 2.77 gm/cc for anorthosite and 3.02 gm/cc for dolerite. The susceptibility ranges of these rocks are 0 – 5000 (granite), 100 – 6150 (gabbro), 0 – 6800 (diorite), 0 – 4800 (anorthosite), 75 – 4100 (dolerite), 75 – 4700 (granulite), 190 - 2600 (charnockite) and 50 – 2900 (gneiss). Thus the range in average density, considering all the rocks, varies between 2.67 to 3.02 gm/cc while the magnetic susceptibility from 0 to 6800 and the values mostly close to average crustal values. Extremely high or low values of density or susceptibility are not

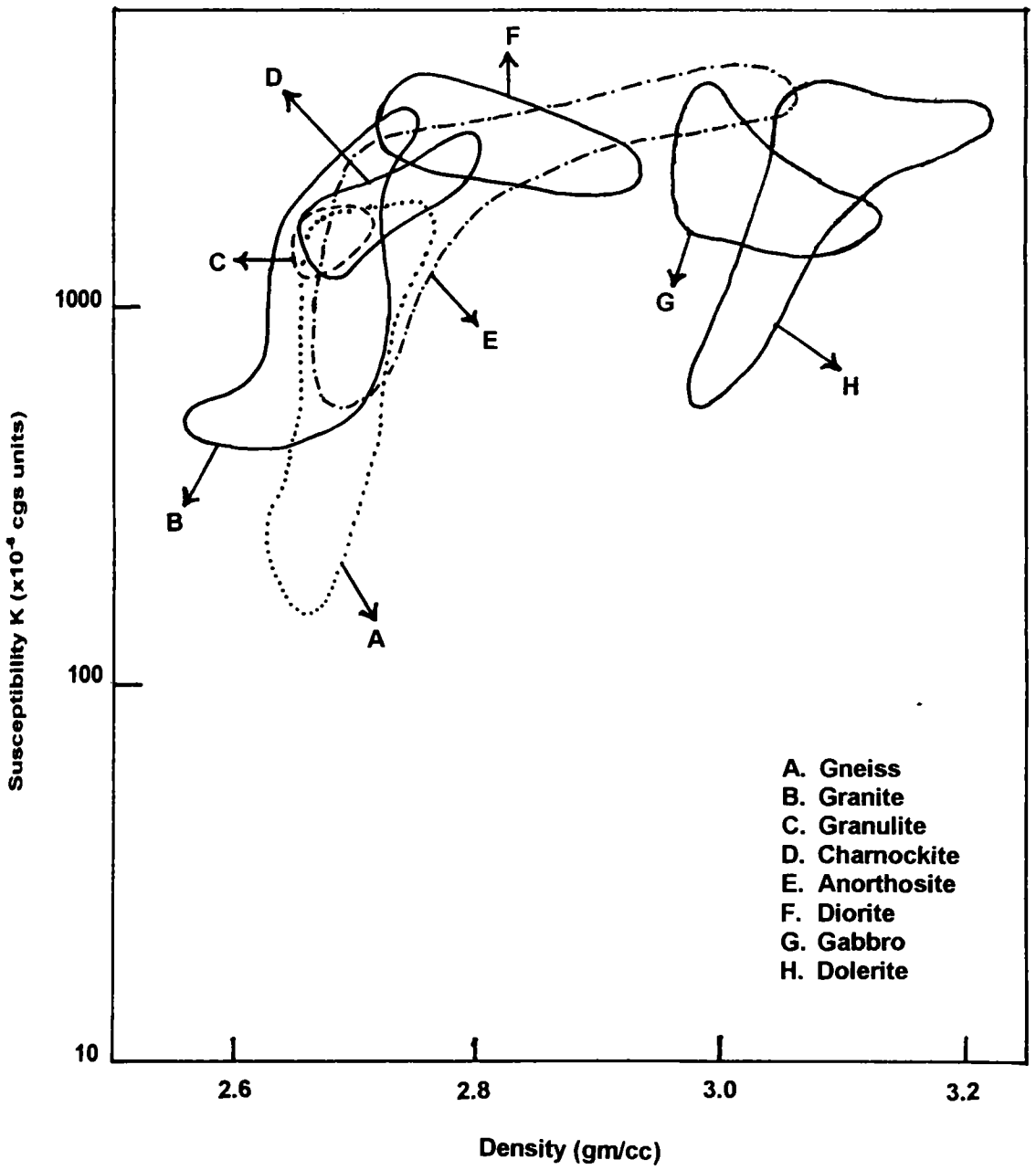


Fig 3.5. Plot showing the representative D-MS fields for all rock types considered in the present study.

recorded. For a few number of samples, where modal mineralogical data is available, an attempt is made to correlate the mineralogical data with the physical properties. For granites and gabbro, since the mineralogical data of samples from different locations are available, the variation in physical properties in samples from different locations is explained with the help of mineralogical data. An analysis of the relationship between modal mafic mineral percentage and density for granite, gabbro, diorite and anorthosite samples establish that the mafic content determines the density of rocks to a great extent.

*Chapter IV*

# Data Acquisition and Reduction

## 4.1 Introduction

The method of gravity prospecting can be divided into three stages. The first stage is field work where gravity and elevation data are collected at various stations distributed in the area. The second step involves the reduction of observed data by making corrections for various disturbances while calculating the anomalies and their amplitudes. The third step is related to the interpretation of these anomalies in terms of plausible geological features. This chapter describes the procedures and methodology adopted for gravity surveys in the study region. A brief history of the gravity surveys in Kerala, is presented and the quantity and quality of data collected, the corrections applied and the various regional-residual separation methods are outlined.

## 4.2 A Brief History of the Gravity Surveys in Northern Kerala and the Adjoining Areas

A number of agencies and workers have been involved in the collection and analysis of the gravity data in the South Indian shield regions. These include the Survey of India (SOI), Geological Survey of India (GSI), Oil and Natural Gas Commission(ONGC), Hawaii Institute of Geophysics, USA (HIG) , National Geophysical Research Institute (NGRI) and the Center for Earth Science Studies (CESS). Though some parts of Kerala were covered during these surveys, the data collected was too scanty to make any meaningful

geological interpretation. The data includes a few pendulum stations established by SOI in the Kerala region (Gulatee, 1956). The accuracy of these pendulum stations is uncertain and also many of the station locations at present cannot be easily traced. Gravity surveys conducted by ONGC cover mainly the coastal regions of Kerala. HIG established a few gravity stations located at permanent places in the Kerala region (Woollard et al., 1969). Radha Krishna et al.(2000) estimated probable uncertainties in the HIG stations and found errors of as much as 1.5 mGal. As part of the regional gravity surveys, NGRI collected a good amount of gravity data in the Kerala region at an average station spacing of 8-10 km along major roads. This data alone is however not sufficient for any detailed work, but can form the basis for more close spaced gravity data. CESS had established nearly 40 permanent gravity base stations (Singh et al., 1985) in and around Palghat gap region. These bases were established with respect to the Coimbatore Airport base and are accurate enough to consider for regional gravity surveys. Details of the data collected by various agencies in the regions in and around Bavali shear zone and adjoining areas are given in Table 4.1.

## 4.3 Establishment of Gravity Bases and Collection of Data

In any gravity survey, a good network of gravity base stations is a prerequisite. As the available pendulum stations of the SOI (Gulatee, 1956) in the area are relatively not that accurate for linking secondary bases and as

**Table 4.1. Details of gravity data in the region of Bavali shear zone and the adjoining areas.**

| Name of organization | No. of gravity bases | No. of gravity observations | Reference |
|---|---|---|---|
| CUSAT | 36 | 850 | Present study |
| NGRI | - | 60 | Qureshy et al. (1981) |
| HIG, ONGC and SOI | - | 40 | Woollard et al. (1969) |
| CESS | 40 | - | Singh et al. (1985) |

many of these locations are presently not traceable, for the purpose of this study, the nearest known base established by Singh et al.(1985) at Vallathol Nagar R.S. (gravity value of 978.13815 gals) was used. This station is located 80 km. SE of Calicut. As mentioned earlier, the Vallathol Nagar R.S. base is part of a network of 40 bases established by Singh et al. (1985) with respect to Coimbatore Airport value of 978.0715 gals(Qureshy and Krishna Brahmam, 1969). The Coimbatore Airport base was in turn connected to the Bangalore Airport gravity value of 978.0386 gals(Manghnani and Woollard, 1963). The Bangalore base corresponds to a value of 978.0640 gals of the Indian National Gravity Base at Dehradun, which in turn corresponds to the Potsdam gravity value of 981.2740 gals.

The base stations were established using the well known method of forward looping, the procedure being, to carry forward the gravity value from an already established base A to a new base B, by making a loop A-B-A. The same method was adopted to carry forward the gravity values. It is necessary to have a reasonably good network of base stations in the study area for the smooth conduct of the survey. So, a network of 36 new permanent gravity base stations has been established in the area whose locations are given in Fig. 4.1. The base stations have been selected to be at well-defined and permanent landmarks such as verandhas of Rest houses (RH), Inspection Bunglows(IB) and other government buildings such as Railway stations(RS), Police

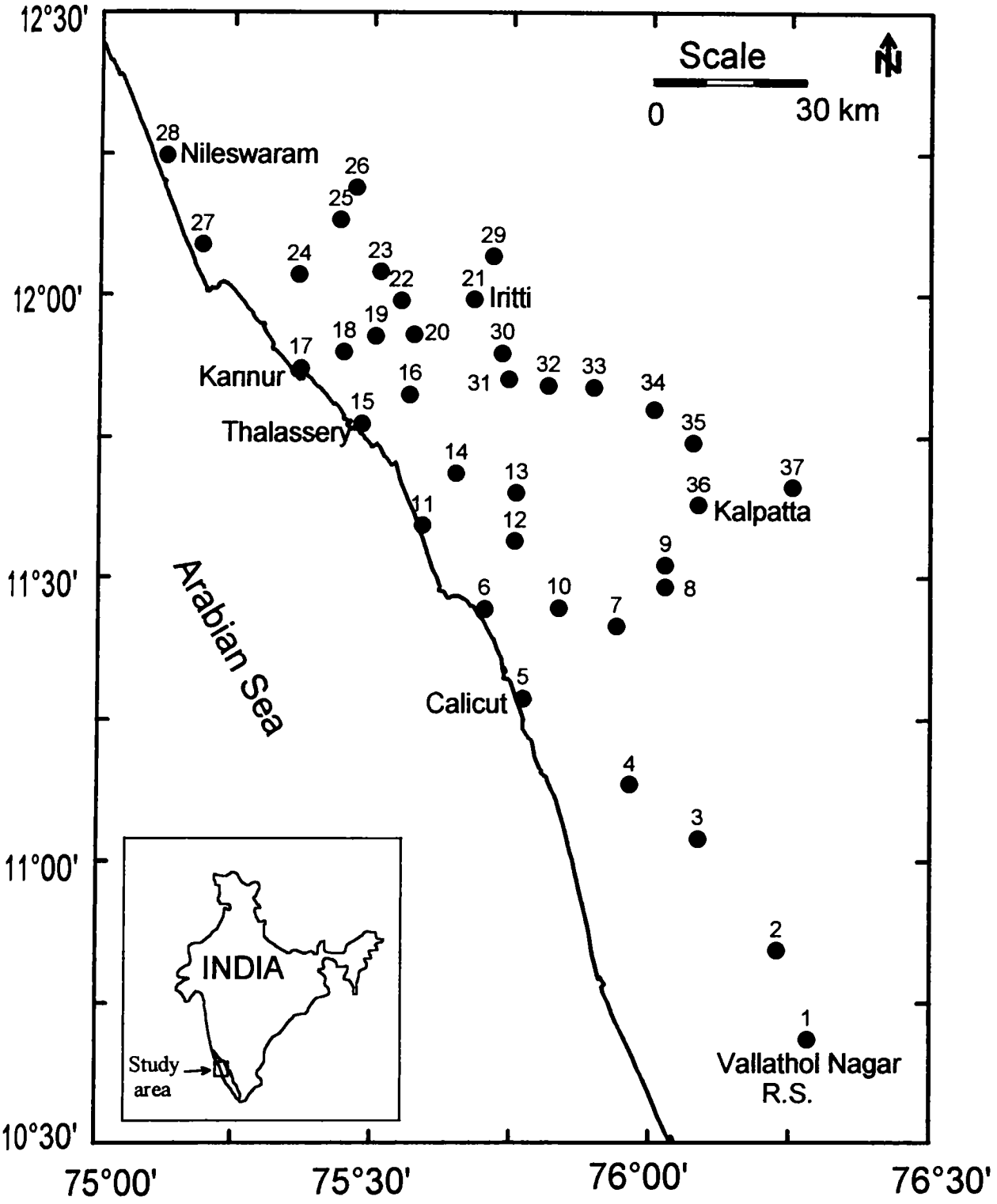


Fig 4.1. Map showing the distribution of permanent gravity bases established in the present study for the purpose o f gravity surveys in northern Kerala. The base station value at Vallathol Nagar RS established by Singh et al. (1985) has been carried forward for this purpose. Numbers refer to the serial number in sketches shown in Fig 4.2 to Fig 4.8.

stations(PS) etc. and also at some major road junctions. Detailed sketch of the locations of all the 36 new permanent base stations are given in Figs. 4.2 - 4.8

The base establishment and collection of intermediate stations were carried out in four phases of field work and with two types of gravimeters. The first phase was done with a Lacoste and Romberg gravimeter (model G-1042), having a worldwide range of 7000 mGals. A total of 16 base stations and around 100 gravity measurements were made with this instrument. The rest of the three phases of survey was conducted by a W.Sodin gravimeter (model no. 100) having a dial constant of 0.24 mGal/s.d borrowed from CEG, Osmania University. A set of twenty base stations were established apart from collecting more than 750 routine field station data using this instrument.

The gravity observations were made at an average interval of 1 km . These observations were taken along all major and motorable roads in the study area and selected to be at easily locatable points on toposheets such as kilometer stones on roads, road junctions etc. During the survey, importance was given to roads cutting geological structures and lithological boundaries and wherever necessary, observations were made at a closer spacing of 0.5 km. In areas far away from the shear zone, observations were made at 2 km interval. A total of 850 gravity measurements were made in the present study. Apart from this, nearly 100 gravity observations collected by various agencies

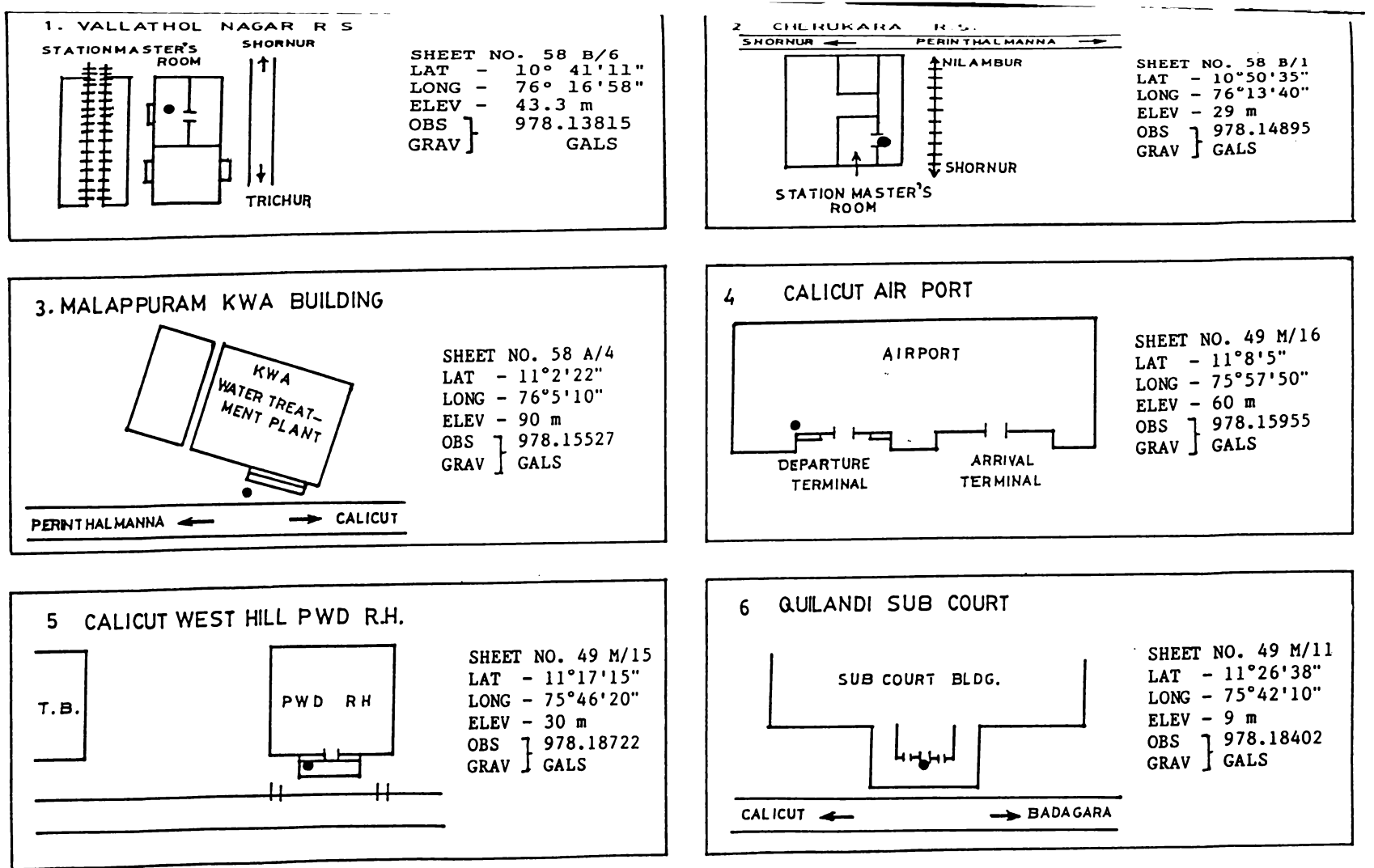


Fig. 4.2. Sketches showing location of six permanent base stations (nos. 1-6). Abbreviations and symbols used are shown in Fig .4.8.

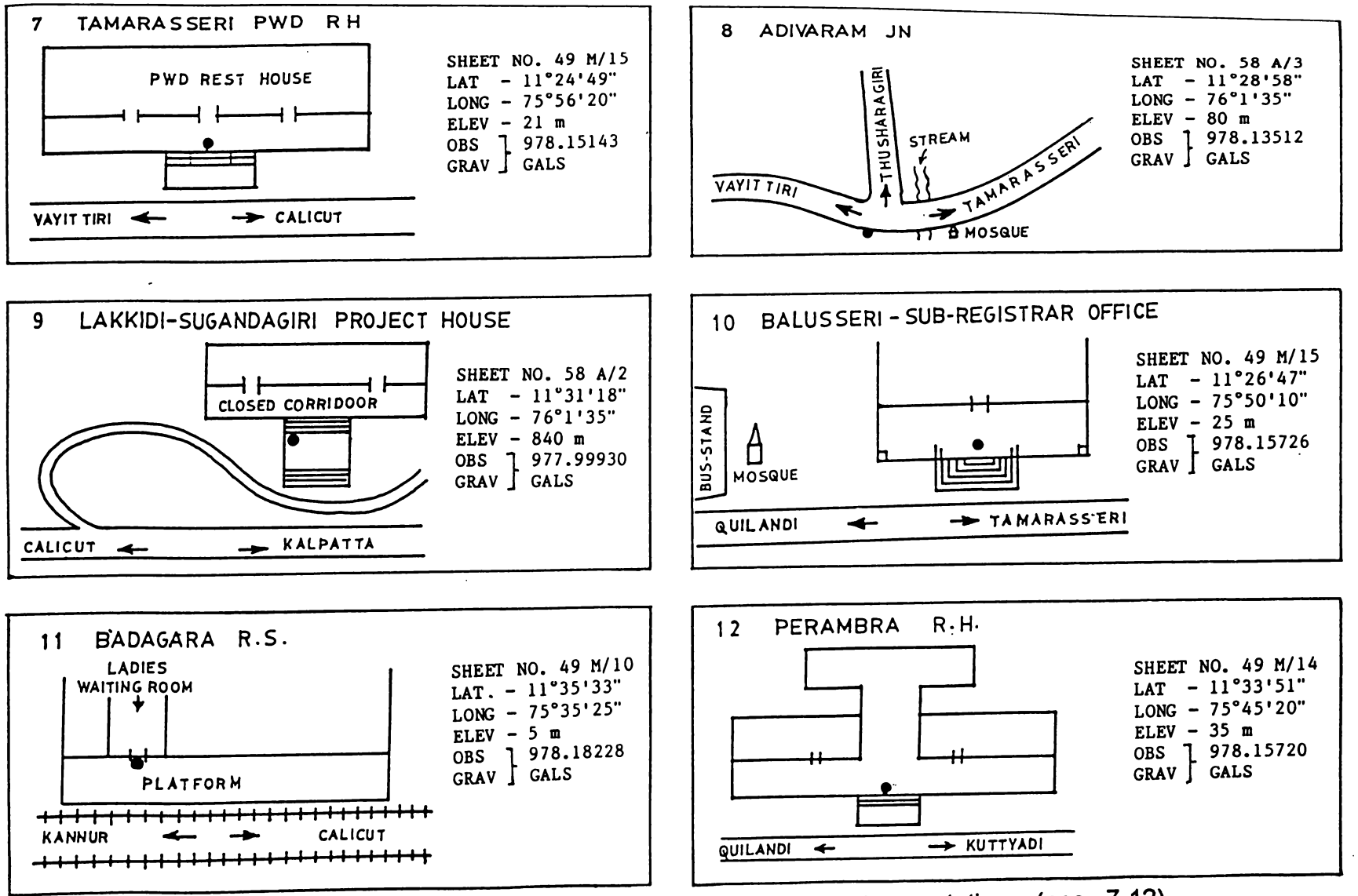


Fig. 4.3. Sketches showing location of six permanent base stations (nos. 7-12). Abbreviations and symbols used are shown in Fig .4.8.

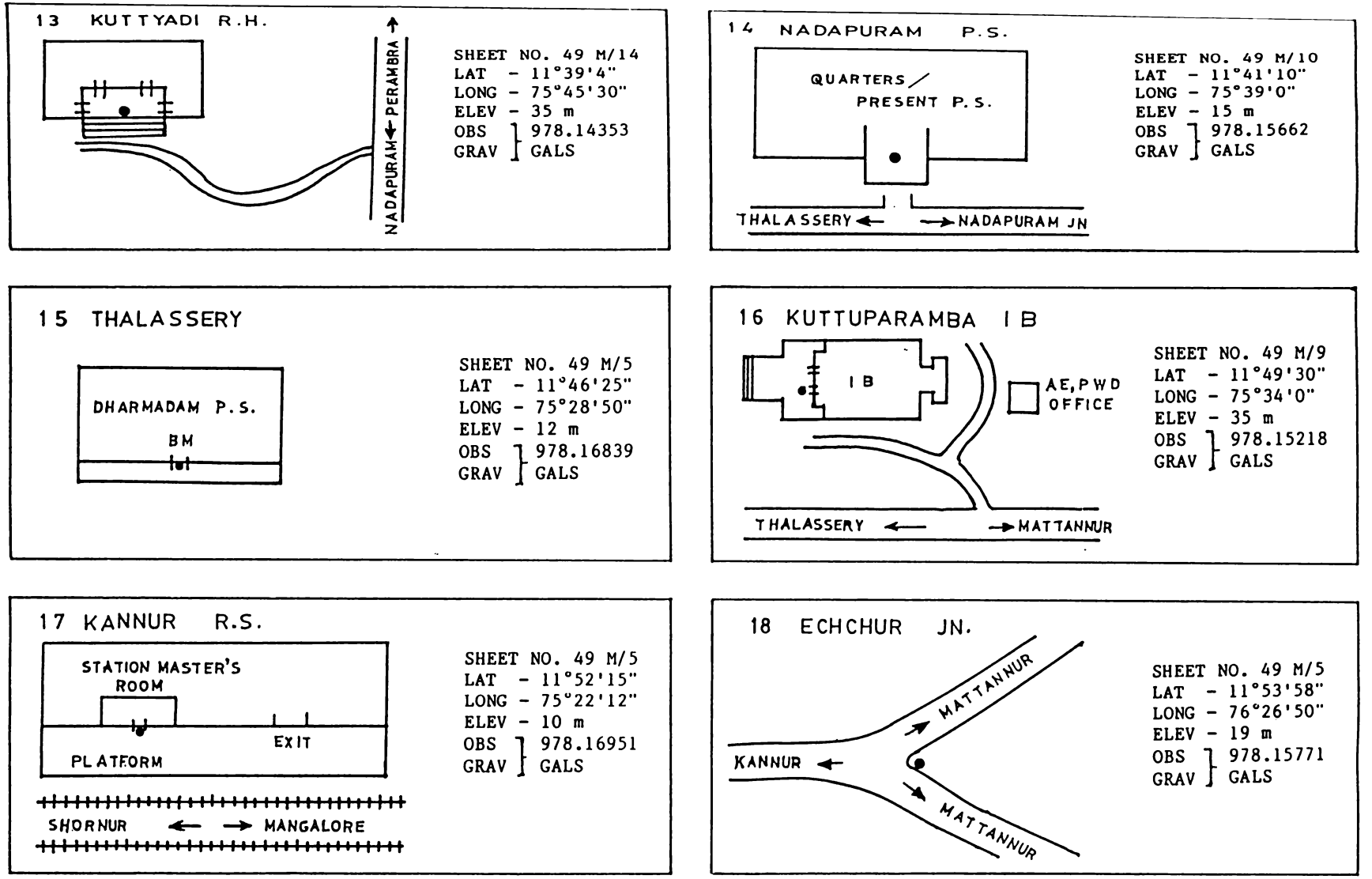


Fig. 4.4. Sketches showing location of six permanent base stations (nos. 13-18). Abbreviations and symbols used are shown in Fig .4.8.

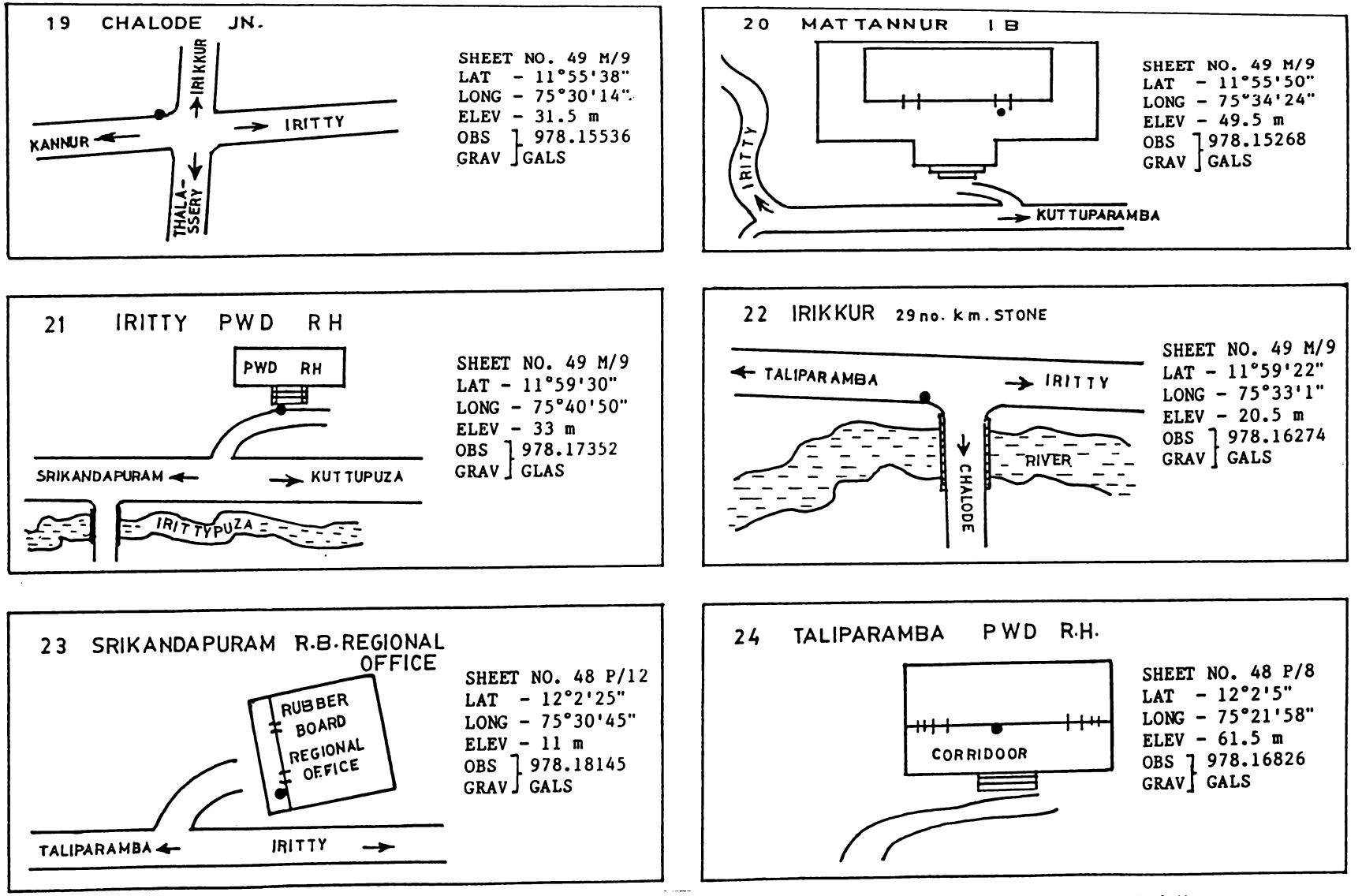


Fig. 4.5. Sketches showing location of six permanent base stations (nos. 19-24). Abbreviations and symbols used are shown in Fig .4.8.

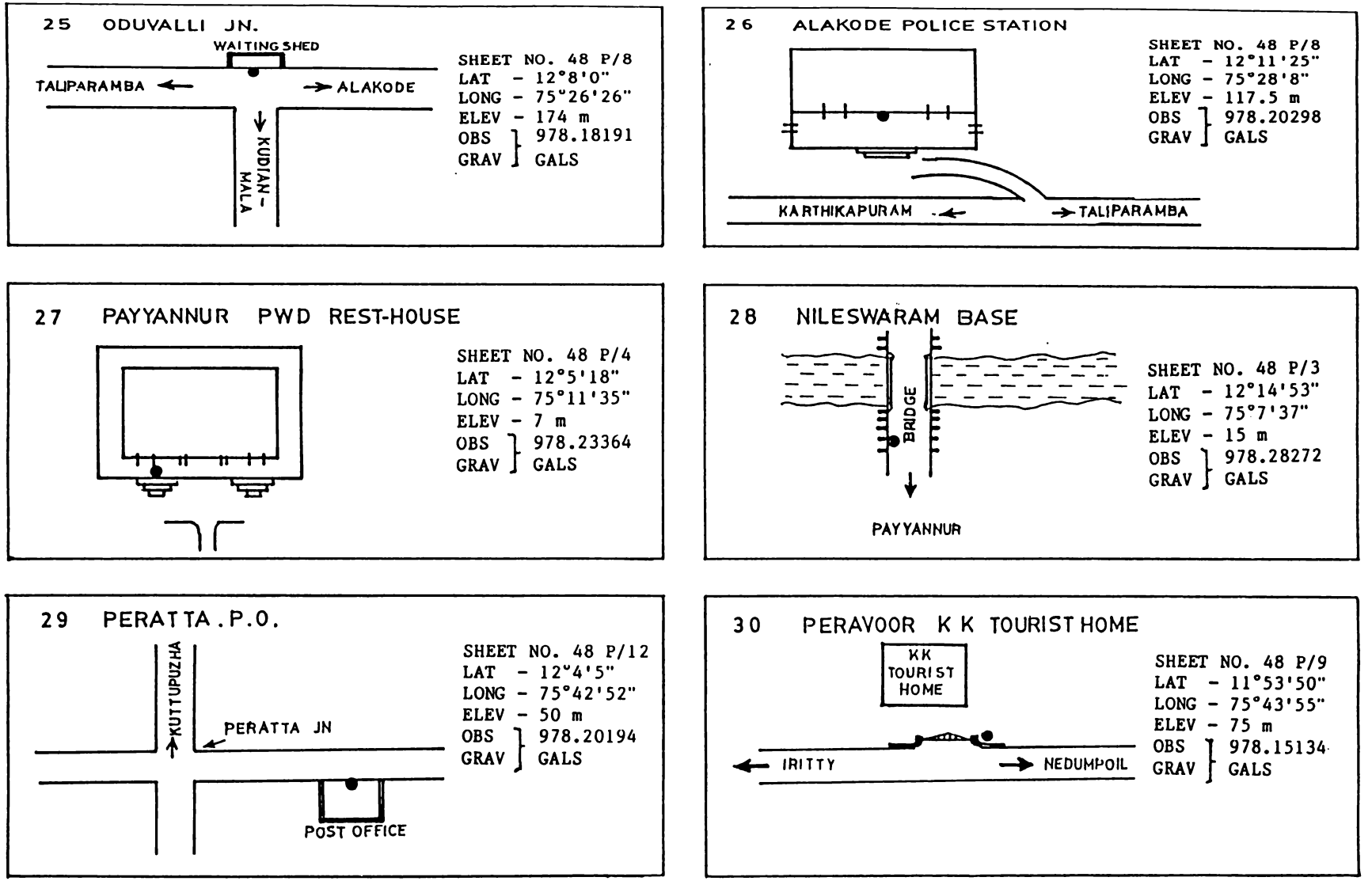


Fig. 4.6. Sketches showing location of six permanent base stations (nos. 25-30). Abbreviations and symbols used are shown in Fig .4.8.

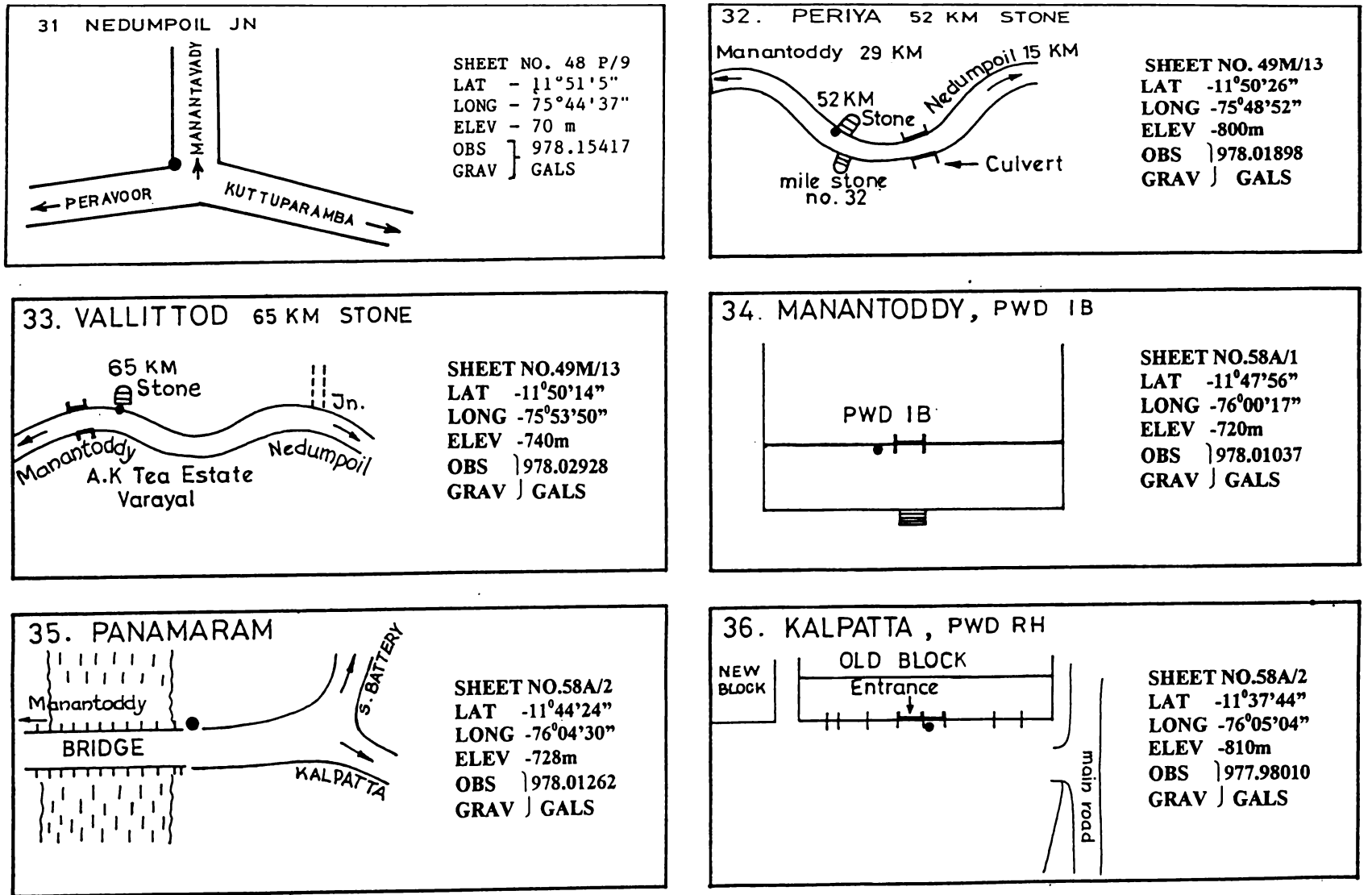


Fig. 4.7. Sketches showing location of six permanent base stations (nos. 31-36). Abbreviations and symbols used are shown in Fig .4.8.

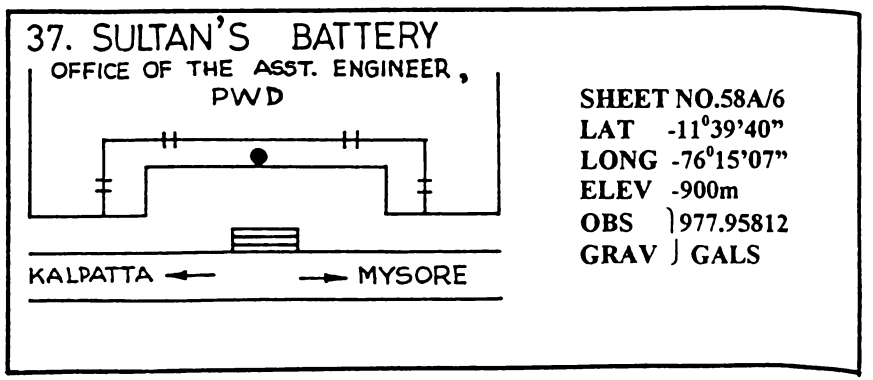


| | | | |
|---|---|---|---|
| ● | GRAVITY BASE | OBS GRAV | OBSERVED GRAVITY |
| ▭ | STEPS | | |
| ++++ | RAILWAY LINE | LAT | LATITUDE |
| RH. | REST HOUSE | LONG | LONGITUDE |
| IB. | INSPECTION BUNGLOW | ELEV | ELEVATION |
| P.S. | POLICE STATION | m | METRES |
| P.O. | POST OFFICE | R.S. | RAILWAY STATION |
| JN. | JUNCTION | BM | BENCH MARK |

Fig. 4.8. Sketch showing location of one permanent base station(no. 37). Abbreviations and symbols used for all stations are shown in the legend.

(see Table 4.1) are available in the region. These data were supplemented to the data collected in the present study mainly to fill the data gaps and to prepare composite gravity maps of the region. Fig 4.9 shows the gravity data distribution in the study region.

## 4.4 Altimeter Surveys

It is necessary to know elevation of the gravity station to make corrections for the observed gravity values. Hence altimeter survey was also conducted simultaneously with gravity survey using an American Paulin altimeter, having an accuracy of around 5 feet. These altimeter readings are correlated with toposheet elevation readings at the end of each day's field work. Wherever altimeter was not employed, elevations of spot-heights, benchmarks and topographic contours from the SOI toposheets were utilized.

## 4.5 Reduction of Gravity Data

Drift of the gravimeter is a thermo-elastic phenomenon associated with the quartz spring system of the gravimeter. Due to this effect, the reading of the gravimeter at any given place changes with time. A correction for the drift of the gravimeter is incorporated in the calculation considering that the effect is linear with time. In order to prepare the drift curve of the instrument, it is necessary to reoccupy the base station periodically during a gravity survey. The

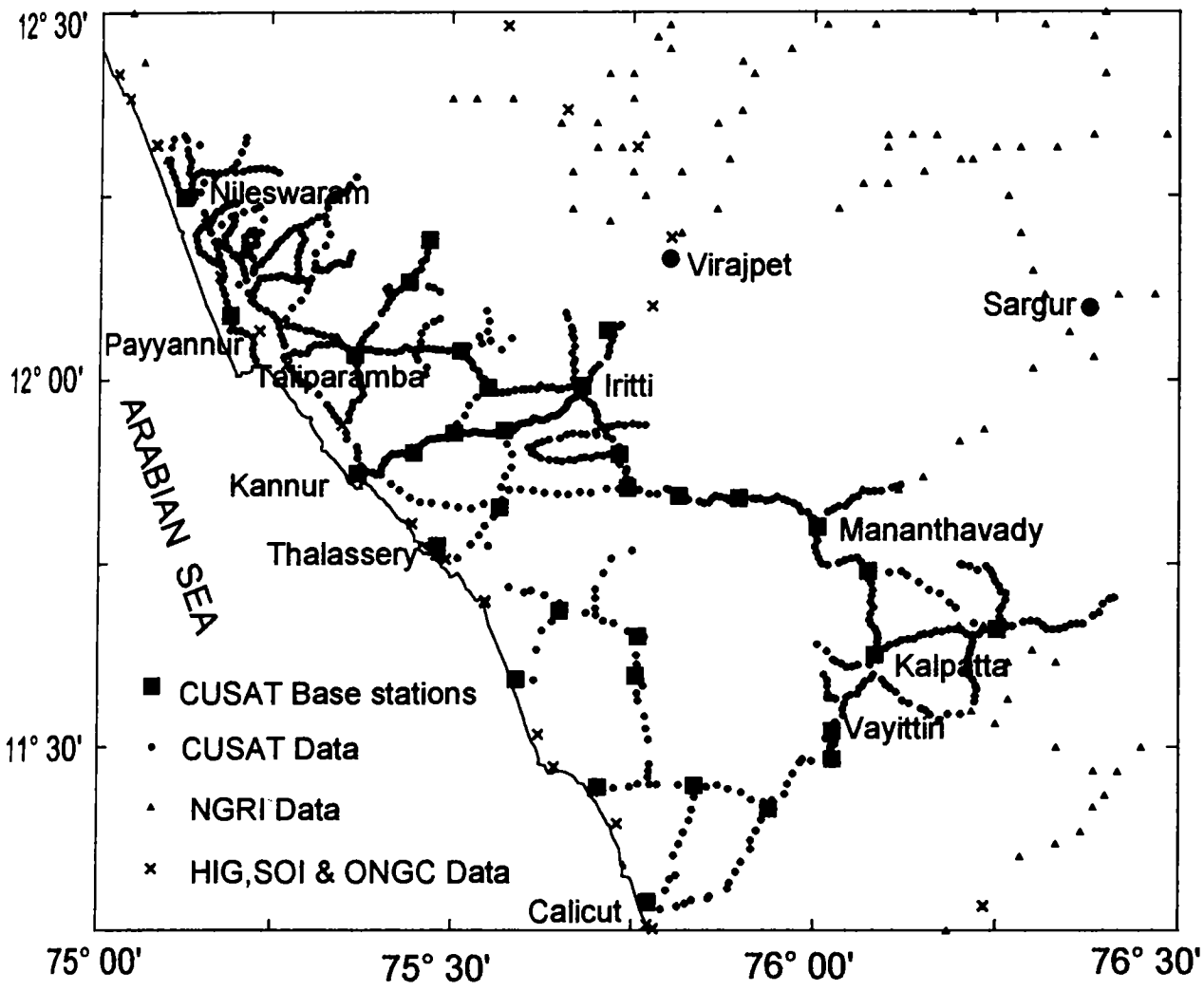


Fig 4.9 :Distribution of gravity stations utilized in the present study. The NGRI stations are from Qureshy et al.(1981) and the HIG, SOI and ONGC data are from Woollard et al. (1969).

maximum time allowable between base repetition would usually be less than 2 to 3 hours. The intermediate gravity stations, which are occupied between two base repetitions can then be corrected for the drift, by considering that the drift is linear with time.

In order to have an idea about the possible error in the assumption of linear drift, the dynamic drift rate of the gravimeter exhibited during the course of networking of base stations was calculated. Histograms for the number of base ties against the dynamic drift for the two phases were prepared (Fig. 4.10). In both the phases, it is seen that most of the drift values are falling below 0.006 mGal/min.

The end product of the gravity survey is a set of gravimeter readings and corresponding elevation values. After correcting readings for the drift of the gravimeter, observed gravity value at each field station is calculated by using the scale constant or the calibration table. This observed gravity value shows a point to point variation not only due to various anomalous sources in the crust which are of our interest, but also due to the earth's topography, centrifugal force of the earth, departure of the earth's shape from that of a sphere etc. Since our interest is only on the anomalous sources, a correction should be made for the other effects.

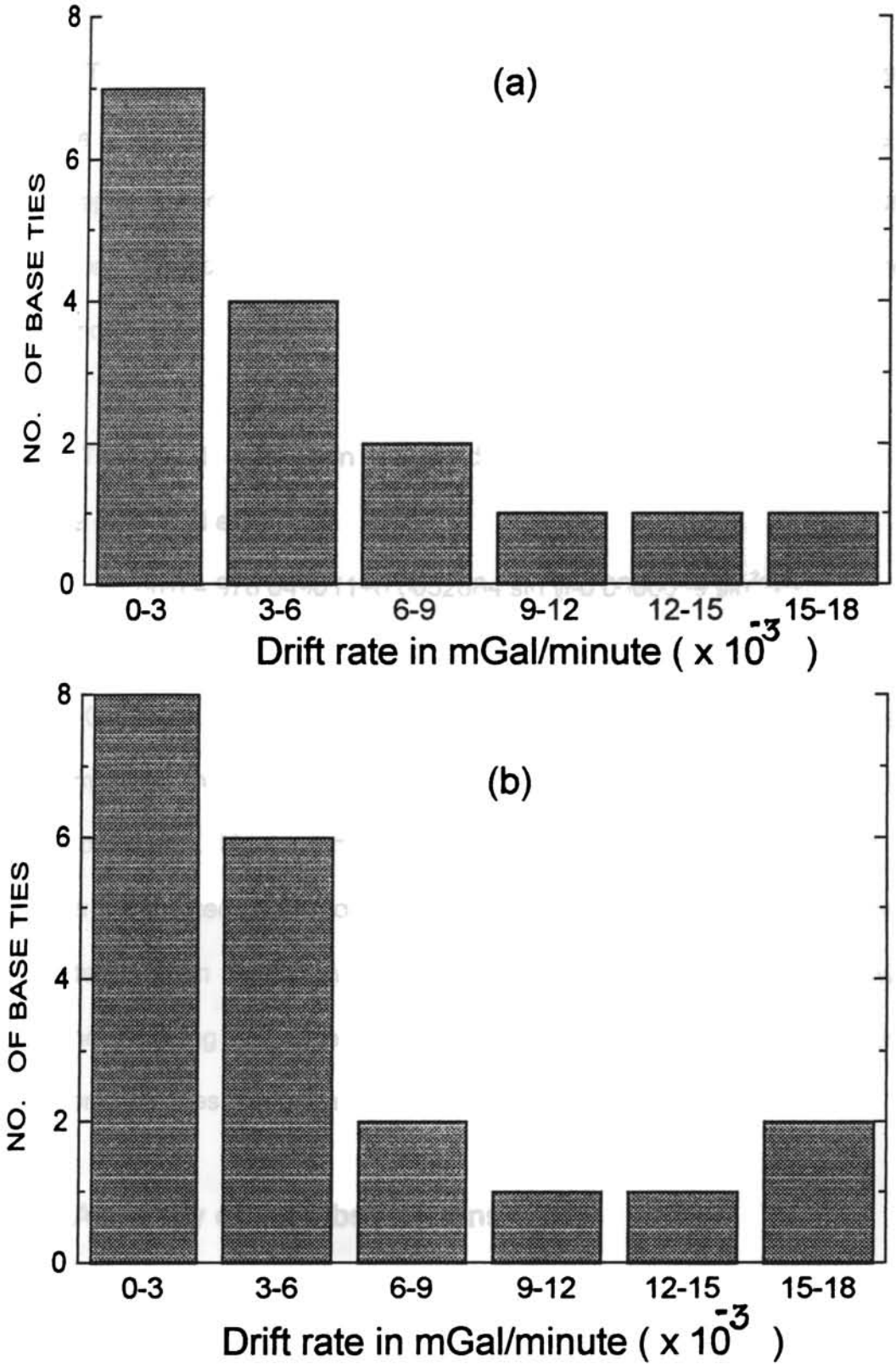


Fig. 4.10. Histograms showing the number of base ties against dynamic drift rate for (a) Lacoste & Romberg gravimeter and (b) W Sodin gravimeter.

The corrections that should be applied to raw gravity data are a) latitude or normal correction b) free-air correction c) Bouguer correction and d) topographic correction. Among these, the second and third being dependent on elevation, can be combined into a single term called the combined elevation correction.

The latitude correction was made based on the International Gravity formula of 1930 ; i.e.,

$$g(\varphi) = 978.0490\ (1+0.0052884\ \sin^2\varphi-0.0000059\ \sin^2 2\varphi)$$

Combined elevation correction was done using the standard density of 2.67 gm/cc for the surface rocks, which gives a correction factor of 0.19686 mGals per meter . No terrain correction was applied to the data as most of the stations are located away from any undulating topography of significance. A computer program written in 'C' language developed for reducing the raw field data incorporating all necessary corrections and to calculate free-air and Bouguer anomalies has been given as Appendix I.

## 4.6 Accuracy of the Observations

To obtain an idea on repeatability of these base values, the already established base at Mattannur during the first phase was reoccupied during the second phase. An observed gravity value of 978.15268 Gal was obtained in the

second phase whereas the value was 978.15260 Gal in the first phase giving a repeatability of 0.08 mGals . Hence, the base stations established in the present study are believed to be fairly accurate for conducting regional gravity surveys.

The major factors that could contribute to errors in the observed Bouguer anomaly are instrument reading errors , error due to drift, location errors and errors due to elevation . Shazina and Grushinsky(1971) gave a formula for estimating the accuracy of the observed Bouguer anomaly as

$$\varepsilon_{B.A.} = \pm[\varepsilon^2_{base} + \varepsilon^2_{h} + \varepsilon^2_{obs} + \varepsilon^2_{\phi} + \varepsilon^2_{terr} + \varepsilon^2_{\sigma}]^{1/2}$$

where

$\varepsilon_{base}$ - error in the base value

$\varepsilon_{h}$ - error in the elevation

$\varepsilon_{obs}$ - error in the observed gravity

$\varepsilon_{\phi}$ - error in the location

$\varepsilon_{terr}$ - error in the terrain correction

$\varepsilon^2_{\sigma}$ - error in the surface rock density

It has been observed from the dynamic drift for base repetitions (Fig. 4.10) that most of the drift values fall below 0.006 mGal/min. Survey of India toposheets were used to locate stations. Except at the bench marks, the locations could have a shift of 6" arc length. This would result in an error of 0.06 mGal due to location uncertainties at these latitudes. For an average density value of 2.67 gm/cc, the combined elevation correction factor comes up to

0.196 mGal/meter. The bench marks and spot height data are very accurate. However, altimeter data and interpolated elevation from topographic contours give rise to a maximum possible error of 2 to 3 meters in the plain areas of low as well as high lands where elevation is uniform and 4 to 5 meters in the hilly ghat regions. Since very few stations are located in the ghat sections, the maximum average error in elevation is considered as 3 meters. This could give rise to an error of 0.5 mGal in the Bouguer anomaly. For estimating errors due in the observed gravity, it is customary to repeat at least 10 - 15 % of the gravity readings. Since the study region is very large and average station spacing is around 1 km, the station points often could not be reoccupied. However, this factor is very low and not very significant in the present study. As mentioned earlier, no terrain correction was applied to the data. The error in density estimate can be considered as 0.07 gm/cc taking the average density of dominant surface rocks (charnockite and gneiss) as 2.74 gm/cc. For an average elevation of 300 m for all the measuring points, this error would give rise to an error of 0.87 mGal in the anomaly. All these error factors combinedly have been used to calculate the maximum error in Bouguer anomaly based on the above mentioned formula which give rise to an error of less than 1 mgal.

## 4.7 Regional- Residual Separation

Bouguer anomalies obtained after applying the various corrections described above is, in fact, due to the total effect of the various disturbances

lying at several depths below the ground surface. The smaller local disturbances or noise at very shallow depths can be smoothed out easily on the map. The noise free anomalies are mainly due to two components namely regional and residual. Regional anomalies are usually due to structures at greater depths and hence exhibit broad and uniform variation. The residual anomalies which are due to sources of our interest (local sources) should be separated from the regional anomalies.

The terms regionals and residuals are relative in their meaning. Regional – residual separation is thus ambiguous since the separation can be done in an infinite number of ways. However, based on the assumption that the regional is broad and uniformly varying and on the basis of the known geology and other factors, the interpreter can decide and go for the best method. A brief review of some important methods of regional-residual separation are discussed here. They are 1) Graphical method 2) Least-square method 3)Grid method 4) Fourier analysis 5)Finite element method.

### 4.7.1. Graphical Method

In the graphical or smoothing method, smooth and undisturbed parts of the anomaly profiles are joined by smooth curves and are considered as regionals by giving due weightage to the known geological data. Difference between the observed and regional anomalies are considered as residual. Two

variations of these methods have been developed. In the first, profiles in two mutually perpendicular directions are chosen so that two values of regional anomaly are obtained at each point. The smoothing exercise is repeated until the same values are obtained for regional at all intersecting points. In the second method, the contour map itself is smoothed for the regional. If the contours exhibit a uniform curvature over sufficient lengths, the portions of uniform curvatures are joined for the contours of the regional anomaly. At all the points where these regional anomaly contours cut the observed, residual is calculated as the difference between the two. Graphical anomalies are fairly accurate if good geological information is available and if anomalies are collected over wider areas. However, in the case of several overlapping anomalies and if the residuals are completely masked by strong regionals, graphical method will become non-operative.

### 4.7.2. Least-square Method.

In the least-square method, the gravity anomalies are assumed to vary systematically according to a mathematical expression. Regional can be represented by a surface of a chosen order defined by a polynomial with terms containing the coordinates of anomaly points (Murthy, 1998). If x denotes the horizontal position on a gravity profile, the regional gravity $\Delta g_R$ may be written as

$$\Delta g_R = \Delta g_o + \Delta g_1 x + \Delta g_2 x^2 + \Delta g_3 x^3 + \ldots\ldots\ldots + \Delta g_n x^n$$

The surface is fitted to the observed anomalies in the least-square sense and the departures of observed anomalies from the best fitting least-square surface are taken as residual. The method has some drawbacks. The least square residuals are truncated in magnitude compared to the true ones and contain several pseudo anomalies bordering each high and low. However, it is a popular automatic method and can be routinely adopted some times to supplement the regional obtained from other methods.

### 4.7.3. Grid Method

In this method, when very little is known about the subsurface, the regional at a point is assumed to be represented by the weighed mean of the observations around that point. This method is very useful when the grid spacing and the coefficients are chosen according to the depth and extent of the sources whose effects are to be identical. When the observations are available at the corners of a regular square grid, anomalies at the discrete gridded points on the periphery of the circle are averaged and subtracted from the central value. Mathematically, the grid residual $\Delta g_R$ at the point of computation can be written as

$\Delta g_R = \Delta g - \overline{\Delta g(r)}$ , where

$\Delta g$ is the gravity anomaly at the point of calculation, ie; center and $\Delta g(r)$ is the average of the gravity anomalies along the circumference of the circle. Woollard (1969) suggested nine point method, ie; for a square of two grid

units, the regional can be considered as the average of nine anomalies, eight on the periphery and one at the center of the square. This method is more mechanical, computer adaptable and devoid of any personal judgement.

Other analytical techniques broadly falling under grid methods are second derivatives and continuation methods. While, higher vertical derivative values magnify the influence of the shallow local features suppressing the regional, the method of continuation magnify the influence of local or regional suppressing the other depending on downward or upward respectively. However, residuals obtained by any of these methods can not be subjected to quantitative interpretation.

### 4.7.4. Fourier Analysis

Any periodic function can be mathematically represented by a Fourier series of sine and cosine terms of a fundamental frequency and their harmonics (Bhattacharya, 1965). If $\Delta g(x)$ is the gravity anomaly and $\lambda$ the wavewlength, the expression

$$\Delta g(x) = \sum_{n=1}^{N} (a_n \cos 2n\Pi x/\lambda + b_n \sin 2n\Pi x/\lambda)$$

is called a Fourier series, where $a_n$ and $b_n$ are constants and N is the number of terms. The Fourier sum of individual terms is replaced by a Fourier integral used to represent non-periodic function such as

$$\Delta g(x) = \int_{-\infty}^{\infty} G(u)\ e^{iux}\, du \qquad \text{where}$$

$$G(u) = 1/2\Pi \int_{-\infty}^{\infty} \Delta g(x)\, e^{-iux}\, dx$$

G(u) is Fourier transform of $\Delta g(x)$ and efficient computer algorithms are available for rapid computation of Fourier transforms in the literature. Spector and Grant(1970) and Treitel et al.(1971) gave methods of calculating depths of anomalous sources from the Fourier spectra of the potential field data. The Fourier method is also useful for preparation of filtered maps. The method is faster, computer oriented and effective. However, the calculated spectra are associated with errors due to finite data size and considerable care should be taken for any quantitative interpretation of these results.

### 4.7.5. Finite Element Technique

The finite element technique has been used by Mallick (1991) and Mallick and Sharma(1997) to compute regional gravity anomalies. The method is based on the concept and properties of the element shape functions used in finite element analysis (FEA). In the solution of differential equations by FEA, the continuous field variables at any point in the element – linear, quadratic or cubic are expressed as a weighed sum of the discrete nodal values, gI in the form of

$$g(x,y) = \Sigma\, Ni\, ((x,y)\, gi \quad , I=1,2,3,.....,r.$$

where Ni(x,y) are the shape functions acting as weighting factors and r is the number of nodes in the element. g(x,y) represent the regional field. The method is very effective as evidenced by several case studies (Mallick and

Sharma, 1997; Mallick and Vasanthi, 2000). However, the accuracy of this technique mainly depends on a)the optimum choice of the reference element so that the survey area is fully taken care of b)the choice of nodal positions, which is very important as Bouguer gravity values at these nodes approximate the regional.

In the present study, the regional-residual separation is carried out mainly by graphical method. This method has been employed because the gravity field in the area is found to be strongly influenced by the underlying geology. The least-square method also has been used in certain cases to aid the graphical regional. The nine-point average method given by Woollard (1969) has been used to prepare free-air, Bouguer and elevation (spatial filtered) maps at different grid levels of 1/8°x1/8° and 1/4°x 1/4° for comparison and to obtain a qualitative picture of the anomalous sources.

*Chapter V*

# The Gravity Anomalies and Elevation Maps – A Qualitative Analysis

## 5.1 Introduction

The gravity anomaly map is an important tool to understand the spatial variations of the gravity field and its correlation with the surface and subsurface geology. Free-air and Bouguer anomalies address different aspects of the deep structures of an area. By a qualitative analysis of the trend, amplitude and wavelength of these anomalies, inferences on subsurface mass distribution can be made. The present study brings out the relationship of broad geological features of the gravity field in more detail than that available for the region from previous studies (Krishna Brahmam and Kanungo, 1976; Subba Rao, 1988; Krishna Brahmam, 1993). The observed gravity field is discussed in relation to the geological features and inferences are drawn on the presence of anomalous masses in the crust, their extent and possible depth of occurrence.

Elevation map was prepared based on the altimeter data and spot heights, bench-marks and digitized topographic data from Survey of India (SOI) toposheets (Fig.5.1). Based on nearly 850 gravity observations generated during the present study and also utilizing the data generated by other organizations totaling to about 1000 stations, the free-air and Bouguer anomaly maps were prepared and are presented in Fig 5.2 and Fig 5.3 respectively. The maps prepared cover the area between 11°15'N to 12°30'N latitudes and 75°E to 76°30'E longitudes.

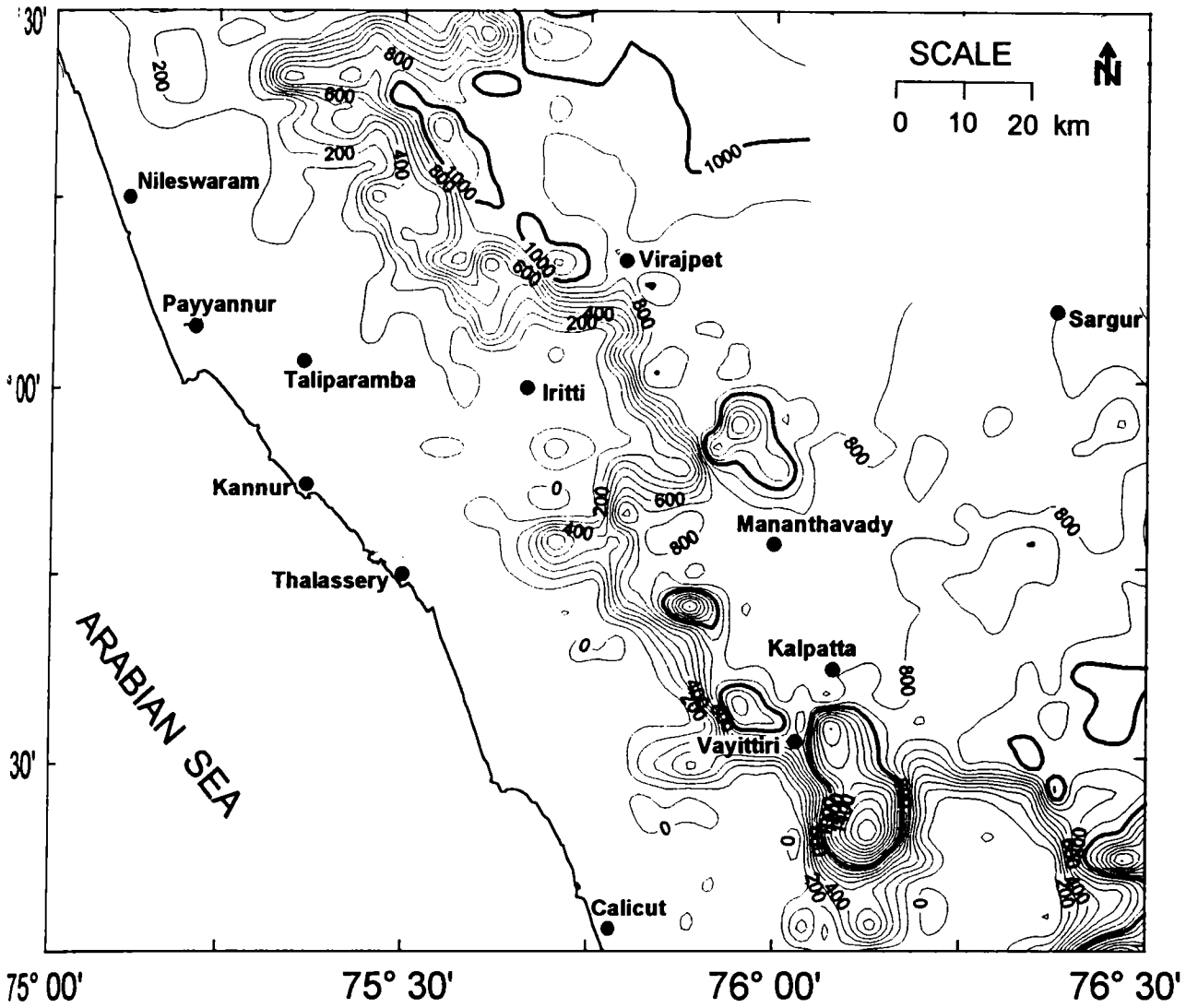


Fig 5.1. Elevation map of the northern Kerala region based on bench mark and spot height data from Survey of India topographic maps (1: 50000) and the altimeter measurements along gravity traverses. Contour interval 100 meters.

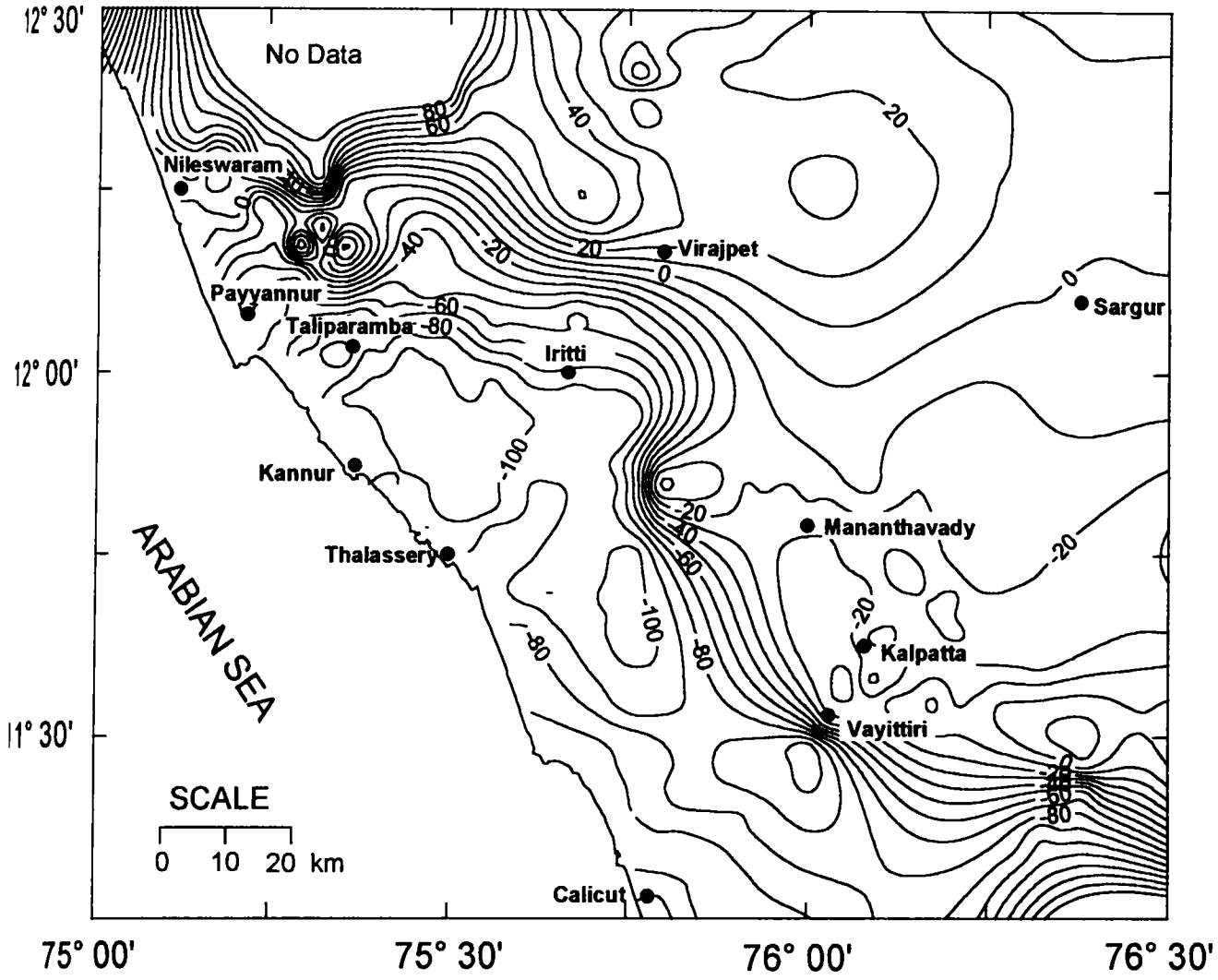


Fig 5.2 . Free-air anomaly map of the Bavali Shear zone and adjoining regions. Contour interval 10 mGals. Though the original data permits a 5 mGal contour interval, 10 mGal contour interval is chosen to avoid overcrowding especially along steep gradients.

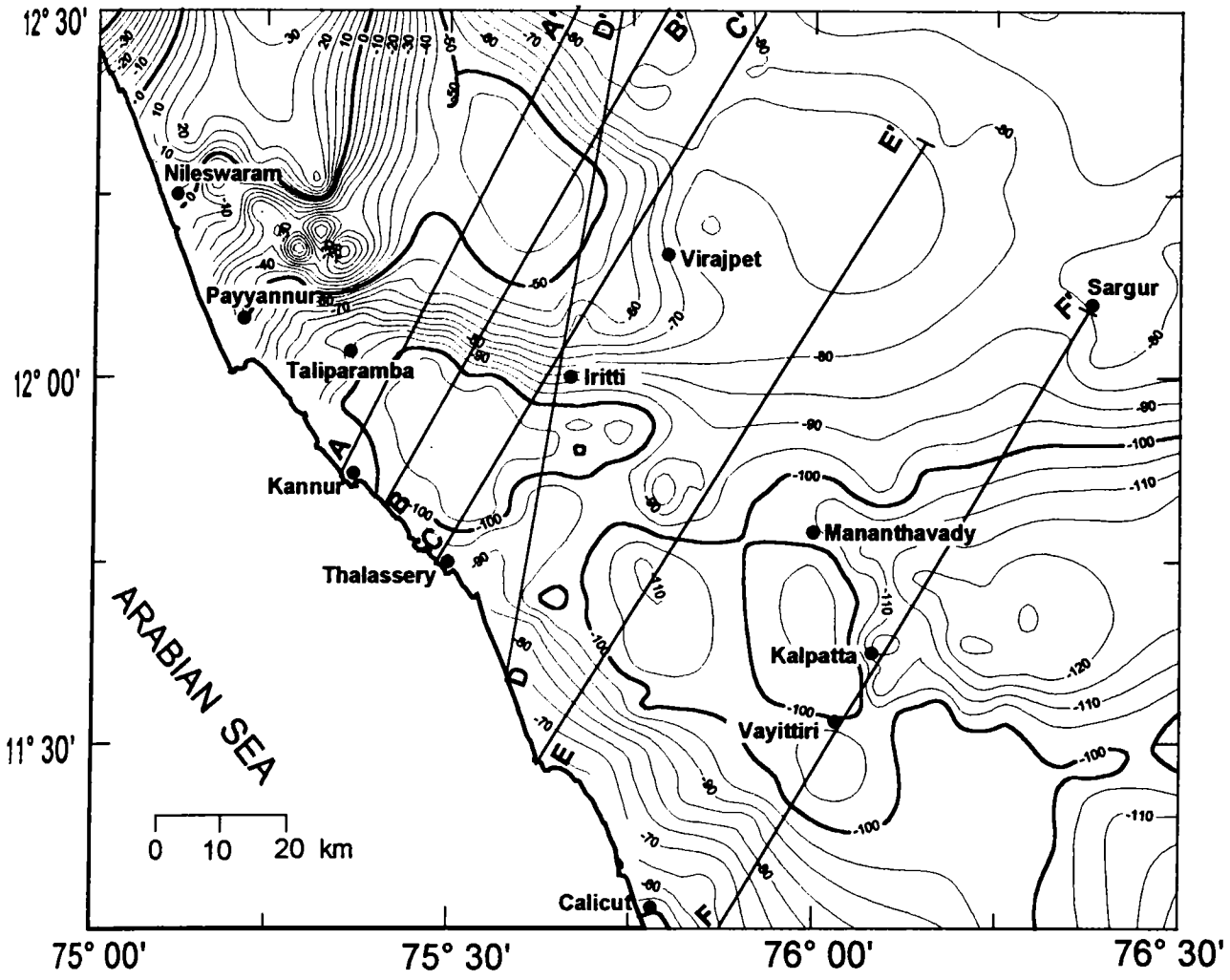


Fig 5.3. Bouguer anomaly map of the Bavali shear zone and adjoining regions. Contour interval 5 mGals. Lines AA' through FF' represent profiles selected for 2-d modeling.

## 5.2 Elevation Map

The NNW-SSE trending Western Ghats is the major topographic feature in the region. In the western portion of the map, the coastal plain and lowlands lie below 100m elevation and constitute more than 25% of the area. The Western Ghats pass through the central portion of the map, where elevation sharply rises from 100 m to as much as 800-1000m with several isolated topographic peaks touching maximum heights of 1500m at a few places along the Ghats. Further east, the highlands have an uniform average elevation of 800-1000m. It can be seen from the map that at around 11°50' latitude and 75°50' longitude, between Mananthavady and Iritti, the Western Ghats trend has been offset eastward by approximately 20 km

## 5.3 Free-air Anomaly Map

The free-air is the simplest type of anomaly as no assumptions are made about the surface rock densities. Since the attraction of mass above the datum remains in-built in the free-air anomaly, the increase in elevation partly gives rise to more positive values. However, it is significant in that, the average free-air anomaly value over an area approximately equals the isostatic value and therefore, is related to deeper features. Thus, the effect of surface and crustal masses as well as crust-mantle boundary contribute to the free-air anomaly.

The free-air anomaly map prepared in 10 mGal interval for the study region (Fig 5.2) shows strong correlation with the elevation map. The anomaly values, in general, range from +80 to –100 mGal in the region. The map shows positive free-air anomalies ranging between +20 to +80 mGal in the area north of Nileswaram, Virajpet and Sargur; a low anomaly of -120 mGal in the Wynad plateau south of Sargur and a series of gravity lows characterized by –100 mGal anomaly contours extending southward from Taliparamba to south of Vayttiri. Further west of these lows, the free-air anomalies tend to be more positive and the values increase from –80 mGal to –50 mGal towards the coast. The most prominent feature on the map is a sharp gradient anomaly zone with the values increasing from –80 mGal in the plains to –20 mGal in the high ranges with an average gradient of 4 to 5 mGal per kilometer coinciding with the Western Ghat trend. This sharp gradient zone, follows the topographic trend and takes an E-W curvilinear trend marked by a rise in anomalies from –90 mGal to as much as –40 mGal towards the coast between Iritti and Payyannur through Taliparamba. This E-W trending zone occurs over plain areas and coincides with the gneiss-charnockite boundary. Such an increase in free-air anomalies over a plain topography may be attributed to subsurface mass heterogeneities along the gneiss-charnockite boundary. The map further shows that the charnockite region north of the shear zone extending from the coast up to Virajpet in the NW portion (Fig. 2.2) is associated with large free-air anomaly high ranging from –40 to +80 mGal. it is observed that within this broad high, in the Perinthatta region (latt.

12°10' N and long. 75°20'E) three small positive anomaly closures of 10 to 20 mGal amplitude coincide with the Perinthatta anorthosite massif.

## 5.4 Bouguer Anomaly Map

Under the general assumption that no lateral inhomogeneities exist below the Moho, the Bouguer anomalies would generally reflect the variation in the crustal thickness, the intra-crustal structures and lithologic changes within the crust, the near surface geological structures and changes in surface geology. The Bouguer anomaly map prepared in 5 mGal interval (Fig 5.3) shows some major trends as follows.

- an E-W trending gravity gradient zone extending from Payyannur to Iritti characterized by a sharp gradient of 3.0 mGal/km. across the shear zone. This zone extends further east of Iritti but has a wide and gentle gradient of 0.4 mGal/km.
- a broad gravity low with a relief of 20 mGal in the Wynad plateau east of Kalpatta and Mananthavady
- series of gravity lows characterized by –105 mGal contour starting from east of Kannur region and extending up to south of Vayttiri. The anomalies are seen to increase from –100 mGal to –60 mGal towards the coast between Calicut and Thalasseri.
- a broad gravity high increasing from –70 to –40 mGal in the north-west portion of the map can be correlated with the charnockite body north of the

shear zone. This high further increases up to +20 mGal towards the coast near Nileswaram.

- three positive closures with a relief of 10 mGal coincide with the Perinthatta anorthosite which is situated within the northern charnockite province.

## 5.5 Correlation of Various Anomalies – A Qualitative Analysis

The Bouguer anomaly map when correlated with the surface geology, free-air anomalies, elevation and rock density data leads to some important inferences regarding the subsurface mass distribution.

The E-W gradient zone seen on the Bouguer anomaly map coincides with the gneiss-charnockite boundary west of Iritti where both free-air and Bouguer anomalies sharply increase northward across the boundary. However, east of Iritti, this gradient zone falls within the gneiss-schist province and has a gentle gradient in the anomalies. While the former occurs in the coastal lowlands, the latter is seen on the Wynad plateau region. Further, the high gradient west of Iritti is circumfering the charnockite in the NW part of the region giving rise to a broad Bouguer anomaly high. The northern charnockite province which has mafic granulite and anorthosite occurrences is also characterized by free-air high. It is also associated with an isostatic anomaly high in the published NGRI map (NGRI, 1978). Though the surface rock densities estimated (presented in chapter III) for charnockites (2.76 gm/cc) is higher than for gneissic rocks (2.73 gm/.cc), this density contrast alone would not be sufficient to explain the

observed gravity high over the charnockite body. The Perinthatta anorthosite massif located within the charnockite province gives rise to three small positive closures on both free-air and Bouguer anomaly maps. These localized positive closures indicate that the anomalies may arise from slightly higher density anorthosite (2.77 gm/cc) or its mafic cumulates at shallow depths. In view of this interesting anomaly pattern, the region has been subjected to detailed analysis as given in chapter VII. The E-W gravity gradient zone as well as the broad gravity high encircling the high grade charnockite terrain together may indicate, a regional rise in crust-mantle boundary, presence of high density gabbroic masses in the lower crust, variations in thickness of upper crust or a combination of some of these features. Krishna Brahmam (1993) inferred ultrabasic gabbroic rocks below the region.

The region south of the schist-gneiss province is characterized by series of free-air and Bouguer anomaly lows. East of Kannur, the gravity low coincides with the area of Vengad basin in which quartz-mica schists and quartzites occur. The low densities of these formations may partly or wholly account for the gravity low. However, further south up to the area south of Vayttiri, the gravity lows coincide with the steep south-east slopes of Wynad plateau. Minor faults/ shears have been reported in this region by GSI(1995) (see figure 2.2). It is possible that the gravity lows may be due to faulting or dislocation in the upper crust.

The coastward positive gravity gradient observed between Calicut and Thalasseri was also noticed at many places along the West Coast by several workers and has been explained as due to crustal upwarp or localized thinning of the crust (Qureshy, 1981; Chandrasekaram, 1985; Mishra, 1989). However, north of Thalasseri, the gravity anomalies in the coast indicate that such thinning in the region is either absent or is masked by anomalies due to upper crustal inhomogeneities. The map also shows a broad gravity low east of Kalpatta and Mananthavady in the Wynad plateau region. Krishna Brahmam and Kanungo (1976) inferred that the gravity low could be due to buried granite intrusion. Though the region is characterized by the presence of Kalpatta and Ambalavayal granite bodies, which are small in dimension, the observed low require very large scale emplacement of granite at depth. To check the areal extent , shape and depth of the Kalpatta granite, a detailed analysis of the gravity field is carried out over the Kalpatta granite and adjacent areas as presented in chapter VIII.

In order to ascertain the gravity anomaly trends and depth as well as areal extent of various anomalous subsurface masses in the region, average maps at various grid levels have been prepared and their relation with average elevation has been analyzed as discussed below.

## 5.6 Anomaly-Elevation Relationship

The gravity field in any region depends on several factors such as crustal thickness, mean crustal density, mean surface elevation and density inhomogeneties in the upper mantle besides the density changes in the near surface/subsurface lithology. The nature of isostatic compensation and the geological history of the area also influences the gravity field. It is fairly well established from seismic refraction data that as the elevation increases, the crustal thickness also increases as required by the Airy's isostatic compensation.

Bouguer anomalies generally show inverse relationship with elevation, as the calculation of Bouguer anomalies do not take into account the root formation under elevated areas. Woollard(1959) presented a graph showing the correlation between average Bouguer anomaly and average elevation on the basis of world wide data and his study reveals that the anomaly-elevation relationship is different for several parts of the world. Many previous workers studied the anomaly-elevation relationship in different regions of the world including the Indian sub-continent (Woollard, 1959; Qureshy, 1963; Woollard, 1969; 1970; Qureshy, 1971; Verma and Mukhopadhyay, 1976; Verma et al., 1984). In the isostatically compensated regions, the Bouguer anomalies vary linearly with elevation with the coefficient of regression equal to –112 mGal/km if the density of rock column above mean sea level is considered as 2.67 gm/cc (Qureshy, 1971).

In order to understand the relationship between Bouguer and free-air anomalies with elevation, average maps for free-air and Bouguer anomalies and elevation data for the area under study have been prepared. The map was divided into 1/8°x 1/8° , 1/4°x1/4° and 1/2°x1/2° grid size and the average value for a particular grid level was computed using nine point average method of Woollard (1969).

### 5.6.1 Relationship for 1/8°x1/8° Areas

The free-air, Bouguer and elevation contour maps prepared based on the $1/8^0$x$1/8^0$ averaged values are shown in Fig. 5.4. As mentioned earlier, the average elevation map (Fig 5.4 (a)) reflects the regional trend of the Western Ghats. The map shows slightly broader topography and several minor peaks seen in Fig.5.1 are absent. The coastal areas are characterized by low elevations of 50-200m, while elevations of 800-900m are observed over the Wynad plateau region. A strong correlation can be seen between free-air anomalies and elevation. The free-air anomaly map (Fig 5.4(b)) shows broad low around Kannur and Thalasseri coinciding with the Vengad basin which is seen to be extending southward. A minor free-air high is seen centered around Nileswaram. The 1/8°x 1/8° average BA map (Fig 5.4(c)) reflects slightly smoothed broader wavelength anomalies herein named, such as;

1) Coastward gravity gradient towards Nileswaram leading to strong positive anomalies towards the coast close to Nileswaram , the Nileswaram Gravity High (NGH)

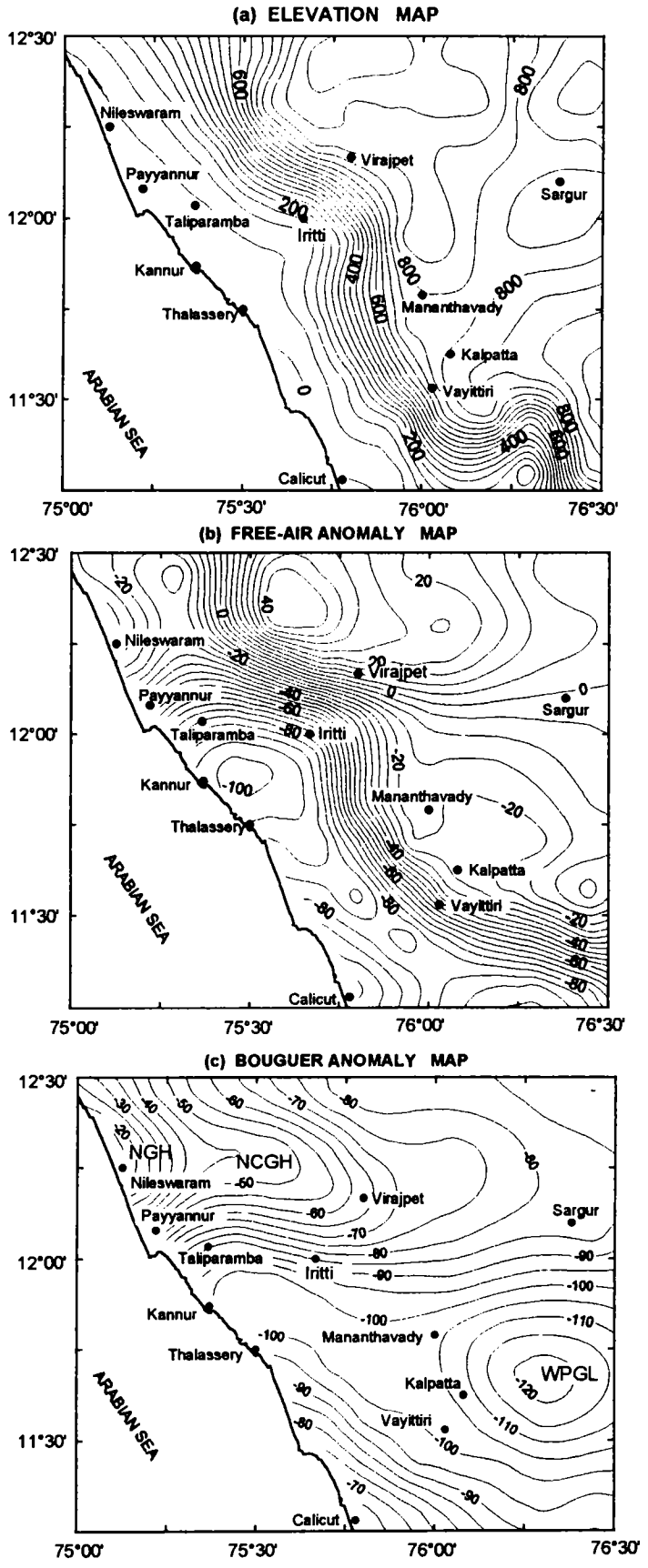


Fig 5.4. The contour map of average values for 1/8°x1/8° grid areas of the study area.

2) A gravity low with a relief of –20 mGal centered over the Wynad plateau, Wynad plateau gravity low (WPGL).
3) Elliptically trending contours showing a gravity high almost circumfering the northern charnockite body, the Northern Charnockite Gravity High (NCGH).
4) E-W trending gravity gradient almost following the Bavali shear zone

Also, it is interesting to note that the three localized closures coinciding with the Perinthatta anorthosite have been smoothed out on the map suggesting that the anorthosite bodies extend only to shallow depths.

The 1/8°x 1/8° average free-air and Bouguer anomaly values have been plotted against elevation as shown in Fig. 5.5. The scatter plot indicates that the free-air anomalies bear a positive correlation with elevation while the Bouguer anomalies have a negative correlation with elevation as is generally expected. The regression relation for free-air anomaly is $y = 0.086\ h - 74.79$ and for Bouguer anomaly, it is $y = -0.020\ h - 71.80$.

### 5.6.2 Relationship for 1/4° x 1/4° Areas

The average elevation, free-air and Bouguer anomaly maps for 1/4°x1/4° areas are shown in Fig. 5.6. The average elevation map shows the dominant Western Ghat trend with uniform rise in elevation from 50m to 800m. Localized high elevated areas have been completely smoothed out on the map. The free-air anomaly shows a strong correlation with the elevation on this average map. The 1/4°x1/4° average free-air and Bouguer anomalies have been

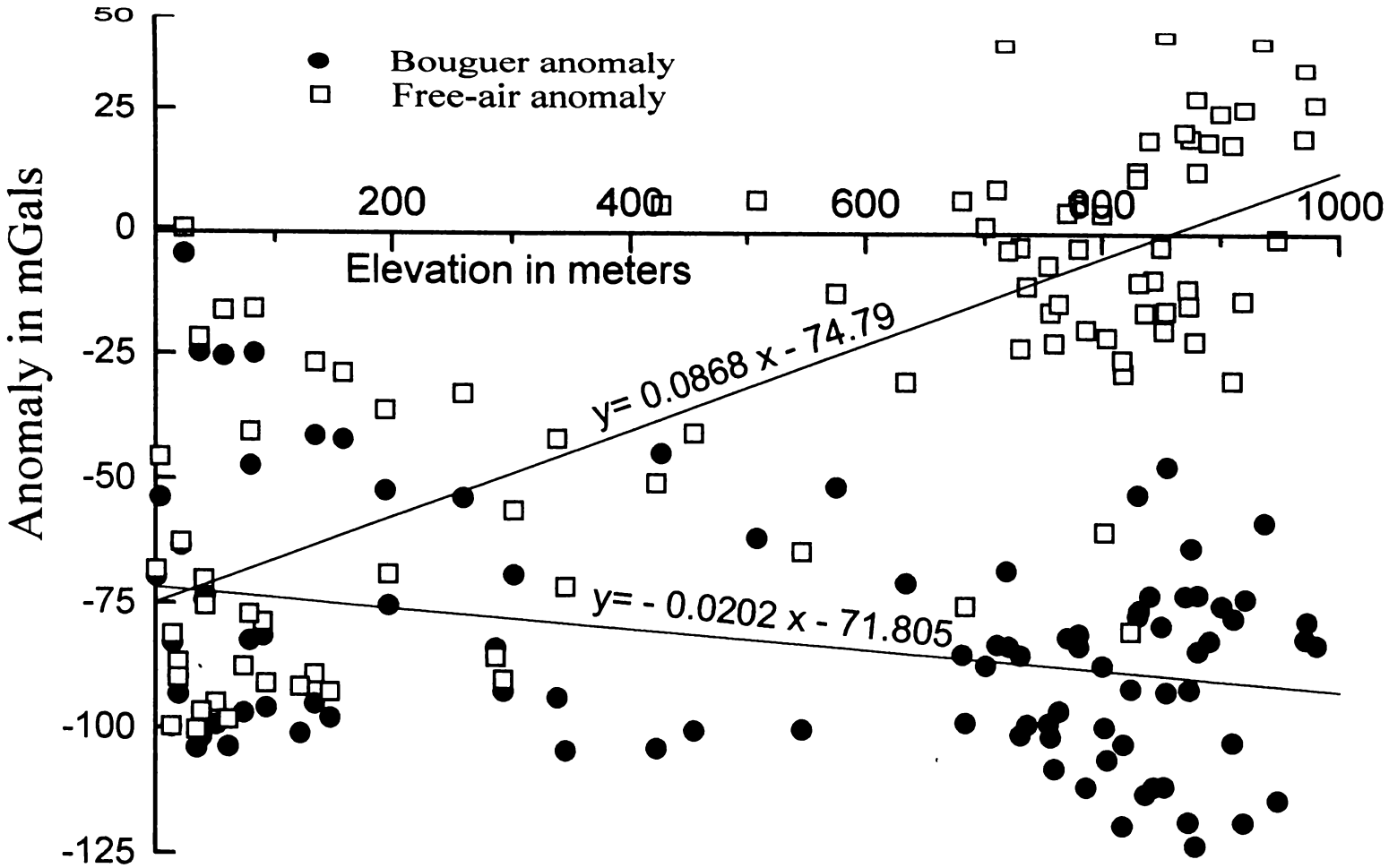


Fig 5.5. Plot showing the 1/8° x 1/8° averaged gravity anomaly values against corresponding elevation values in the study area. The best fit lines with equations are also shown.

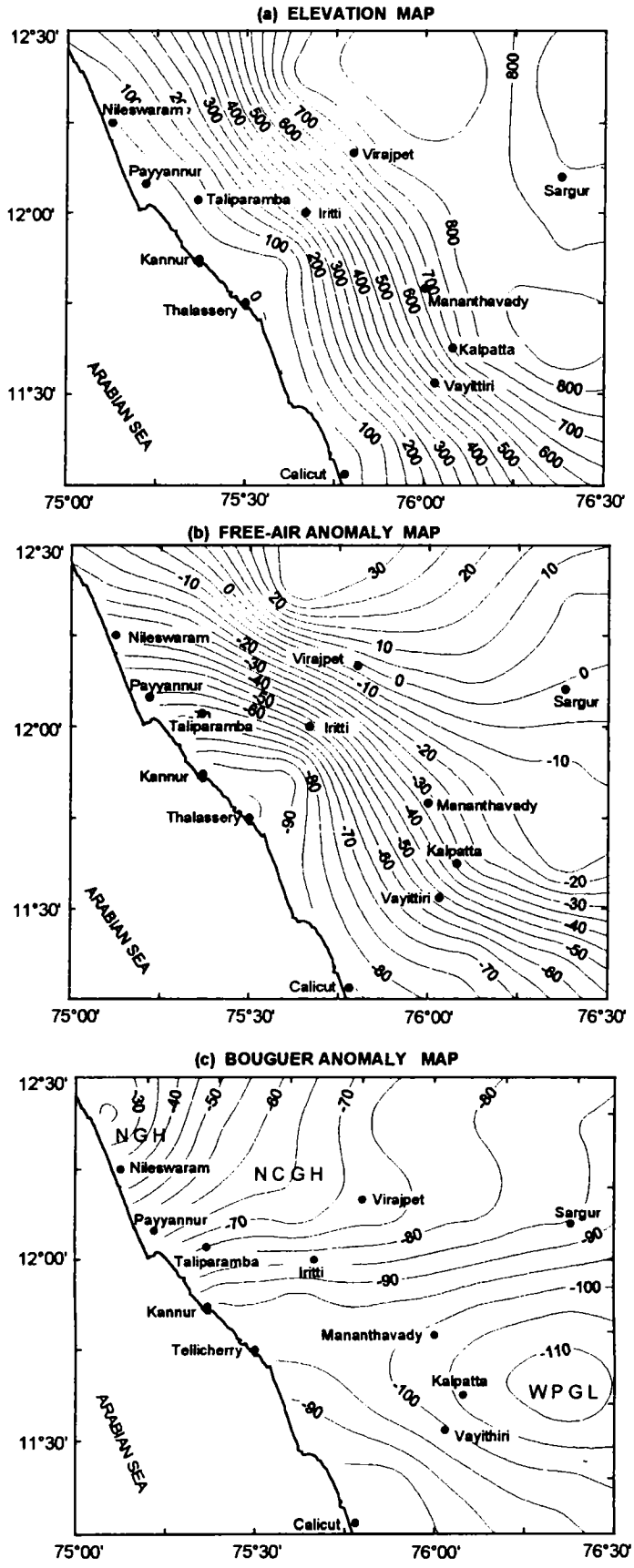


Fig 5.6: The countour maps of average values for 1/4°x1/4° grid areas of the study area.

plotted against elevation as shown in Fig 5.7. The regression relation obtained for free-air anomaly is $y = 0.095\ h - 78.6$ and for Bouguer anomaly, it is $y = -0.017h - 74.6$.

As can be seen from Fig 5.6(c), the WPGL continues to be expressed as a broad low of nearly –15 mGal as also the NGH. However, the NCGH which was well brought out in 1/8° x 1/8° grid average map (Fig 5.4(c)) is fairly smoothed out in this map suggesting that this feature might be related to mid-crustal depths. A significant aspect that emerges by a comparison of 1/8° x 1/8° grid and 1/4° x 1/4° grid average maps is the status of Bavali shear zone (a 10 km wide zone along Bavali lineament) marked by dotted lines in Fig 5.4(c) and Fig 5.6(c) . The shear zone along most of its length (between Payyannur and Mananthavady) separates two distinct gravity fields marked by a gradient along the shear zone. But, beyond Mananthavady, the gradient is seen to be occuring NE of the shear zone. Considering that the anomalies with wavelengths greater than 56 km are reflected in 1/4° x 1/4° grid average map, the observed gradient along the shear could be explained due to mass anomalies within the upper and mid crustal layers. Therefore, it may be tentatively suggested that the Bavali lineament is possibly a major crustal discontinuity zone. Further explanation of this feature is only possible by seismic profiling across this lineament. A more detailed analysis of 1/4° x 1/4° average map in relation to the Moho thickness is discussed in chapter VI.

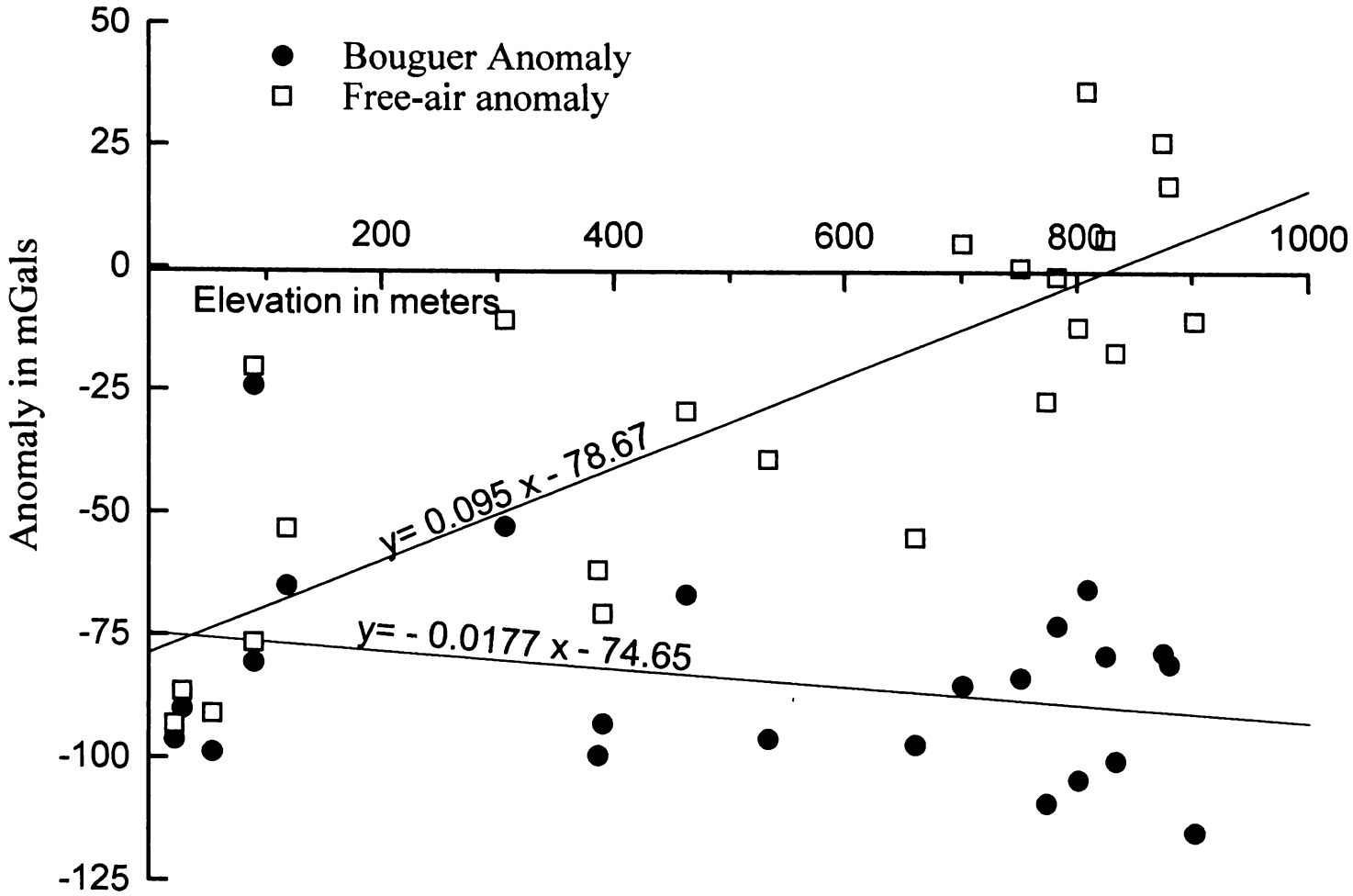


Fig 5.7. Plot showing 1/4°x1/4° averaged gravity anomaly values against corresponding elevation values in the study area.The best fit lines with equations are also shown.

### 5.6.3 Comparison with Other Areas

A 1/2°x1/2° average free-air and Bouguer anomalies have been computed. But there are only very few points in the region. Fig 5.8 shows 1/2°x1/2° average free-air and Bouguer anomalies plotted against elevation in the study region. The regression relation for free-air anomaly is y=0.072 h – 59.6 and for Bouguer anomaly it is y=-0.025 h – 70.8. The correlation coefficient is 0.75 for free-air anomaly and –0.52 for Bouguer anomaly. The regression relation for Bouguer anomaly has been compared with similar relations obtained for 1/2°x1/2° average values in other parts of India as shown in Fig 5.9 and Table 5.1. The differences in regression relation for different regions indicate variations in crustal densities and crust-mantle relationship. Positive or low negative regression coefficients for Aravallis, Satpura mountains and Eastern Ghats have been attributed to high density masses underlying these regions (Verma et.al., 1984). The low regression coefficient observed for the present study region (-25 mGal/km) could also probably be due to high density material at depth. The isostatic anomalies in the region (NGRI, 1978) show 0 - 20 mGal in the northern part of the area with anomalies falling down to –80 mGal in the southern part of the region. Such variations in the isostatic anomalies suggest lateral inhomogeneities in the crustal masses or changes in crust-mantle interface.

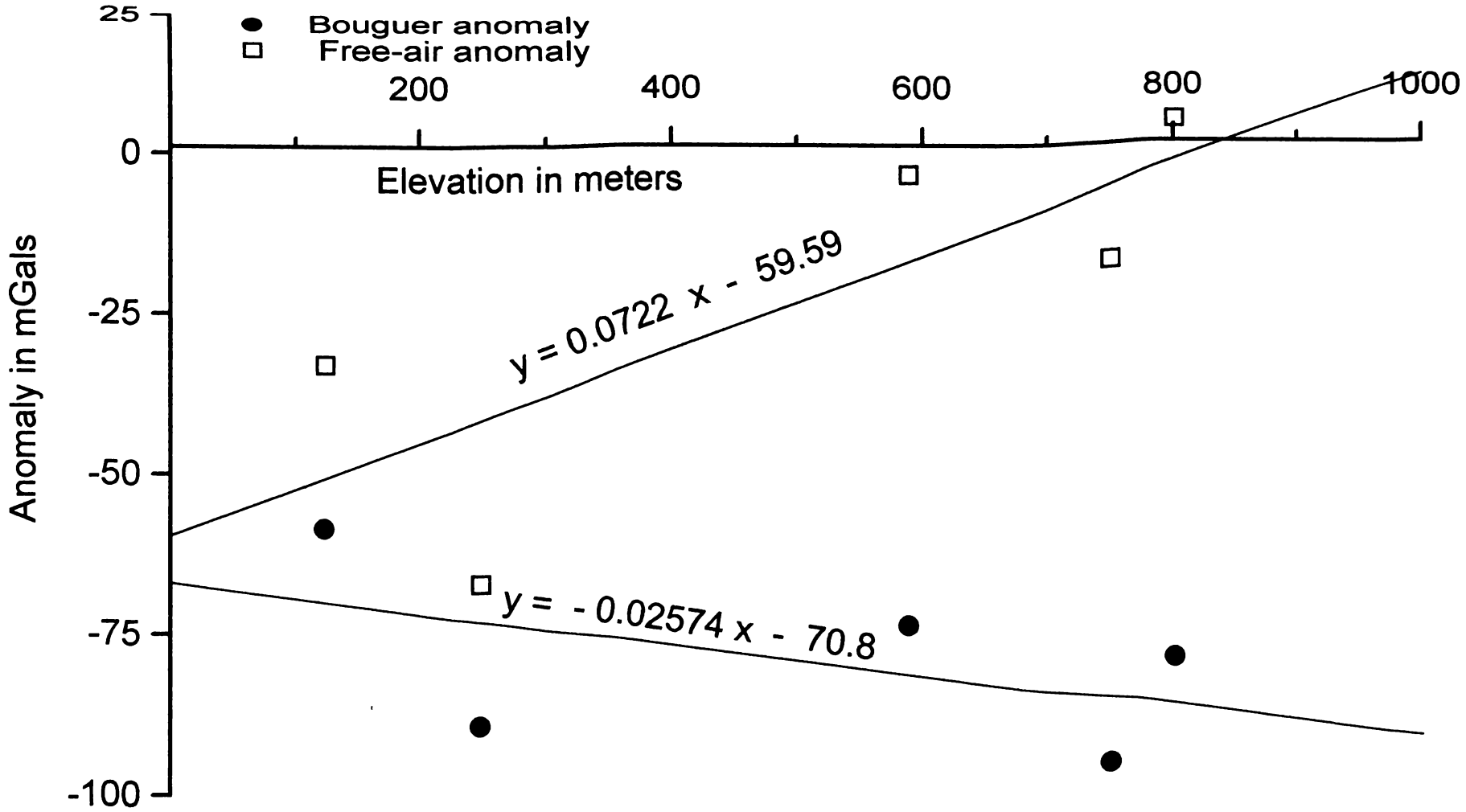


Fig 5.8. Plot showing the 1/2° x 1/2° averaged gravity anomaly values against corresponding elevation values in the study area. The best fit lines with equations are also shown.

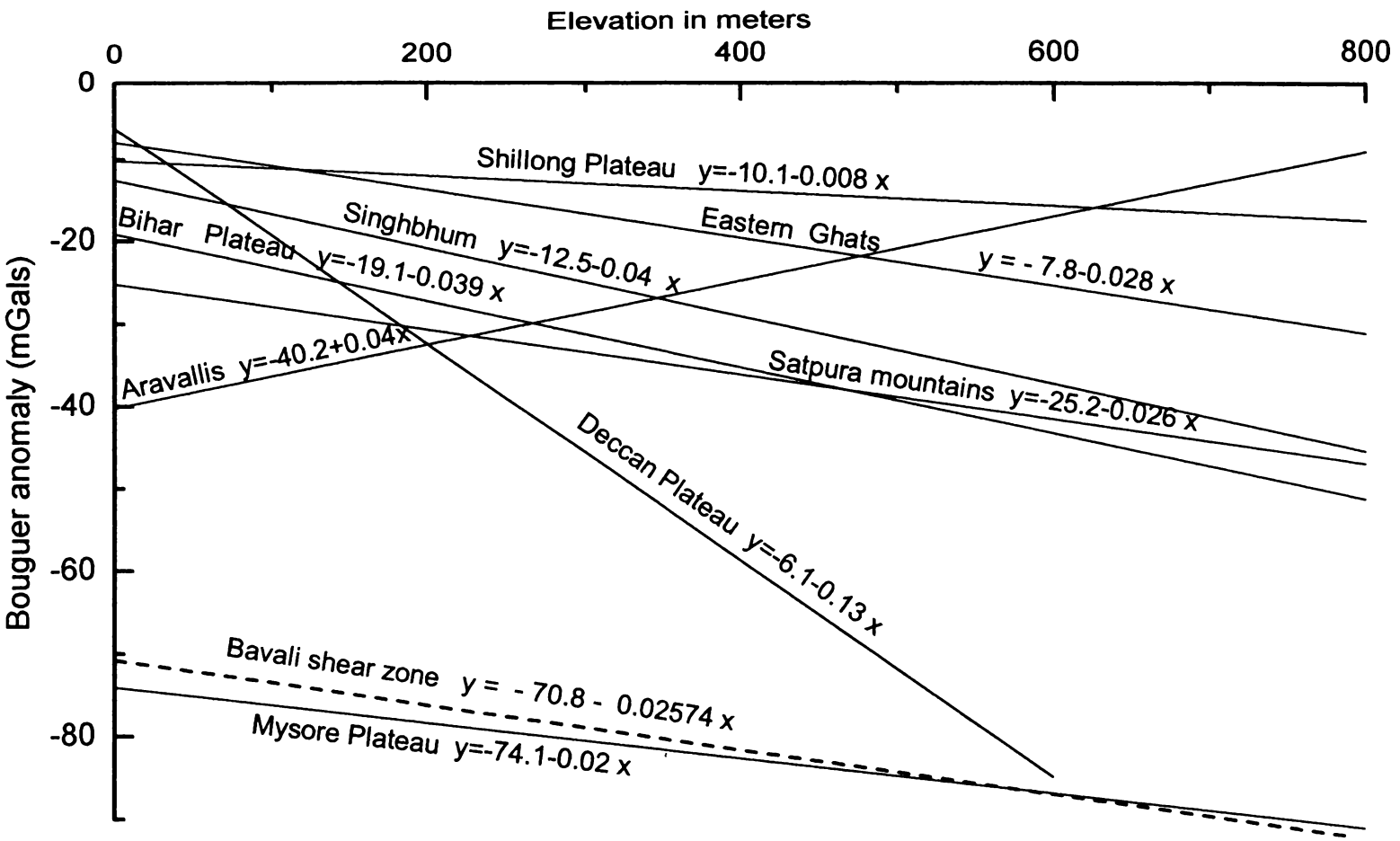


Fig 5.9. Comparison of average Bouguer anomaly vs. elevation with other parts of the Indian peninsula for 1/2° x 1/2° areas.

**Table 5.1. Average free-air and Bouguer anomaly versus elevation relationship for different parts of Indian peninsula based on 1/2°x1/2° grid values.**

| Sl No | Region | | Correlation coefficient | Slope | Interce-pt | Average | | Reference |
|---|---|---|---|---|---|---|---|---|
| | | | | | | Anom-aly | Eleva-tion | |
| 1 | Bavali | FA | 0.77 | 72.2 | -59.6 | -23.3 | 503 | Present |
| | Shear zone | BA | -0.52 | -25.7 | -70.8 | -83.7 | | Study |
| 2 | Mysore | FA | 0.72 | 110.0 | -85.1 | -12.0 | 664 | Verma et |
| | Plateau | BA | -0.20 | -20.0 | -74.1 | -87.4 | | al. (1984) |
| 3 | Singhbhum | FA | 0.79 | 70 | -18.3 | 3.65 | 313 | Subba Rao |
| | | BA | -0.61 | 40 | -12.45 | -27.22 | | (1990) |
| 4 | Arvallis | FA | 0.69 | 120 | -32.7 | 14.10 | 391 | Verma et |
| | | BA | 0.42 | 40 | -40.2 | -24.6 | | al. (1984) |
| 5 | Shillong | FA | 0.78 | 154 | -31.6 | 29.9 | 401 | Verma et |
| | Plateau | BA | -0.09 | -8 | -10.1 | -13.5 | | al. (1984) |
| 6 | Eastern | FA | 0.559 | 42.8 | -8.6 | 5.0 | 319 | Verma et |
| | Ghats | BA | -0.434 | -28.2 | -7.8 | -16.8 | | al. (1984) |
| 7 | Bihar | FA | 0.52 | 49.6 | -10.6 | 9.6 | 409 | Verma et |
| | Plateau | BA | -0.534 | -39.3 | -19.1 | -35.2 | | al. (1984) |
| 8 | Satpura | FA | 0.79 | 93.8 | -35.1 | 5.6 | 434 | Verma et |
| | mountains | BA | -0.386 | -26.0 | -25.1 | -36.1 | | al. (1984) |
| 9 | Deccan | FA | 0.05 | 3.5 | -16.2 | -13.7 | 458 | Verma et |
| | Plateau | BA | -0.01 | -130 | -6.1 | -65.7 | | al. (1984) |

## 5.7 Conclusions

The free-air and Bouguer anomaly maps prepared for the study region indicate the following:

- an E-W gradient zone coinciding with the gneiss-charnockite boundary west of Iritti and the gneiss-schist province east of Iritti.
- A broad gravity high circumfering the northern charnockite province (NCGH). The Perinthatta anorthosite massif in this province is characterized by three localized gravity highs.
- A positive gravity anomaly towards coast near Nileswaram (NGH).
- Broad gravity low with a relief of –20 mGal in the Wynad plateau (WPGL). Though the Kalpatta granite falls within this broad low, the anomaly due to granite body is not well reflected in a regional field.
- A series of gravity lows south of the Bavali shear coincide with the western slopes of hill ranges and the supracrustals in the Vengad basin.
- A coastward gradient anomaly between Calicut and Thalasseri.

Spatial filtering through averaging at 1/8°x1/8° and 1/4°x1/4° grid levels of the map carried out in the present study clearly demonstrated various broad wavelength anomalies and their probable depth. The anomalies over the Perinthatta anorthosite gets smoothed out on 1/8° x1/8° average map indicating that anorthosite occurs at shallow crustal levels. Similarly the NCGH loses its presence in 1/4°x1/4° average map. In the 1/8°x1/8° and 1/4°x1/4° average

maps the Bavali shear zone separates two distinct gravity fields with a gradient zone almost following the shear. While the anomalies are more positive on the northern side, the region south of the shear is characterized by large negative anomalies. The gravity field variation in the region and the high gradient observed across the Bavali shear zone may probably indicate lateral mass heterogeneities in the crust. The low regression coefficient (-25 mGal/km) obtained for the study area based on 1/2°x1/2° averaged anomaly-elevation relationship indicates the presence of high density material at depth. In order to resolve these factors, a detailed gravity modelling is attempted across the Bavali shear zone as given in chapter VI.

*Chapter VI*

# Gravity Modelling of the Crustal Structure

## 6.1 Introduction

The gravity modelling is basically a tool to obtain knowledge of the subsurface extension of the exposed geological units and their structural relationship with the surroundings. For this purpose, a priori knowledge on the densities of crustal rocks and crustal thickness is required. Seismic data do provide much information required for gravity modelling. Therefore, seismically constrained models are considered to be more robust. However, in the absence of such data, the surface rock densities, regional tectonics and Moho configuration by other geophysical means can also be effectively used under certain broad geological assumptions.

Fairly adequate gravity coverage over the Bavali shear zone and the adjoining areas allows us to carry out a quantitative analysis of the data in terms of 2-D gravity models. For this purpose, six regional gravity profiles located across the Bavali shear zone and the adjoining crustal segments are considered for gravity modelling. The study is expected to throw light on the nature of the shear zone, crustal configuration below the high grade granulite terrain and the tectonics operating during geological times in the region.

## 6.2 Shear Zones and Their Tectonic Significance

Shear zones are narrow, planar, sub-parallel sided domains where strain is concentrated relative to their surrounding regions (Ramsay, 1980). They are prominent features defining boundaries of the deeply eroded orogenic belts as well as zones of more intense deformation within the belt. Deformation of the continental lithosphere is principally concentrated at all scales in networks of shear zones (Bak et al., 1975; Tapponier and Molnar, 1977). Brittle, brittle-ductile or ductile shear zones are known in various lithologies and structural levels down to the upper mantle (Vissers et al., 1991). The shear zones range from microscopic to a few hundred kilometers in extent. Identification and recognition of ductile shear zones is important because of their significance often as terrain boundaries, sites of large strain and reactivation, hospitable locations for igneous activity, fluid conduits and mineralization. The mid-crustal shear zones exposed in deeply eroded Pre-Cambrian orogenic belts transfer or accommodate large scale relative displacements between the terraines. Numerous structural investigations on regional geology and tectonics of major shear zones in the Pre-Cambrian terraines have been made by several workers (eg., Bak et al., 1975; Daly, 1986; Coward and Park, 1987; Friend et al., 1988; McCourt and Vearncombe, 1992; Vissers et al., 1995; Pili et al., 1997; among others). However, some recent geophysical studies particularly gravity and seismic investigations combined with geology over certain major shear zones world over revealed the crushed dynamics, crust-mantle interactions and lithospheric structure (Fountain and Salisbury, 1981; Lambeck, 1983; Lambeck et

al., 1988; Reston, 1990; Plomerova et al., 1993; Ibrahim et al., 1996; Pili et al., 1997; among others).

## 6.3 Major Shear Zones in the Southern Granulite Terrrain (SGT) of India

Major shear zones in the SGT include the Moyar-Bhavani shear, Bavali shear, Palghat-Cauvery shear and the Achankovil shear. Moyar shear zone separates the Biligirirangan hills to the north and Nilgiri charnockite block to the south. Around 70 km long dextral displacement effective across a zone of more than 20 km was proposed by Drury and Holt(1980) for the Moyar-Bhavani shear zone which trends east-west. Naha and Srinivasan (1996) suggested that the Moyar shear zone is neither as extensive or its effect as pervasive as formerly believed. They restricted the most intense shearing to a width of 2 km, and proposed that the Moyar shear is characterized by a predominantly dip slip transport and the veering of the 'trends' in southern Karnataka, northern Tamil Nadu and northern Kerala is an inherent feature of the superposed fold systems there. The Bhavani shear zone merges with Moyar shear and it extends in a NE-SW direction.

A major E-W trending shear system occupies the Palghat-Cauvery lowlands. This shear system represented by a distinct geomorphic expression known as Palghat gap is connected to the N-S thrust system of Eastern Ghats by many arcuate shears. The Palghat-Cauvery region is characterised by roots of

supracrustals and dismembered layered basic complexes (Ramakrishnan, 1988). Recent structural studies along Palghat gap indicate that it is a ductile dextral shear (Eric D'Cruz et al., 2000).

The Achankovil shear belt in southern India is a prominent lineament that has been interpreted as a major shear zone (Drury et al., 1984). This shear zone coincides with the boundary between charnockites of Madurai block to the north and khondaliltes of the Trivandrum block to the south. Achankovil shear zone is 10-20 km wide and more than 100 km long (Drury et al., 1984). The southwestern boundary of the shear zone coincides with another major shear zone called Tenmala shear zone (Chacko et al., 1987; Ramakrishnan, 1993). The kinematic indicators along the southwestern edge of the Achankovil shear belt are suggestive of the essentially dextral nature with a reverse component for the shear (Sacks et al., 1997).

The Bavali shear zone, the major structural feature in the present study area is nearly 100 km long with a width of 10 km. The shear zone is regarded by some workers as the western extension of Moyar shear. But there is a definite change in the trend and nature of Bavali with Moyar shear. Pili et al. (1997) classified the shear zones into 'Major shear zones' of length > 350 km, 'Minor shear zones' of length < 140 km. If Bavali shear zone is an extension of the Moyar shear, the two together would merit to be qualified as 'Major shear zone' and then one would expect to find the attributes assigned by Pili et al. (1997) to

such shears. Recent structural studies along the Bavali shear revealed more than one episodes of shearing along this zone and that the shear has essentially dextral displacement with some normal component (Soney, 2000).

## 6.4 Structure and Evolution of the SGT: Constraints from Geological and Geophysical signatures

Since the exhumed lower crust on either side of the Bavali shear zone is a part of the large lower crustal domain of the SGT and several shear zones are believed to have juxtaposed crustal blocks with differential exhumation in SGT, a comprehensive review of several previous works on structure and geological models would be relevant and are outlined below.

The SGT is one of the different segments of high grade domains encircling the central Archaean cratonic region called the greenstone-granilte domain in Peninsular India (Mahadevan, 1994; 1996). The major shear zones are often linked to processes of exhumation of the lower crust. Fountain and Salisbury (1981) analysing several exposed cross-sections of deep continental crust point out that distinctive Bouguer anomaly patterns reflect the dipping basement structures and anomalously deep mantle. Percival et al. (1990) suggested several process related to the exhumation of the crust in the high grade domains. They include (i) repeated phases of compression, shortening and thickening of the crust followed by denudation (ii) extensional stretching, thrust stacking and denudation (iii) a progressive and random underplating by mafic igneous rocks providing elevator mechanism followed by denudation (iv) transpressional uplift

from a vertical component of motion along large transcurrent faults (v) hyper velocity meteoric impact causing rebound of deep crustal materials along major faults. They have also mentioned that all except the last may act singly or in combination.

Mahadevan (1998) believes that several of the ductile shear zones of SGT are the result of the differential uplift of the high grade domains. In the case of SGT, the northerly tilt of the Indian subcontinent proposed by Fermor (1936) also acts as an additional factor of exhumation of the lower crust.

Drury et al. (1984) proposed a late Archaean crustal shortening and thickening in South India prior to the development of major transcurrent shear belt. This model was supported by Chetty (1996) citing structural evidence like westward verging imbricate thrust zones along Cauvery and Salem-Attur shear zones. Radhakrishna and Ramakrishnan (1988) and Radhakrishna (1989) suggest that the Archaean segment south of Palghat-Cauvery lineament juxtaposes the Karnataka nucleus along the lineament as a result of collision and thrusting. Ramakrishnan (1993) proposed that the Eastern Ghat belt extends southwards into the SGT and is truncated against the Palghat-Cauvery shear system. Gopalakrishnan (1994) presented a model of amalgamation of microterranes, which have been sutured along the major lineaments. The P-T paths proposed by several workers indicate a complex but broadly isothermal decompression path in the SGT with a P-T range of 5-10 kb and 750° to 950°C

(Harris et al., 1982). To sum up, it is debated whether the shear zones in the SGT are the result of differential exhumation or whether they represent sutures welding microplates.

The geophysical studies in the southern Indian shield indicate that the crust below SGT is in general thicker than that below gneiss-greenstone region. Such an observation is consistent with the conclusions drawn by Durheim and Mooney (1991) of the crustal thickness in the Archaean and Proterozoic continental blocks. However, Iyer et al. (1989) observed deep tectospheric roots of high P-wave velocity between depths of 60 to 300 km in both these regions. It is generally believed that such deep roots were formed as early as the mid-Proterozoic in most continents.

Several attempts were made to understand the structure and evolution of southern Indian shield by analyzing the geophysical data as summarized below. The most conspicuous gravity anomaly in the SGT is a distinct gravity low centered near Kodaikanal to the south of Palghat-Cauvery lineament. This gravity low is interpreted as due to a concealed granite batholith (Krishna Brahmam and Kanungo, 1976; Krishna Brahmam, 1993) or due to crustal thickening (Mishra, 1988; Subba Rao, 1988; Mishra and Rao, 1993; Rai et al., 1993). Harinarayan and Subrahmanyam (1986) observed that Palghat-Cauvery shear system is not associated with a significant gravity anomaly. However, Mishra (1988) is of the opinion that the Palghat-Cauvery shear separates gravity

high on the north and the Kodaikanal gravity low in the south and the crust below the shear is thickened due to overriding of these two blocks. Subrahmanyam (1978) and Harinarayan and Subrahmanyam (1986) are of the opinion that the smooth gravity contours observed along the greenstone-granulite transition zone indicate extension of granulites (SGT) beneath the Dharwar craton. However, based on 3D-seismic tomography, Rai et al. (1993) observed structural dissimilarities between Dharwar craton and SGT and the exhumation in SGT has been explained due to southward subduction of Dharwar craton beneath granulites thereby doubling the crust subsequent isostatic uplift and erosion. Ramachandran (1985) and Ramachandran et al. (1986) qualitatively analyzed the aeromagnetic map of SGT and observed several magnetic low and high axis zones based on the intensity, gradient, relief and anomaly orientation. Their study reveals that except Achankovil shear which correlates with a negative magnetic axis, most of the other lineaments have no associated magnetic anomalies. Reddi et al. (1988) made a detailed interpretation of the aeromagnetic map of SGT and concluded that the SGT is composed of a mosaic of individual crustal blocks involved in vertical movements along major breaks or faults. Many of these breaks or faults do not correspond to known outcropping major shear zones in SGT and a one to one correlation may not also be expected (Mahadevan,1998). Thakur and Nagarajan (1992) suggest that uplift of high grade domains has been due to repeated rifting along the eastern and western margins followed by crust-mantle interactions. Krishna Brahmam (1993) observed a paired gravity anomaly with a steep gradient following Moyar-Bhavani

lineament and inferred that the anomaly represents an ancient suture between SGT and the Dharwar craton.

## 6.5 Gravity Modelling

In the present study, the gravity field variation along six profiles AA' through FF' across the Bavali shear zone and the adjoining areas have been considered to interpret in terms of 2d-crustal models.

### 6.5.1 Gravity Profiles

For the six gravity profiles, considered in the present study, the free-air, Bouguer anomalies in relation to the elevation and surface geology for all profiles are shown in Fig. 6.1. The profiles selected are primarily to cut across the shear zone and the major geological formations, taking into account the gravity anomalies and data control. (See figure 2.2 for locations of these profiles on the geological map). The profiles have a near NE-SW alignment running from the coast to the interior. Four profiles (AA' through DD') essentially cover the northern charnockite province and cut the shear along its western portion, one profile (EE') in the central part of the shear zone and another profile (FF') cover the southern part passing the Wynad plateau. While Bavali shear is observed within the coastal plains west of the high lands in profiles AA'-DD', in profiles EE' and FF' it is located on Wynad plateau.

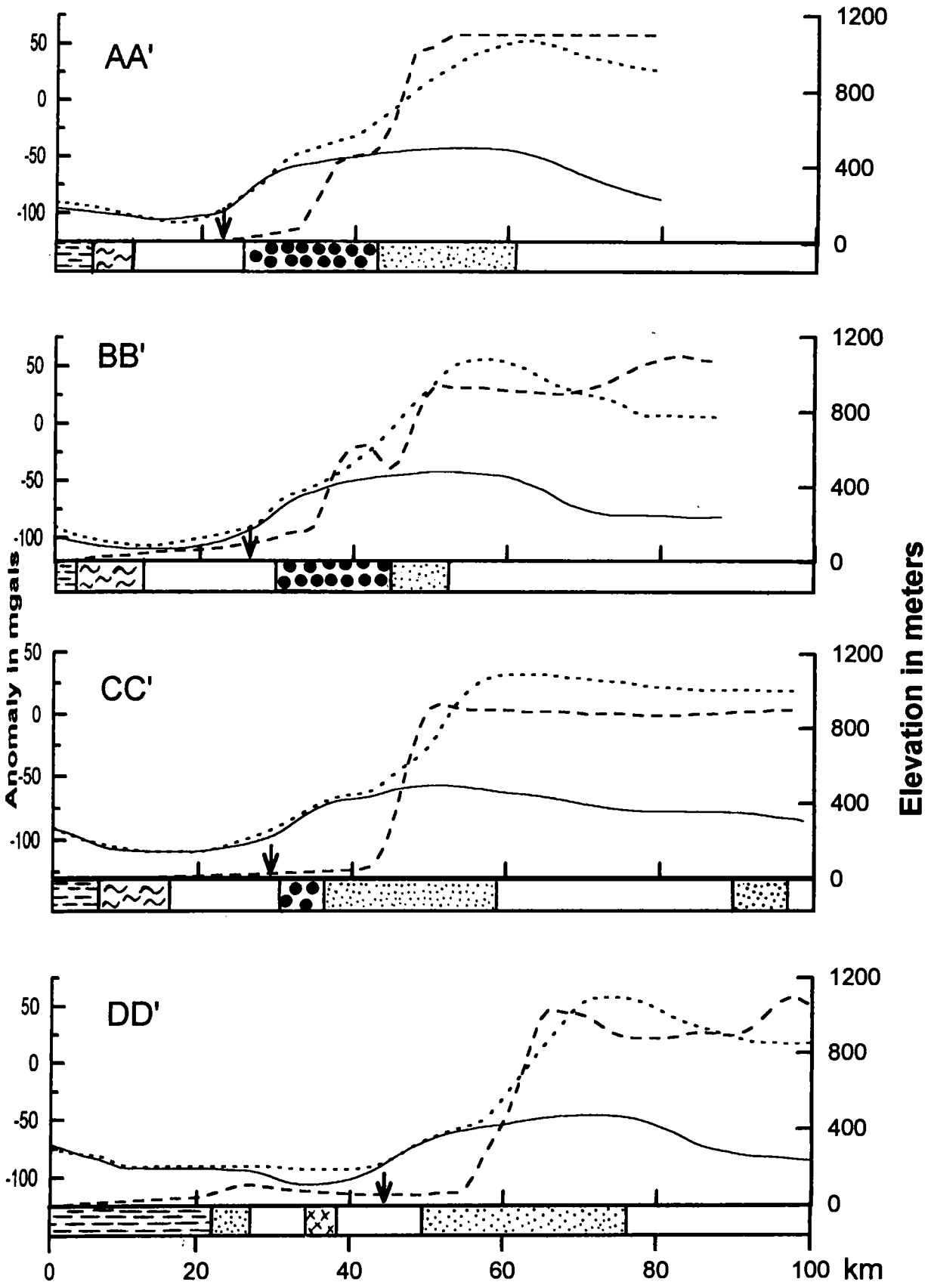


Fig. 6.1(a). Nature of the gravity field and elevation along four profiles AA' through DD' in the region (See Fig. 2.2 and Fig. 5.3 for their location). Details on the Bavali shear and surface geology are adopted from Fig. 2.2 as given in Fig. 6.1 (b)

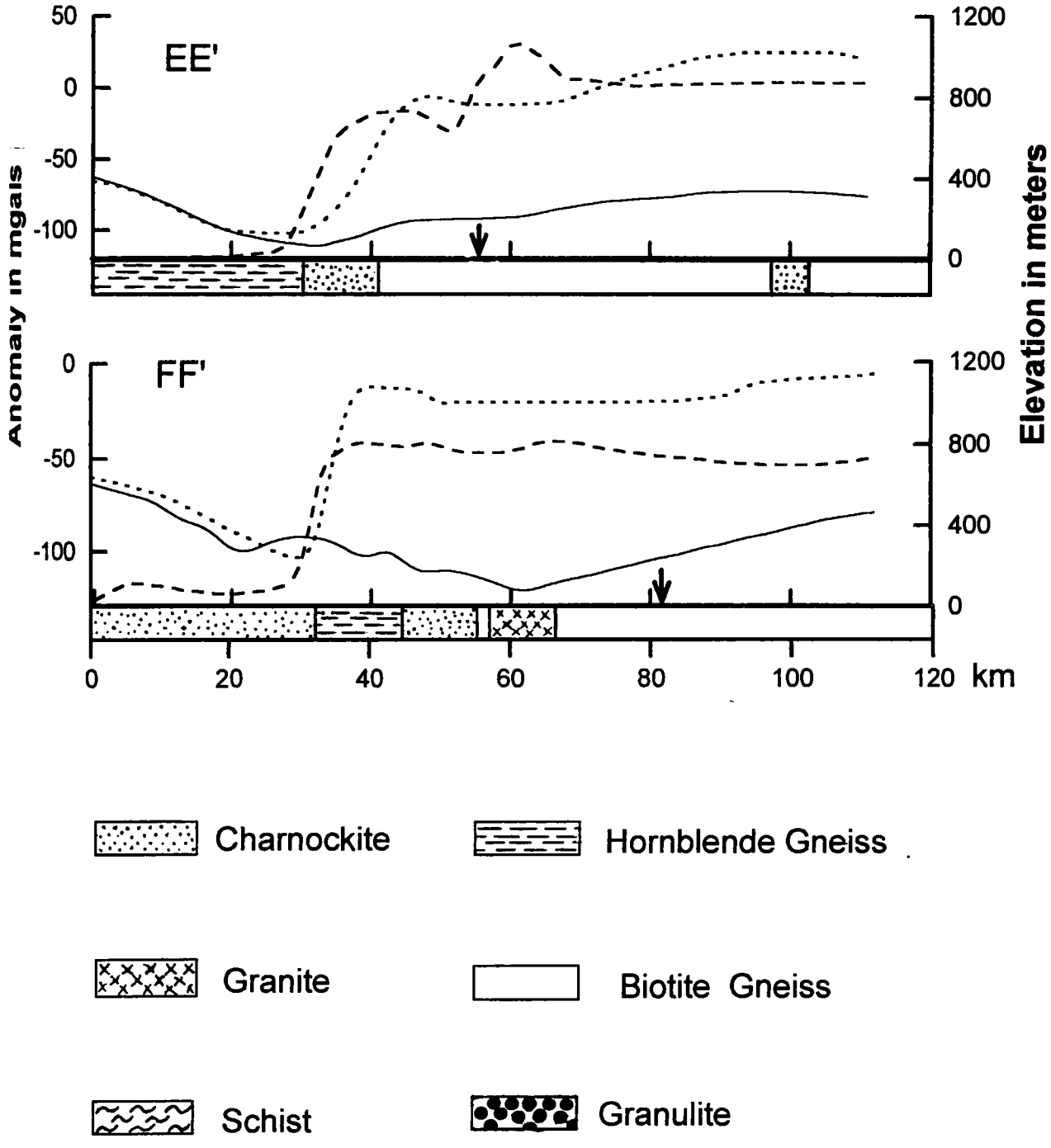


Fig 6.1(b). Nature of the gravity field and elevation along two profiles EE' and FF' in the region. Other details are same as in Fig. 6.1 (a).

In all the first four profiles AA' to DD' (Fig. 6.2 a), the most conspicuous feature is the Bouguer anomaly high of around 50 mGals. This high occurs essentially near the northern charnockite province. While the southern part of charnockite correlates with the gravity high, the northern limit of the gravity high goes well beyond the charnockite region as far as 20 km. The SW margin of this anomaly coincides with the Bavali shear zone. South of the shear, the elevation as well as free-air and Bouguer anomalies are with very low values and even the gradient of the Bouguer anomaly over the shear is quite steep varying from 3.3 to 5.1 mGal/km which is successively decreasing from AA' to DD'. This steep gradient may probably indicate the steep dip of the shear zone as well. The elevation profiles show steep slopes on the northern block but located around 20-40 km from the shear zone well within the northern charnockite province. In the two southern profiles (EE' and FF') outside the northern charnockite province, no such gravity high is observed. However, a small gradient in the Bouguer anomalies is seen over the shear zone. A generalized increase of the Bouguer anomalies are noticed towards coast in all the profiles, more prominently in profiles EE' and FF'.

### 6.5.2 Crustal Thickness Data

As mentioned in the introductory paragraph of the present chapter, for modelling the crust, a prior knowledge about the total thickness of the crust in the region is necessary.

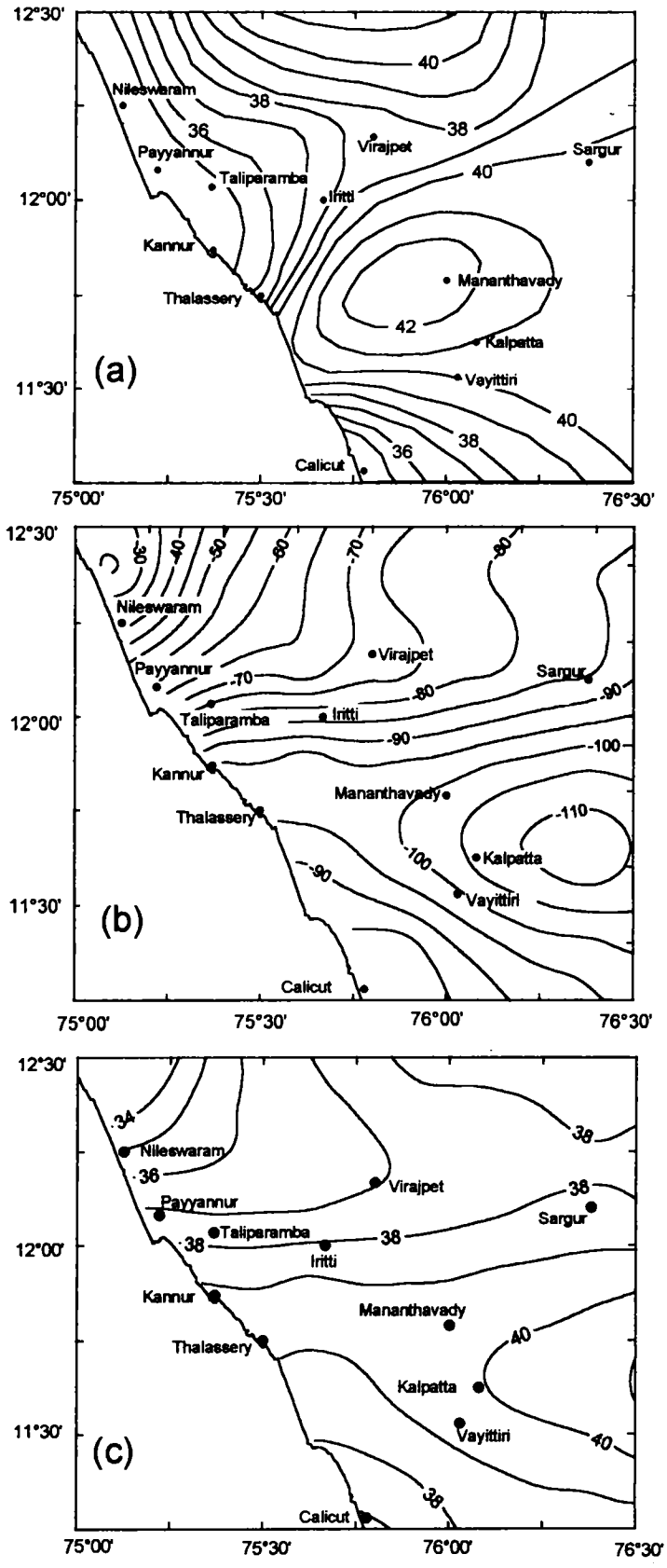


Fig 6.2 (a). The crustal thickness map of Subba Rao (1988) pertaining to the study region.

(b). 1/4°x1/4° average Bouguer anomaly map in the study region.

(c). Crustal thickness map obtained in the present study based on (b). The details of the procedure for crustal thickness estimation is outlined in the text.

The Kavali-Udipi DSS profile which is just north of the present study region suggests a crust of 38-39 km thick in the western part below Karnataka plateau. Kaila and Bhatia (1981) modelled the gravity field along this profile and suggested that the Moho boundary rises gradually from 40 km under the western edge of Karnataka plateau to 35 km under the west coast near Udipi. Though such DSS data is not available for the SGT, certain generalized crustal thickness estimates have been attempted by a few workers. Subba Rao (1988) computed the crustal thickness for the whole of Peninsular India from the 3-D fit (prism shape) to Bouguer anomaly data assuming a sea level crustal thickness of 33km and density contrast of 0.45 gm/cm$^3$ between crust and mantle over a 1/2°X1/2° grid. The Moho depth map prepared by him indicates crustal thickening of 5-6 km in the SGT with depths varying from 34-38km in the coastal areas and 39-43 km in the interior of the SGT. Moho depths estimated by Rai et al. (1993) based on 3D seismic tomography for the south Indian shield are around 35-37 km in the SGT.

The variation in crustal thickness estimates in the SGT from different methods mentioned above is due to the fact that the methods are addressing different properties of the lithosphere and also have intrinsic limitations. However, all these data show thickened crust in SGT and similar trends within SGT (Rai et al., 1993).

The crustal thickness map of the present study region after Subba Rao (1988) is shown in Fig 6.2. Based on more closely spaced data generated in the present study, a refined picture of the crustal thickness could be obtained from the regional Bouguer anomalies. The 1/4°x1/4° average Bouguer anomaly map prepared and discussed in chapter V indicated anomalies of a wavelength of 60 km and above (Fig. 6.2b). This map may be treated as a regional anomaly map and under the assumption that the region has attained isostatic equilibrium, 1/4°x1/4° grid average values can be used to compute the crustal thickness using the empirical formulae suggested by some of the previous workers (Worzel and Shurbet, 1955; Woollard, 1959). Qureshy et al. (1967) arrived at the following relationship between crustal thickness (T) and Bouguer anomaly ($\Delta g$) for Peninsular India.

$$T = 31.6 - 0.078 \times \Delta g$$

Using the above relationship, the 1/4°x1/4° average grid values have been utilized to compute the crustal thickness in the region under study. The main feature that emerges from the Moho contour map is that the crustal thickness in general ranges from 38 – 39 km over a large part of the area thickening to 40-41 km below Wynad plateau coinciding with the WPGL. The Moho becomes shallower towards the coast in the northwest to depths of around 34 km coinciding with the Nileswaram gravity high (NGH). As already mentioned in section 5.4, the thinning of crust towards the coast at Nileswaram is consistent with the Moho upwarp (Qureshy, 1970) or crustal thinning generally observed along the west coast (Chandrasekaram, 1985; Mishra, 1989). It is noteworthy that such thinning of the

crust characteristic of the west coast is not manifested in the region between 11° 30' and 12° 00'. More data beyond the coast is needed to explain this feature.

A comparison of crustal thickness map of Subba Rao (1988) and the map generated in the present study reveals a generalized picture of Moho configuration across the area. However, it may be seen that the Moho highs and lows have slightly shifted in space in the two maps. This may be the result of larger and more closely spaced data base used in the preparation of the present map. Thus the crustal thickness map shown in Fig. 6.2(c) is taken as the basis for the present modelling. The relationship of various geological features in the area to the Moho configuration particularly in relation to the Bavali lineament is discussed in section 6.5.4.

### 6.5.3 Density of Crustal Layers

The SGT being an exhumed lower to middle crustal rock, the occurrence of formations above the Conrad in this region will depend on the levels of exhumation of the deep crust (Mahadevan, 1994). In the area under study, the coexistence of high grade granulites facies rocks of obvious lower crustal origin with low to medium-amphibolite facies rocks implies an exhumed crustal level from below the Conrad. This is borne out by the fact that the average density estimates reported in chapter 3 are dominantly above 2.73 g/cc with values not lower than 2.65 g/cc in the region. Considering several diaphthoretic changes the lower crust may undergo during processes of exhumation one may expect

overall lowering of densities of these rocks but not to the extent of eliminating the lower crustal density signatures in these rocks.

A major approach to modelling crustal densities is through seismic velocites obtained by seismic methods. In India, Deep Seismic Sounding carried out across several profiles provides the basis for building up density models of the crust. For the south Indian shield, Kaila and Bhatia (1981) have generated a density model along Kavali-Udipi (K-U) profile across the Dharwar craton, where the upper lower crustal transitions are well evident. As no DSS profile is available across the SGT, the lower crust (2.85 gm/cc) and upper mantle (3.3 gm/cc) densities estimated in the K-U profile can be used to constrain the densities of the lower crust and upper mantle. Keeping in view all the above considerations, especially I) the average densities obtained for the surface rocks reported in chapter III, ii) the mid- to lower-crustal exhumation in this region and iii) the densities obtained by seismic velocity referred to above, a two layer crustal model is adopted with the following density configurations.

The upper layer is some what heterogeneous with a variety of surficial rocks of varying density and their downward extent. The average densities of the dominant outcrops of charnockite and hornblende gneisses are assigned densities of 2.73 and 2.76 gm/cc respectively. The granitic plutons are assigned a density of 2.67 gm/cc and the supracrustals of Vengad sedimentaries a value of 2.65 gm/cc. The lower part of the crust underlying the above layer is assigned

a uniform density of 2.85 gm/cc and the upper mantle is assigned a density of 3.3 gm/cc, based on the seismically constrained density model of Kaila and Bhatia (1981). This two layer density model is consistent with the simplified two layer crustal model proposed for the SGT by Ramachandran (1992) based on velocity-density relations of major rock types and other tectonic considerations.

### 6.5.4 Gravity Models

In this section the calculated Moho depths along six profiles are outlined and the bearing of the Bavali shear zone to the Moho configuration is discussed. Subsequently, the modelled crustal structure along these profiles in terms of distributed densities is presented.

#### 6.5.4.1 Moho Configuration

The calculated Moho depths along these profiles based on 1/4°x1/4° average Bouguer anomalies are presented in figure 6.3. It may be seen that in all the profiles except FF', a gradual but minor rise in Moho is observed from a depth of 39 km to about 37 km below the northern charnockite province. In the FF' profile which is across the Wynad plateau having some of the supracrustals, there is a lowering of the Moho from 38-41 km. The relationship of Bavali shear to the Moho configuration in these profiles can be constrained to some extent. The position of the Bavali shear zone is indicated in these profiles and it may be seen that its downward projection considering its southerly steep dips (>70° SW) would intersect the Moho close to where it starts rising. This pattern is seen in all

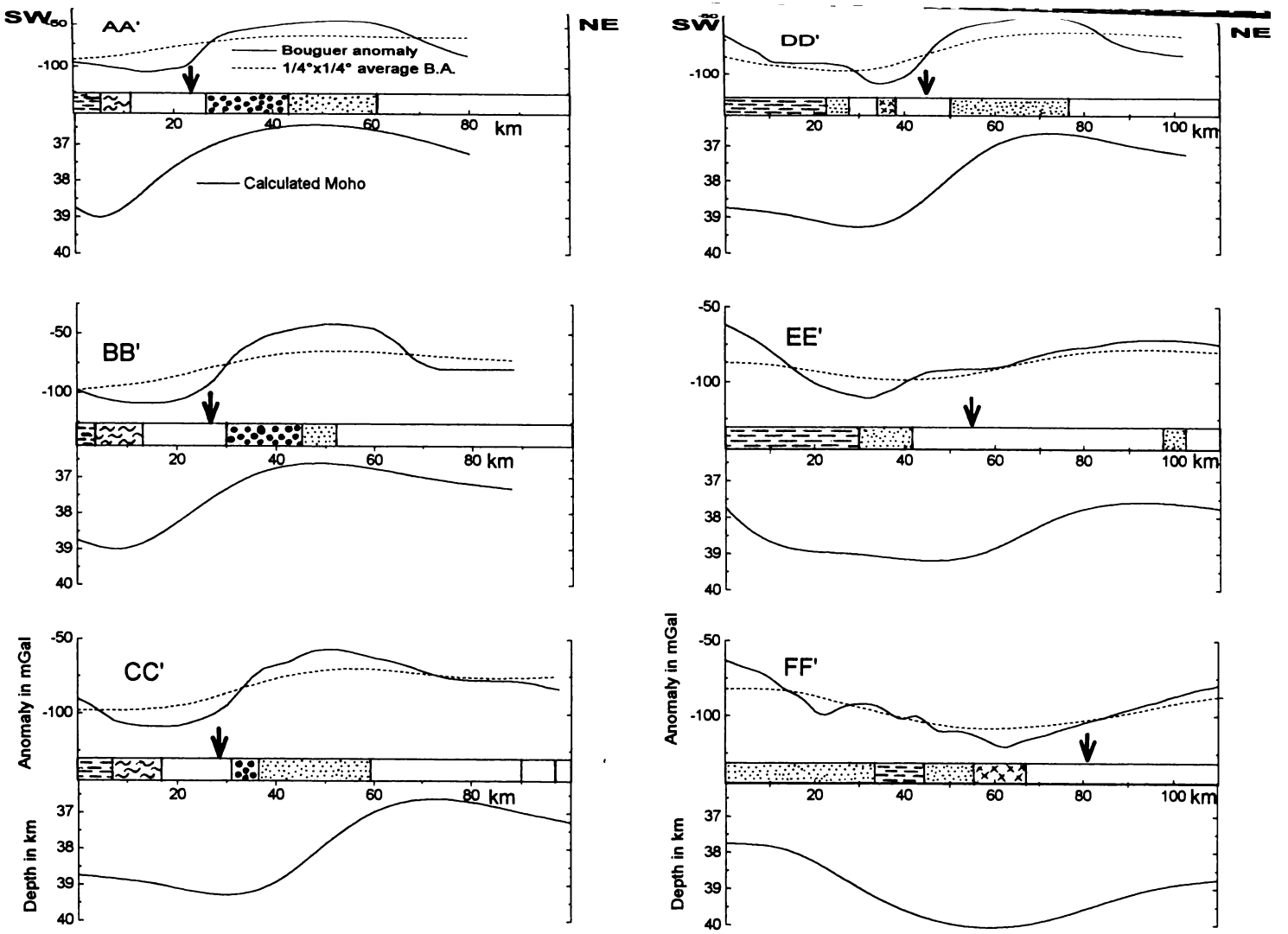


Fig 6.3. Moho configuration estimated along six gravity profiles based on1/4°X1/4° average Bouguer anomalies. Details on the geology are adopted from Fig. 2.2. Thick arrow shown on each profile indicates the location of the Bavali shear zone (Since the Moho rise observed is around 2km in all the profiles, the Moho configuration shown here is vertically exaggerated for the purpose of correlation with surface features).

profiles except in CC', in which case, the intercept of the shear zone and the Moho sways slightly towards SW of where Moho starts rising. The thinning of the crust (mentioned in section 6.4.2) towards the coast is more evident in profiles EE' and FF'.

### 6.5.4.2 Crustal Structure

The gravity anomalies along the six profiles AA' to FF' referred earlier have been modelled based on the consideratons of densities and Moho configuration discussed above. The 2-D gravity modelling was carried out using the SAKI program of USGS (Webring, 1985). The crustal models arrived at along these different profiles are presented in figures 6.4 to 6.10.

The hornblende gneiss SW of Bavali shear zone with an average density of 2.73 gm/cc extends down to depths of 20-25 km in profiles AA', BB', CC', about 15 km in DD' and down to about 32 km in EE'. It can be seen from all these profiles that the Bavali shear delimits this thick upper crust on the NE and juxtaposes it against the high grade granulites. The charnockitic rocks to the NE of the shear with a density of 2.75 to 2.76 gm/cc seem to extend down to depths of 5 – 10 km (AA' to DD') and perhaps merge with the lower crust of density 2.85 gm/cc. Interestingly, the pyroxene granulite band within this charnockite mass is more or less a lensoid body with shallow extension. The gneisses further to the NE of the charnockitic province also extend down to shallow depths of less than 10 km in profiles (AA' to CC') and in DD' it has deeper extension to 20 km. The

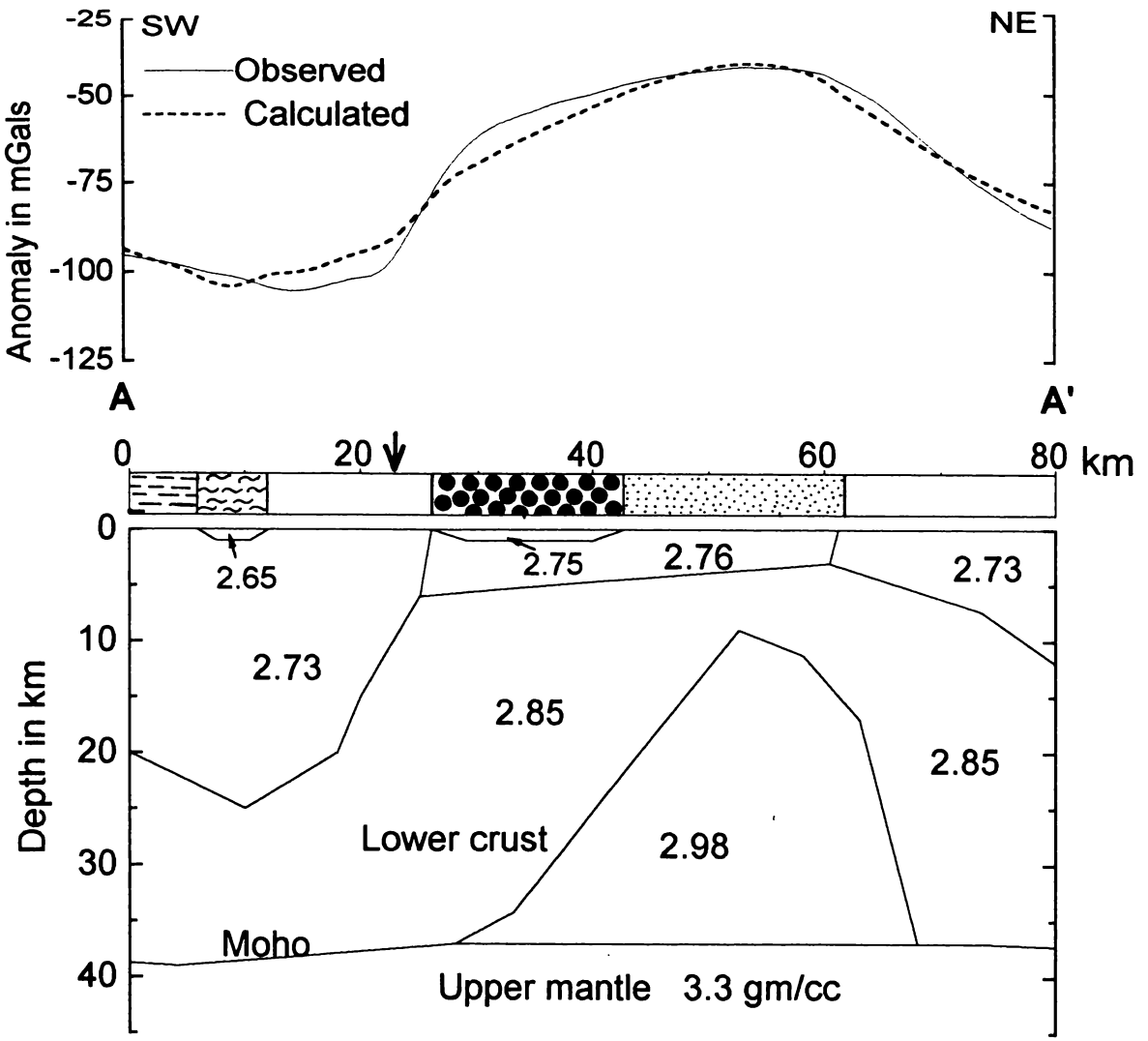


Fig. 6.4. Interpreted crustal structure along profile AA'. Details on geology and Bavali shear zone are adopted from Fig. 2.2. Other details are discussed in the text.

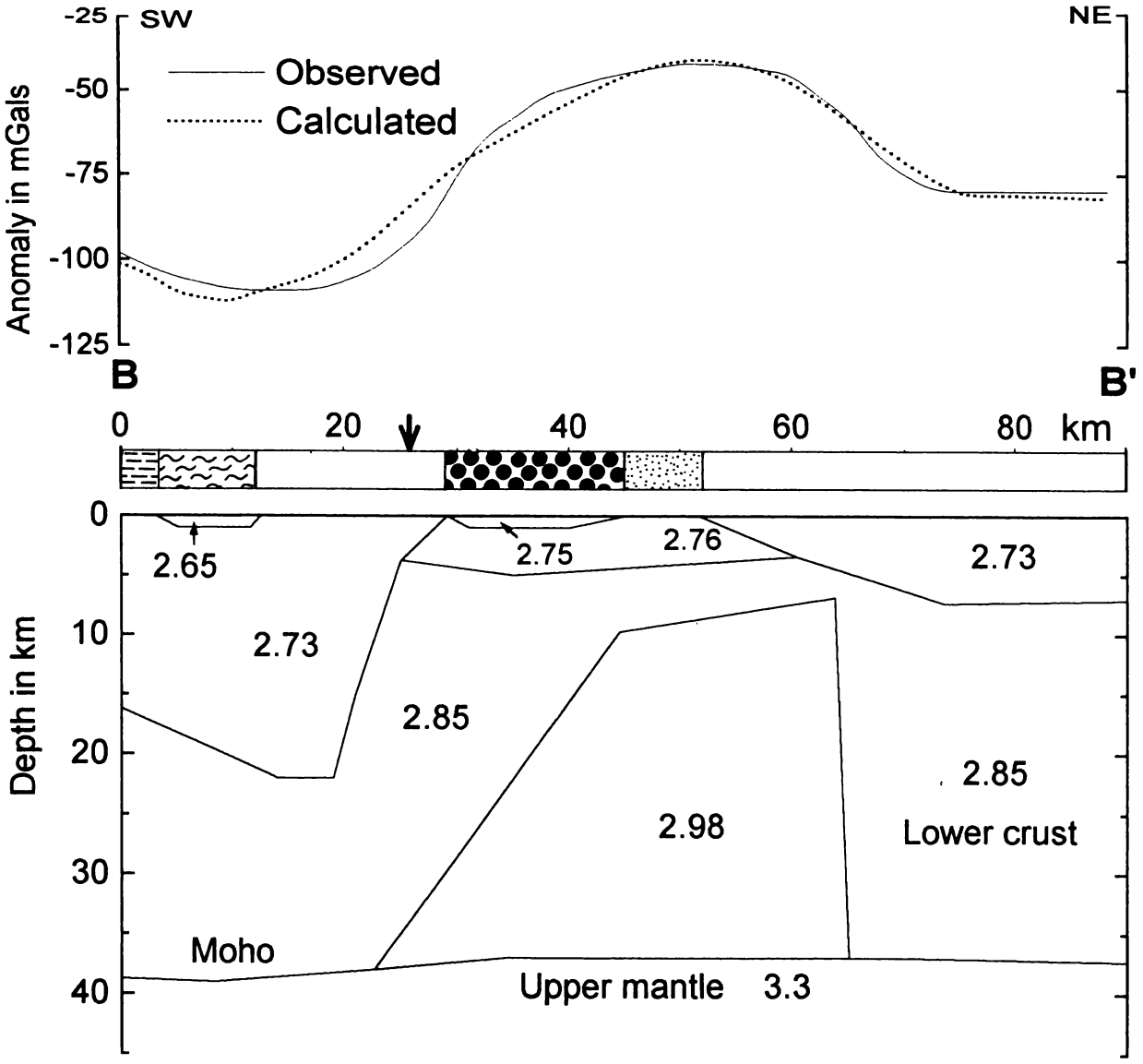


Fig. 6.5. Interpreted crustal structure along BB'

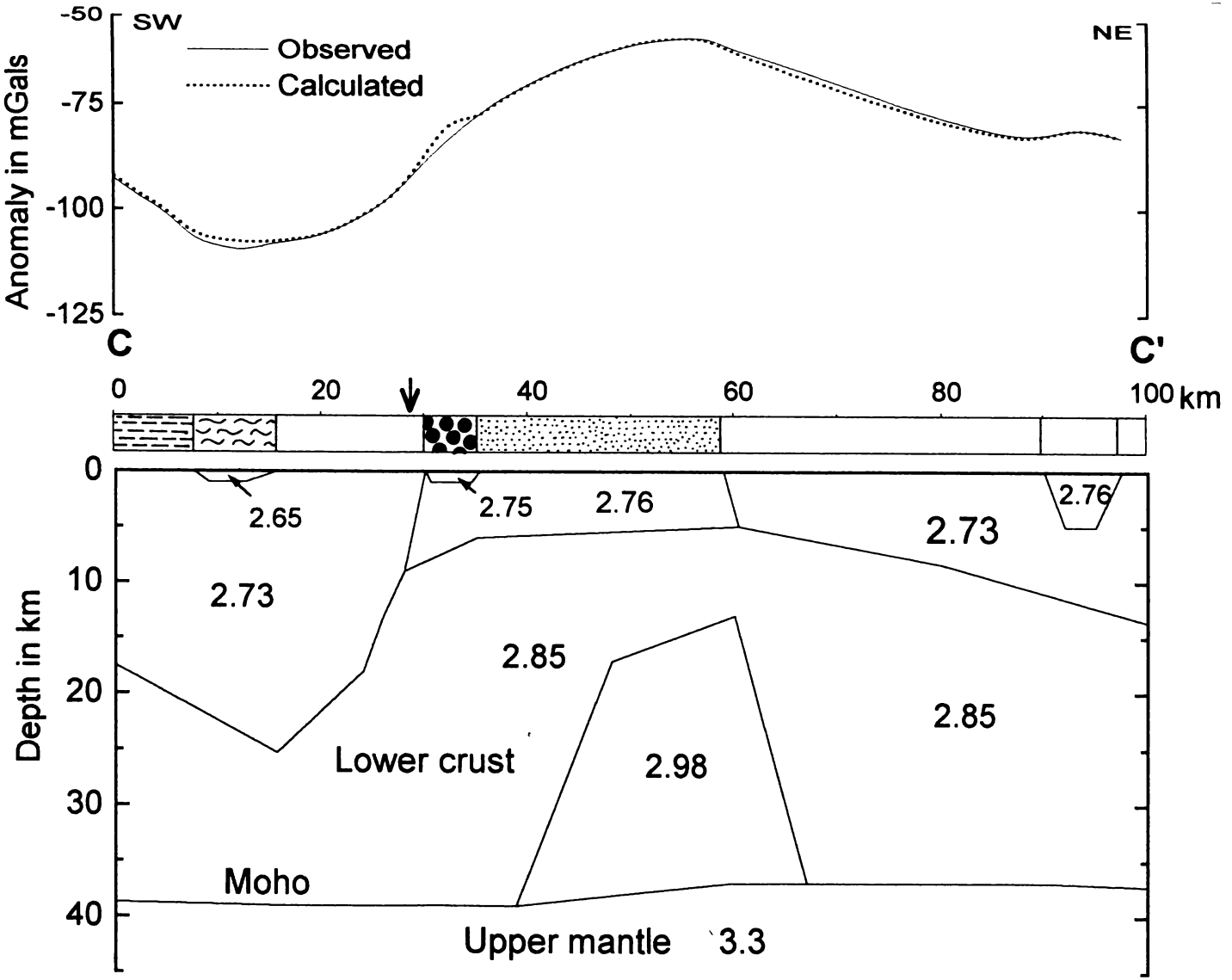


Fig. 6.6. Interpreted crustal structure along CC'

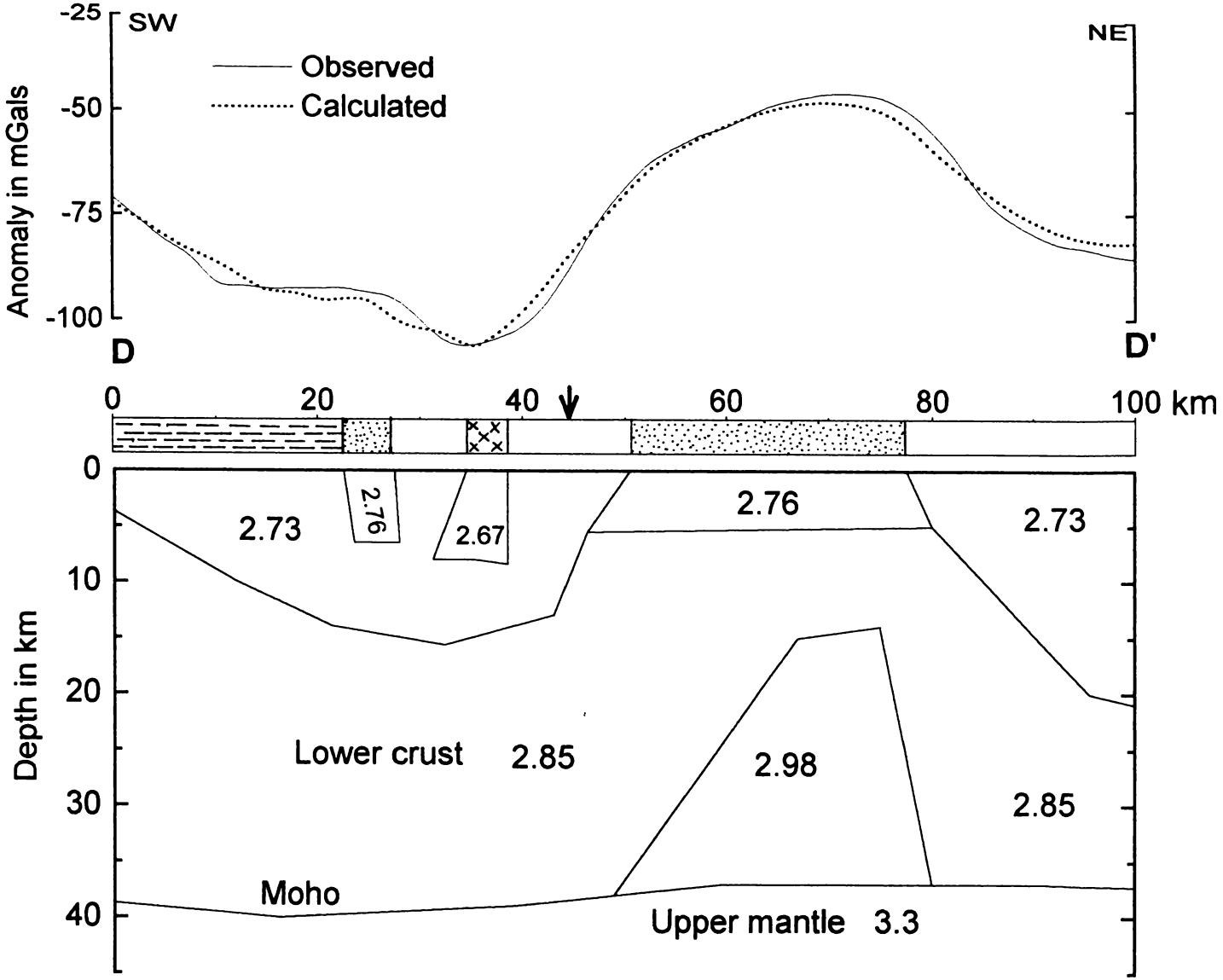


Fig. 6.7. Interpreted crustal structure along DI

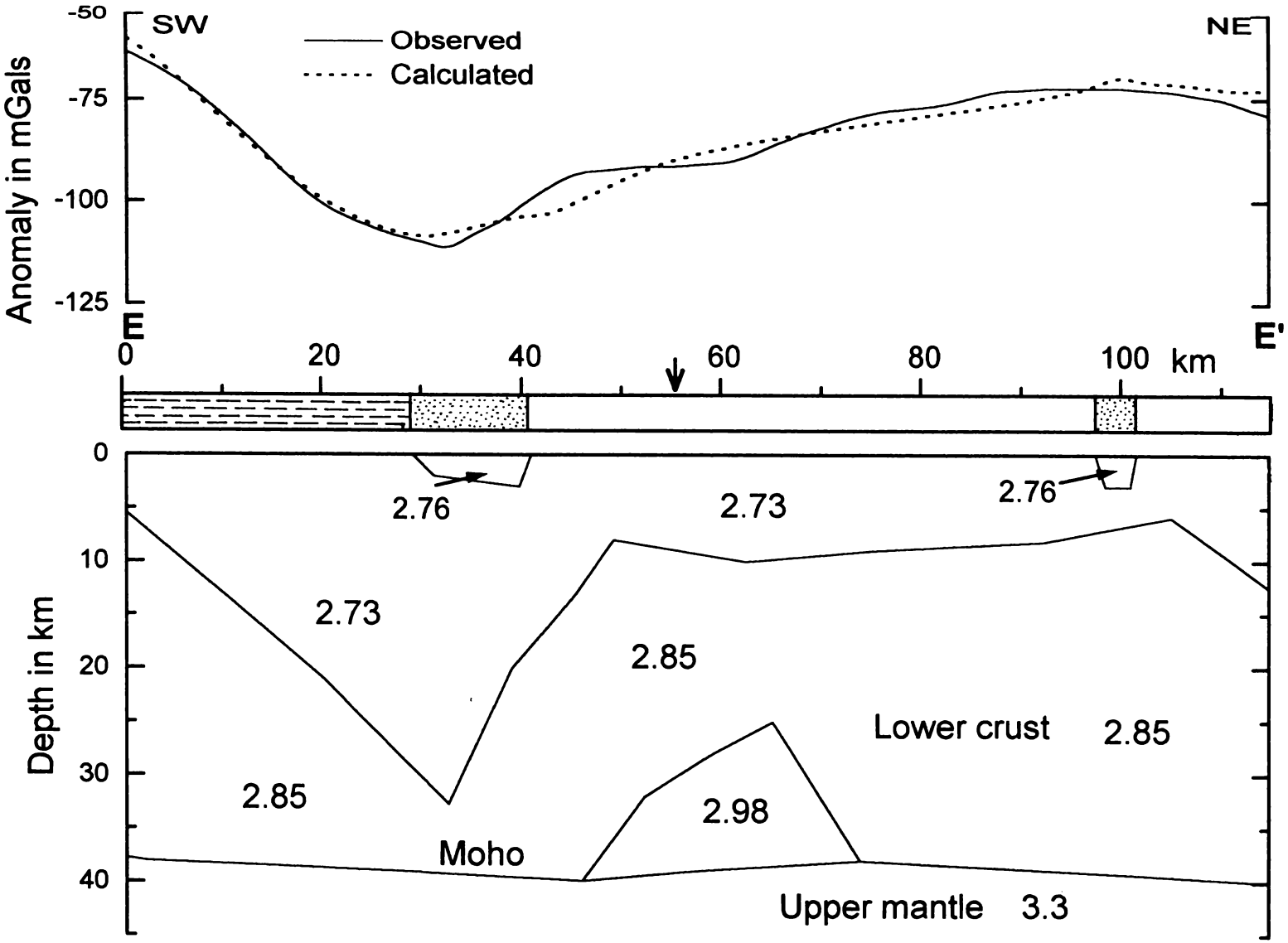


Fig. 6.8. Interpreted crustal structure along EE'

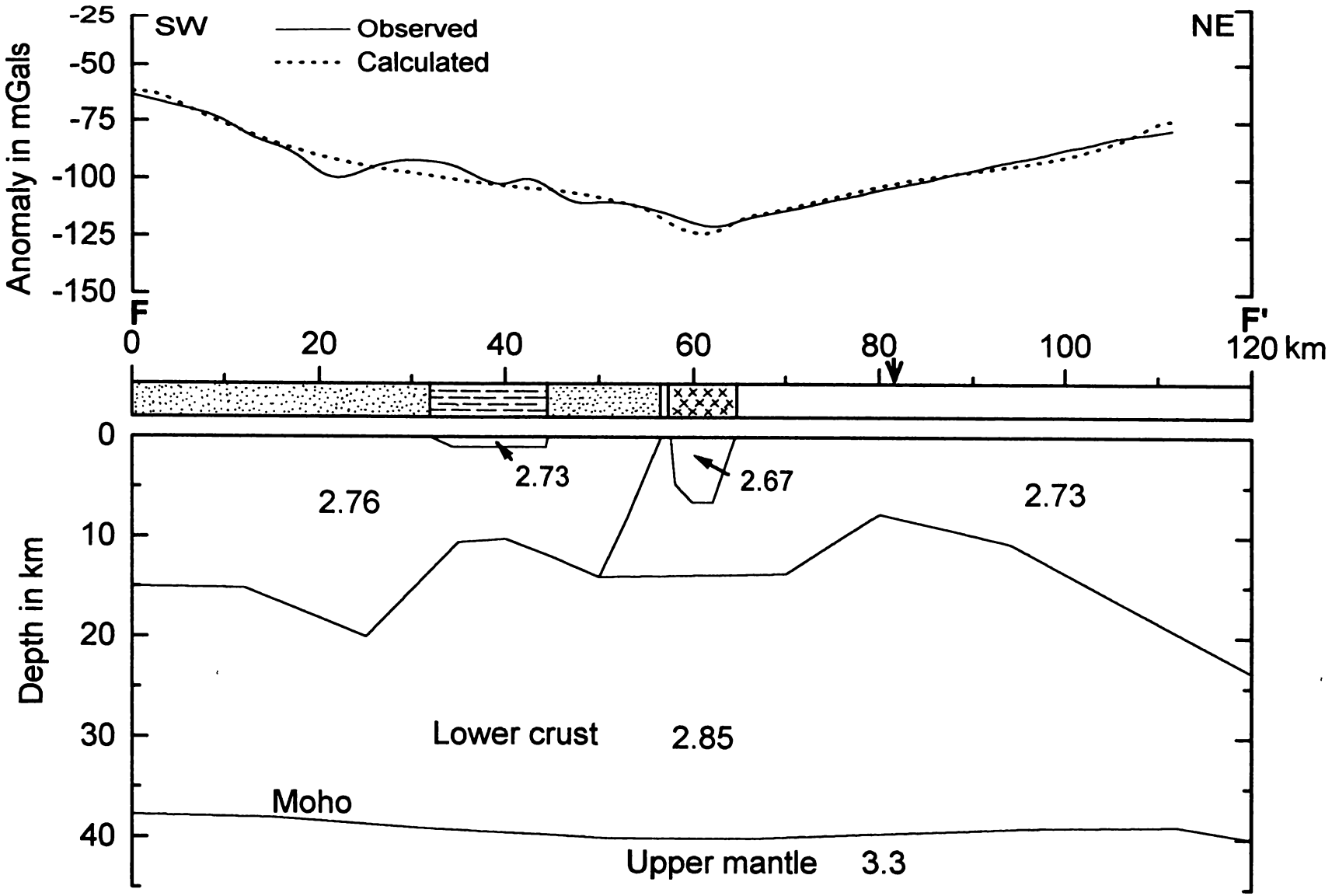


Fig. 6.9. Interpreted crustal structure along FF'

surface that separates these gneisses from the high density charnockitic block and its extensions in the lower crust could represent a gradual transition from the granulite terrain to granite-greenstone terrain or a low angle near listric fault for which no surface expression has been mapped so far. The most dominant feature in the lower crust in all the profiles except in FF' is the presence of a layer of high density (2.98 gm/cc) material which contributes significantly to the gravity high over the charnockite province. This high density body having larger dimensions in profiles AA' and BB' diminishes progressively to the southeast and practically disappears in profile FF' below Wynad plateau.

The EE' profile cuts across the gneisses bounded by the charnockites west of Mananthavady and has some distinctive features. The charnockite mass itself has a shallow extension to less than 5 km and appears to be a floating body. The Bavali shear is traceable by a steep but prominent line of separation of crustal units with different densities extending down to a depth of 30 km. The gneisses with 2.73 gm/cc density in the SW part of the profile EE' (north of Calicut) may constitute a synclinal structure terminating along the shear.

Unlike the above profiles, the profile FF', as mentioned earlier, presents a distinct crustal structure, in that, the lower part of the crust (2.85 gm/cc) is more homogeneous, characterized by the absence of high density material (2.98 gm/cc) present in the above profiles. In the SW part of the profile, below the southern charnockite province, the charnockitic rocks (2.76 gm/cc) are seen to

extend down to depths of 15-20 km and merge down with the lower crust (2.85 gm/cc). The contact shows some sharp discontinuities with ~ 45° slope. This may be an expression of faulting and is consistent with surface faults mapped in the region (see figure 2.2). The boundary of the southern charnockite terrain with the gneisses in the NE is also a sharp boundary which may also be a faulted contact. Further to the NE, the down dip extension of the Bavali shear also merges with a low dipping density discontinuity in the crust. This may indicate that the shear has a tendency to become listric in this part of the region.

#### 6.5.4.3 Alternative Model

The gravity anomalies along the profile AA' to EE' were modelled with Moho configuration obtained from the crustal thickness data inferred from regional Bouguer anomalies (as outlined in section 6.4.2). For this Moho configuration, the models required a high density material (2.98 gm/cc) with large dimensions diminishing from profile AA' to EE' in the lower part of the crust. Alternatively, the observed gravity high over the northern charnockite province can be explained solely by a Moho rise. In order to check the possibility of such a feature, two profiles (AA' and BB') were selected. The profiles AA' and BB' modelled on this basis are presented in Fig. 6.11 and 6.12. It may be seen from the models that a sharp rise of the Moho in AA' and BB' by about 25 km would be necessary to account for the gravity high. Such sharp rises in the Moho within a strike length of approximately 100 km seems unlikely. However, a slight rise (of the order of 2-3 km) of the Moho in the region has already been inferred from the

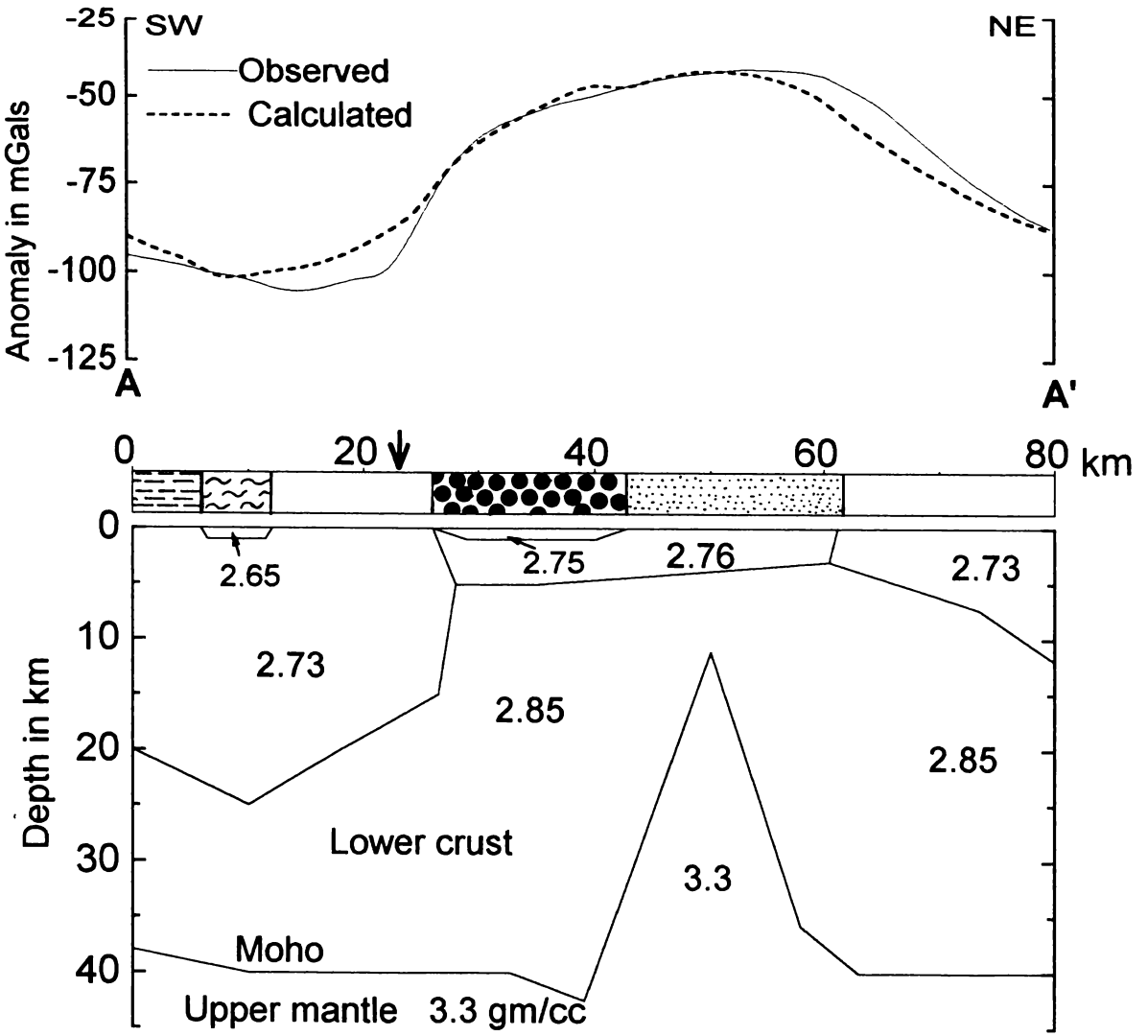


Fig. 6.10. Interpreted crustal thickness (alternative model) along profile AA'. See text for more details.

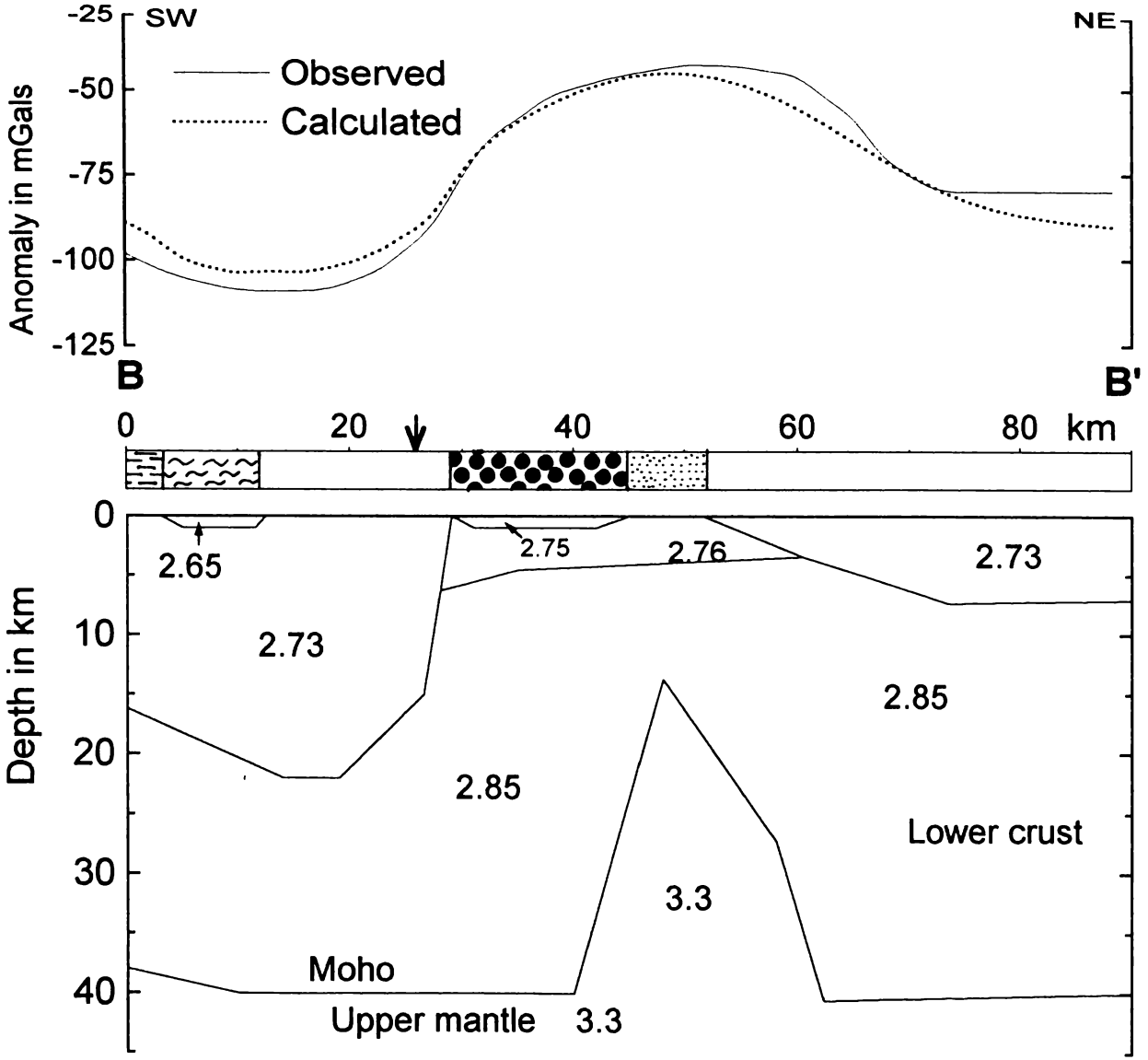


Fig. 6.11. Interpreted crustal thickness (alternative model) along profile BB'. See text for more details.

crustal thickness estimated from the 1/4° x 1/4 ° averaged Bouguer anomalies as discussed earlier (section 6.4.2). A proper matching of the contributions from a rise in the Moho and the presence of high density layer at the bottom of the crust can be resolved only by constraining the models with seismic data.

## 6.6 Geological Implications

The gravity modelling, applying different techniques have generated insight into several crustal characteristics below the part of the SGT studied in this work. Although it is difficult to construct a generalized model of crustal evolution for the terrain from the now available gravity data alone, the features do constrain several aspects of crustal evolution and throw light on some of the major events involved in it.

A major outcome of the present study is the recognition within the SGT, the coexistence of crustal segments with different gravity signatures on either side of the Bavali shear. The NE block defines a major gravity high towards its western half, the northern charnockite gravity high (NCGH), while the SW block encompass a gravity low towards its eastern side, the Wynad Plateau gravity low (WPGL).

As evident from the Bouguer anomaly map and the modelled profiles, the gravity high over the northern block corresponds very characteristically with the boundary of the charnockite in the area. The crustal models arrived at especially

in the AA' to EE' profiles, point to the presence of a thick crust (~ 38 km) with a high density mass (2.98 gm/cc) at its bottom that dwindles in its dimension towards Mysore-Wynad region in the east. The presence of such a high density mass would correspond to seismic velocity of nearly 7.2 km/sec and is consistent with the existence of such velocities in many Proterozoic crustal segments of major Precambrian cratons elsewhere in the world (Christensen and Mooney, 1995). Such a velocity layer is also present in the lower crust below the Karnataka craton along the Kavali-Udipi DSS profile (Kaila et al., 1979). The presence of high density layers in the lower crust therefore is not an uncommon feature. However, it is possible that instead of such a high density mass in the lower crust the gravity high is actually due to a rise of the Moho. The alternate modelling attempted with Moho rise as the source for the gravity high (presented in Fig. 6.10 and Fig. 6.11) reveals that a 25 km of rise of the Moho would be needed to account for the gravity high. Such a rise in the Moho would imply large scale rifting and the related tectonics in the form of, for example graben formation, for which the area does not provide any evidence. Further, the crustal thicknesses estimated from 1/4°x1/4° average Bouguer anomaly values preclude such extreme localized thinning of the crust in the region though minor undulations of 2 to 3 km in the Moho are inferred.

The block SW of the shear is characterized by a crustal thickness of 38-41 km and has a more or less homogeneous crustal configuration, wherein not much density variations are seen. The observed gravity in this region can easily

be accounted for by the two layer crustal model with minor variations in the thickness of the upper part of the crust (see model along FF').

The Bavali shear (which is a steeply southerly dipping structure of around 100 km length and 10 km width) is manifested in the gravity profiles by a steep gravity gradient. The gravity models consistently exhibit a plane separating two contrasting crustal densities below the Bavali shear. This plane dipping steeply towards south can be regarded as the downward extension of the fault. It has been possible to model the downward extent of the structure to a depth of 32 km. However, in the models (AA', BB' and DD') this downward extension meets a slight rise in Moho indicating that this could be a mantle fault. The behaviour of the Bavali shear along Wynad region tends to become listric which may be a reflection of the differences in the stress field in Wynad region compared to the NW region.

A study of the shear sense indicators in the mylonites along the Bavali shear zone by Soney (2000) reveals that the horizontal component of the shear has a dextral mode. The dip slip component of the shear is such that the northern block has moved up with reference to the southern block, and since the mylonite foliations dip along the hade of the fault the shear zone itself is a normal fault (Soney, 2000).

A major debate centers around whether the several shear zones in the SGT are due to collision of micro continents or due to the differential exhumation of the high grade domains. The P-T estimates of the metamorphic rocks on either side of the Bavali shear indicate that the northern block recorded 10 to 12 Kb pressures at which the rocks were evolved, while those south of shear zone register only 6 to 8 Kb pressures (Soney, 2000). The exhumation levels inferred for the northern block is ~ 35 km and the southern block is ~ 25 km, implying differential uplift of the two blocks.

The high density material in the lower crust seen along the profiles AA' to EE' profiles below the northern charnockite province characteristically dwindles to the SE and disappears in the FF' profile across the Wynad plateau. Such a behaviour may imply that this material is an intrinsic part of the crustal structure below the province. A number of possible inferences on the genesis of this high density mass could be made.

- It may have evolved along with the protoliths of the charnockitic rocks which were metamorphosed around 2500 Ma (Radhakrishna et al., 1990). The charnockitic rocks of the region have formed at pressures of some 10 – 12 Kb (Soney, 2000) equivalent to a depth of ~ 35 km. The present crustal depths estimated by gravity are 38-40 km. It is therefore possible that the crustal thickness during the late Archaean in the region may have been ~70 km (cf. Harris et al., 1982). Such a thickening may have been due to underplating by a protoliths of the charnockites.

- It may have originated along with the intrusives of gabbro or anorthosites and have been localized in deeper portions by virtue of the higher density of the magmas from which they were evolved. It is relevant to mention that the gabbro and anorthosite rocks are seen exposed on the surface in and around the northern charnockite province. In an independent analysis of gravity field over the anorthosite of northern charnockite province (presented in chapter VII), the Ashwal (1993) model of genesis has been discussed. According to his model the denser residual fraction, after separation of anorthosite, sinks into the lower crust. The high density material of 2.98 gm/cc may have emplaced in this process.
- It may be possible that the high density body was emplaced during the Pan-African anorgenic event, to which the alkaline and other granitoids in the region have been related. Some of these granitoids such as Kalpatta are in fact in the region of a homogeneous crust, where no high density materiel is present. It is therefore tentatively concluded that the high density mass observed in the lower crust may not be the product of Pan-African orogeny.

Apart from the large massive bodies of charnockites north of the shear zone and west of Virajpet, (Fig.2.2), there are some enclaves or bands of charnockitic rocks of much smaller outcrop dimensions associated with hornblende gneisses and biotite-hornblende gneisses ( migmatite). In the gravity field, these charnockitic rocks , being relatively more dry, may be expected to show up as distinct masses of higher density compared to the associated

hornblendic rocks , which may have a lesser density. This density contrast has been utilized in modelling the charnockitic bodies. In the profiles C-C' to E-E' these bodies show up as bands extending down to a maximum depth of 7 km.

Charnockitic bodies of this nature have been characterised as relics of the transformation of charnockites to gneisses and also as charnockites being formed from hornblende- gneisses Such distinctions in origin have to be necessarily based on petrological studies. Gravity, however, reveals that these are shallow rooted bodies.

## 6.7 Conclusions

Gravity modelling across the Bavali shear zone and adjacent areas has led to the following major conclusions.

- Crustal thickness estimates based on regional gravity anomalies, on assumptions of isostatic equilibrium, leads to values of 38-41 km in the region.
- The region consists of two distinct terraines as identified by gravity anomalies, the western part characterized by both vertical and horizontal heterogeneity in density distribution and eastern part characterized by fairly homogeneous density distribution. In the western part a large high density body of 2.98 gm/cc occupies lower part of the crust and is seen over the northern charnockite province. A slight rise in Moho by 2 to 3 km is also observed below the high density material. An alternative model

appealing to a Moho rise alone in order to explain the observed gravity high over the charnockite province required almost 25 km rise. It has been concluded that such large uplift of the Moho is unrealistic and is not in keeping with tectonics of the region, though a combination of dense masses and a Moho rise is not ruled out and will have to be based on seismic data.

- The Bavali shear is manifested in the gravity profiles by a steep gravity gradient. The gravity model exhibits a plane separating two contrasting crustal densities below the Bavali shear. The steeply dipping plane is seen to extend down to a depth of 30 km and in some profiles meets with a slight Moho rise. This characterizes Bavali fault as possibly a mantle fault. However, in the eastern part it has a tendency to become listric at a depth of around 15 km. Such a change in fault behaviour may indicate variations in the stress field.
- Several plutonic bodies in the region, such as granite, gabbro, supracrustals like Vengad and several bands of charnockites seem to be shallow bodies that do not extend upto great depths.

*Chapter VII*

# Interpretation of Gravity Field over the Perinthatta Anorthosite

## 7.1 Introduction

Gravity investigations over anorthosite massif regions have been a subject of interest to many researchers ( Simmons, 1964; Bukharev et al., 1973; Hodge et al. 1973; Verma et al. 1975; Kearey, 1978; Mukhopadhyay, 1987; among others) and have provided valuable constraints on their tectonomagmatic setting. Unlike other plutonic masses, there is no definite gravity signature assigned to anorthosite plutons. Since anorthositic rocks are generally interpreted as accumulations of magmatically differentiated plagioclase crystals, large bodies of mafic (gabbroic) rocks can be expected at shallow crustal levels. The gravity field analysis thus may provide valuable information on the shape and extent of the pluton, petrological variations within the body, presence or absence of large quantities of mafic units complementary to the anorthositic rocks and their relation with major structures.

The Perinthatta anorthosite is one among the series of mafic to felsic intrusives associated with the Bavali shear and Wynad schist belt (Nair et al. 1976). The anorthosite massif is emplaced within the high grade metamorphic rocks of northern Kerala mainly surrounded by charnockites and pyroxene granulites (Fig.7.1). The Ezhimala igneous complex which is 10 km. southwest of Perinthatta is another major pluton in the region. The Perinthatta anorthosite, first reported by Vidyadharan et al. (1977), has an approximate areal extent of 60 $km^2$ and is presumably of late Proterozoic age. As the area is partly covered by laterites and coastal sedimentaries, the actual areal extent of this pluton is not

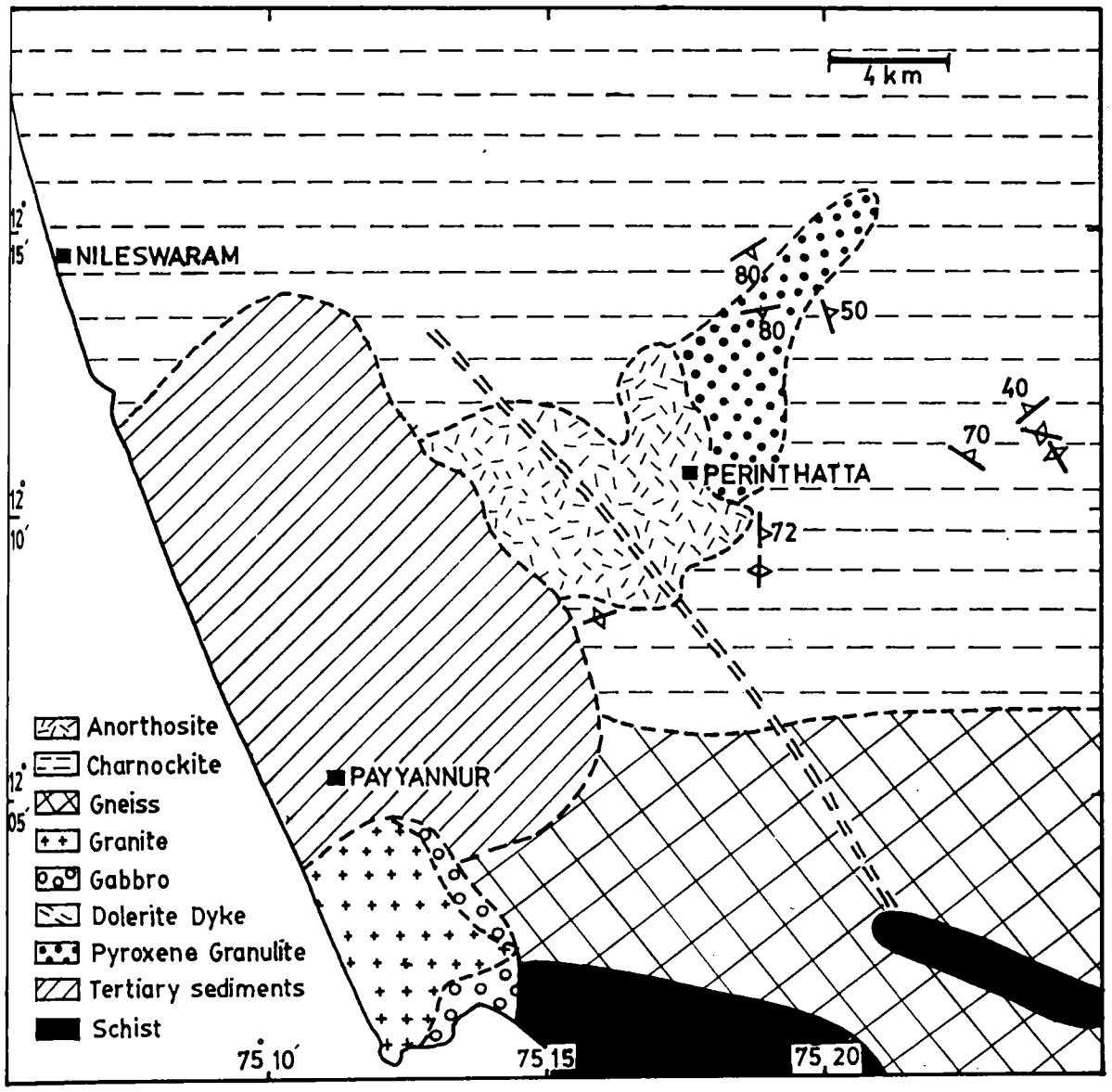


Fig. 7.1. Detailed geological map of the Perinthatta anorthosite and surrounding regions.

certain. Petrographic and geochemical analysis of the rocks were presented by Nambiar et al. (1982), Ravindrakumar(1986) and Nambiar et al.(1997). Petrographically the pluton is essentially made up of anorthosite ( with more than 90% plagioclase) and mafic variants like dioritic anorthosite and anorthositic diorite and rare occurrence of Fe-Ti oxide rich rocks ( Nambiar et al. , 1997). In order to understand the nature and subsurface extent of this pluton, a detailed gravity survey has been conducted along all possible roads in the region with an approximate interval of 1 km.

## 7.2 Density Measurements

As a prerequisite to gravity modelling, density measurements were done for representative samples of anorthosites and country rocks viz; charnockites, granulites, gneisses and gabbros and the results are summarized in chapter III (Fig.3.1). The anorthosites show an average density of 2.77 gm./cc and most of the samples range between 2.70 - 2.84 gm./cc. The charnockites, which form the dominant country rock, are essentially felsic type with minor enclaves of mafic granulites (Nambiar,1987) and give rise to an average density of 2.76 gm/cc, slightly lighter than the anorthosite rocks (Fig.3.1). This density value is in good agreement with the density estimates for acid to intermediate charnockites given by Subrahmanyam and Verma (1981); however, density for anorthosite rocks given by them is much higher than our estimate because their samples were more gabbroic in composition.

## 7.3 Bouguer Anomaly Map and Its Interpretation

Based on nearly 150 gravity observations collected over Perinthatta and adjoining regions of northern Kerala, a Bouguer gravity anomaly map was prepared with a contour interval of 2 mGal. and the same is shown in Fig. 7.2. The outlines of major geological features are also shown in the figure for comparison. The gravity anomaly map, when correlated with the geology of the area, brings out a few interesting aspects. The gravity high gradient zone seen in the southern part of the map correlates with a major shear (Bavali shear) which lies almost along southern border of the map area and takes a curvilinear trend towards the coast south of Ezhimala The NW part of the region is characterized by a gravity high centered over Nileswaram. Though the gravity field over the anorthosite region conspicuously does not show any anomaly, two minor closures within the anorthosite are noticed. Further, the contour pattern suggests that the anomalies due to the anorthosite have been masked by the regional gravity field over the surrounding high-grade metamorphic province. In order to isolate the gravity field of the anorthosite body from the rest of the geological features, we carried out regional – residual separation of the observed anomaly map. For this purpose, a total of six parallel profiles AA' to FF' ( profiles location shown in Fig.7.2) were considered covering the whole area. The regional gravity field for these profiles was obtained by using both graphical method and by defining a first order least-square polynomial curve to the data (Radhakrishna Murty, 1998) (Fig. 7.3). The residual anomalies were obtained by subtracting the regional from the observed anomalies. In both the cases the residual anomaly

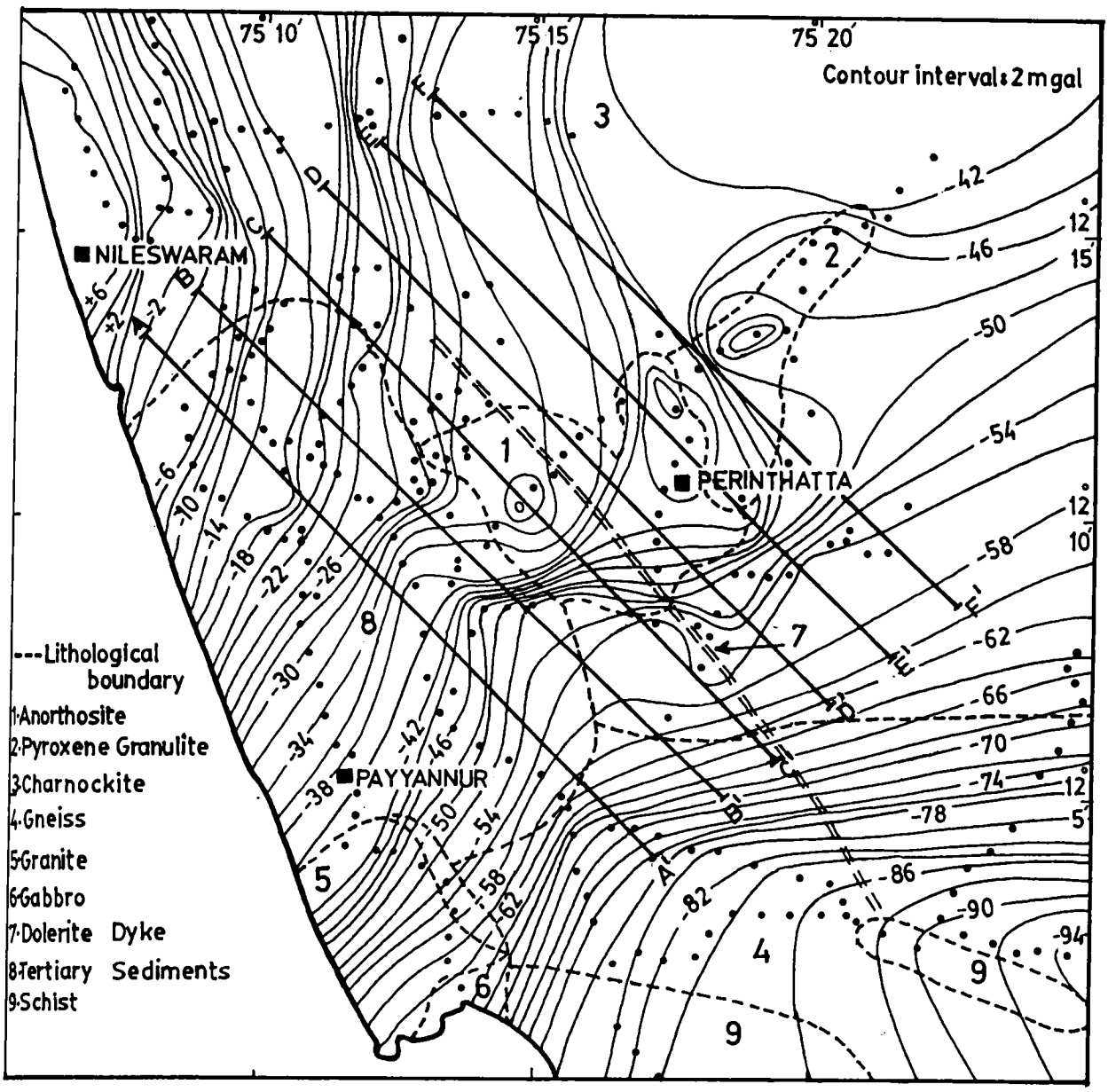


Fig. 7.2. Bouguer anomaly map of the Perinthatta anorthosite and adjacent regions. The dashed line and the inside numbers indicate lithological boundaries as shown in the legend. The location of six profiles AA' through FF' considered for regional-residual separation are also shown in the map.

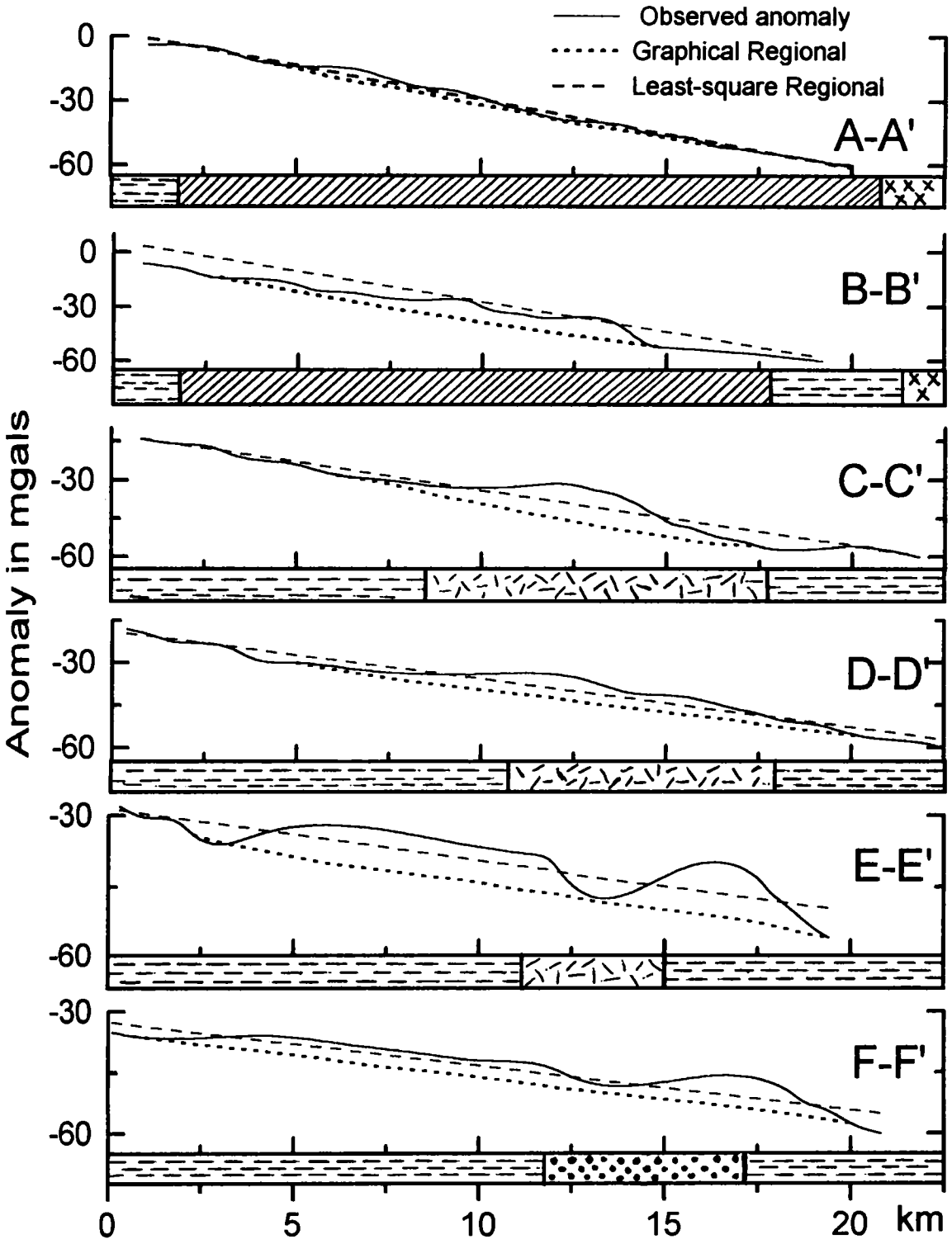


Fig. 7.3. Map showing the six profiles AA' through FF' considered for regional-residual separation. The regional gravity field for these profiles were obtained by using both graphical and least-square techniques. The dashed line indicate the least-square regional while the dotted line indicate the graphical regional. (see section 7.3 for details). Symbols for the rock types are same as those in Fig. 7.1.

shows a gravity high over the anorthosite body except that the least-square residuals were smaller in amplitude and contain pseudo-anomalies. Since graphical regionals were guided by the anomaly trend and based on surface geology, we considered the residual anomalies obtained from graphical method for further analysis. The residual anomalies were contoured, and as can be seen from the map (Fig.7.4), the outcrop of the pluton nicely matches with the estimated positive residual anomaly and the contours display nosing in all four directions. The map suggests subsurface extension of the pluton covering an area of more than 100 $km^2$. It also brings out four gravity high closures with highest anomaly of 12 mGal occurring in the central part of the anorthosite body. The trend of contours and the localized gravity high closures indicate that the gravity anomalies cannot be attributed to a single high density mass at depth. In spite of Perinthatta anorthosite being higher in density with respect to the surrounding rocks, the overall gravity field is much lower, in contrast to gravity field observed over Bankura anorthosite (Verma et al., 1975) or Bengal anorthosite ( Mukhopadhyay, 1987).

## 7.4 Gravity Models

Three profiles (**I I'**, **J J'** and **K K'**) selected from the residual anomaly map were interpreted in terms of structures of anorthosite body (see Fig. 7.4 for location). The observed gravity highs cannot be explained due to anorthosite alone as the density contrast between the anorthosite rocks and the charnockite is only 0.01gm/cc. Profile **I I'** shows two distinct gravity highs, one in the central

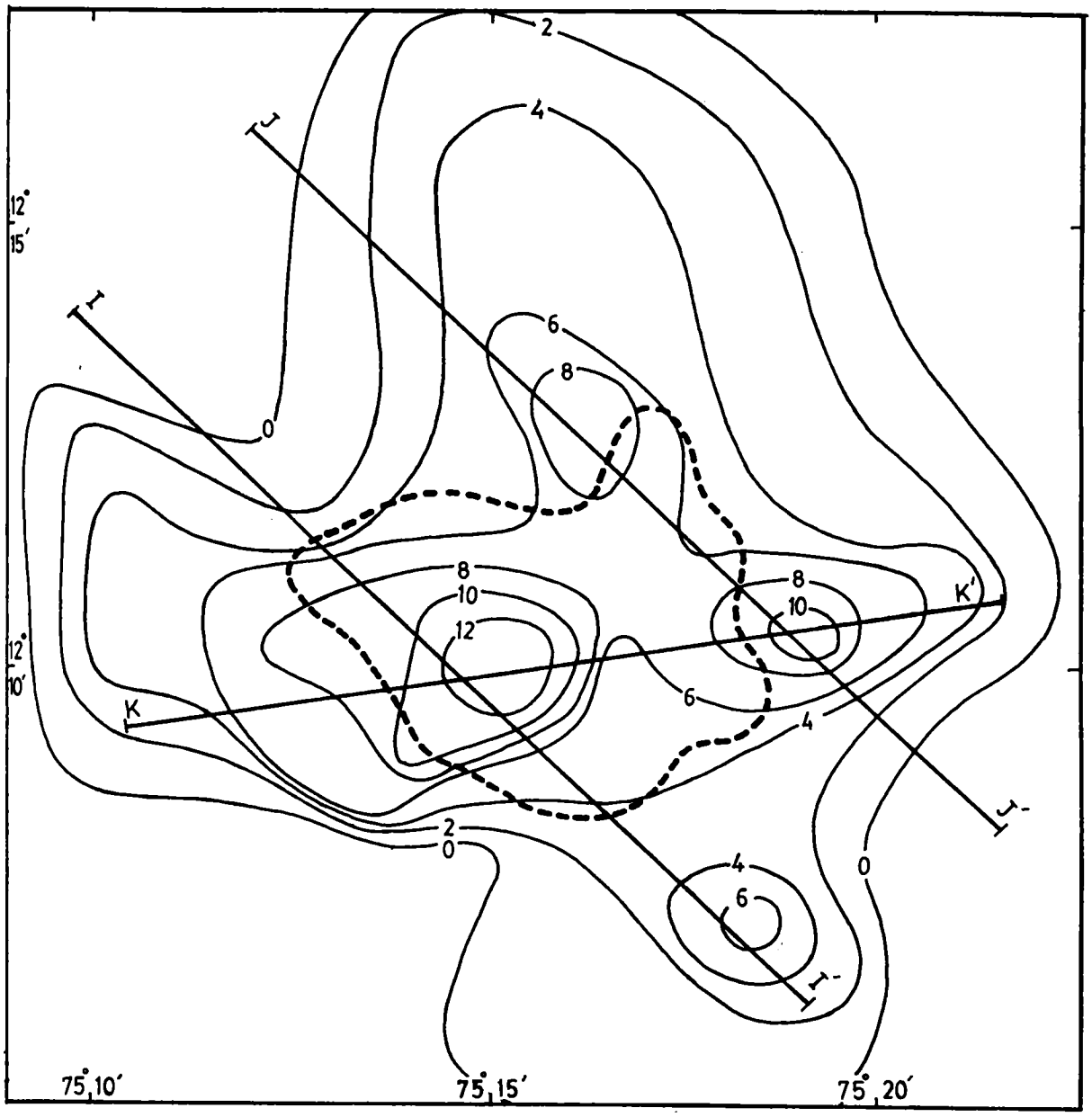


Fig. 7.4. Residual gravity anomaly map of the Perinthatta anorthosite region. The dashed line shows the surface exposure of the pluton. The profiles II' to KK' were considered for gravity modeling.

part of the anorthosite and the other high near the anorthosite- charnockite boundary (Fig.7.5). A body with higher density (2.9 gm/cc) approximately of cylindrical shape ( $\simeq$ 2.5 km diameter) extending down to 7 km is required to explain the central high while the other gravity high also requires a similar body but of smaller dimensions. Profiles **J J'** and **K K'** also display similar gravity signatures(Fig. 7.5). The interpreted models indicate a 2 km thick lens shaped anorthosite body which subjacently extends into the surrounding rock types giving a total area of >100 $km^2$. Four approximately cylindrical shaped bodies were inferred to lie beneath this lens shaped body. These bodies are of 2.9 gm/cc density and extend to 3 to 7 km depth. The rocks corresponding to this density seen associated with the Perinthatta anorthosite are the mafic variants with very high contents of mafic minerals or the sporadically seen Fe-Ti oxide rich rocks.

## 7.5 Discussion

Various theories on the genesis of massif type anorthosites involving contrasting magma composition and mechanism of intrusion assign different possible forms and structures to such plutons. Anderson and Morin (1968) classified anorthosites into labradorite anorthosites occurring as funnel shaped bodies with a mafic root and the andesine anorthosites which are usually sheet like or domical. Shapes of massif type anorthosites are extremely variable owing to factors like buoyancy force of rising as in the case of Morin massif (Martignole and Schrijver , 1970) or solid-state deformational affects as seen in

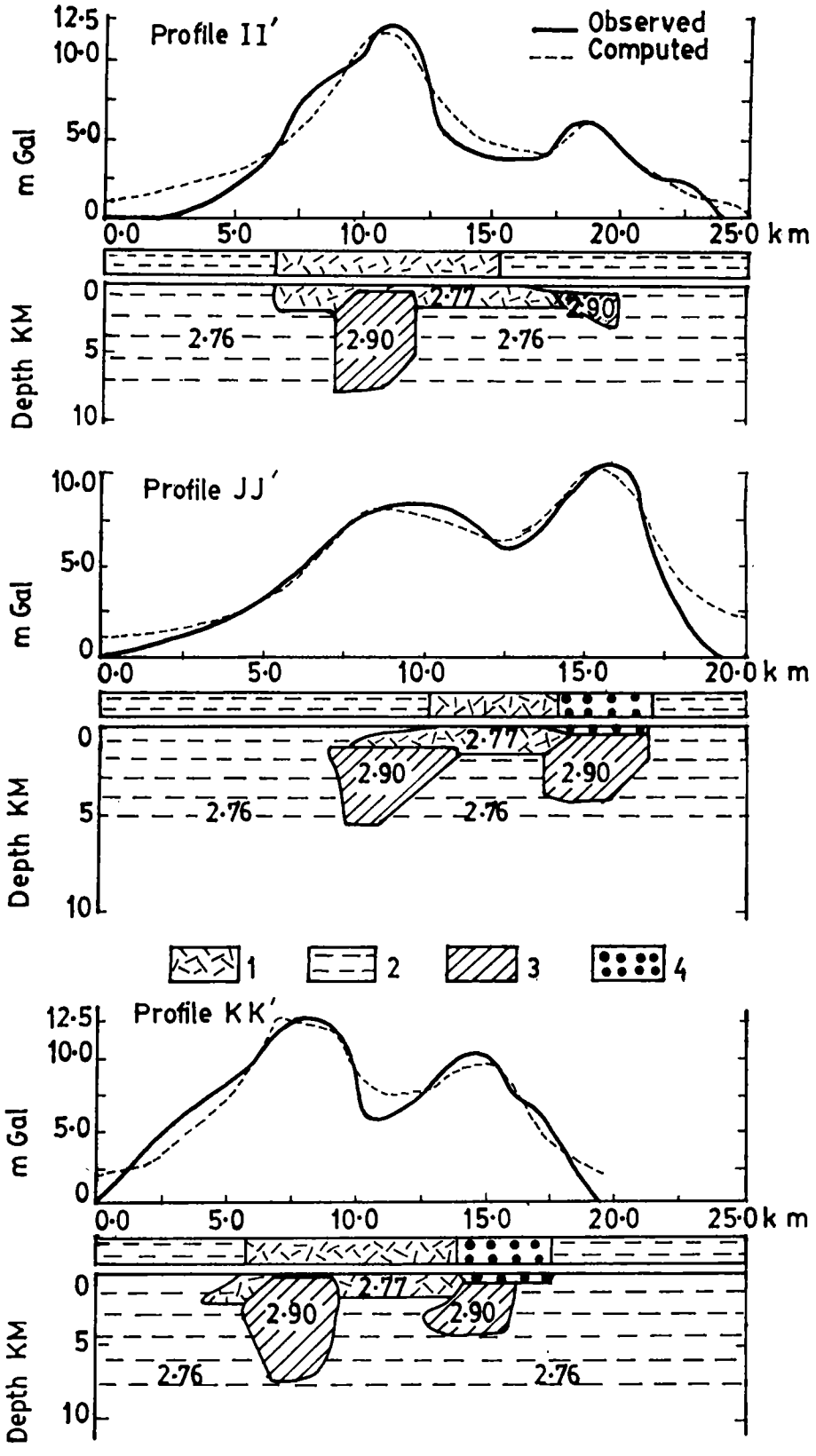


Fig. 7.5 . Gravity models showing the structure of Perinthatta anorthosite along three selected profiles. Location of the profiles are shown in Fig. 7.4. 1. Anorthosite 2.Charnockite 3.High density cylindrical body 4.Pyroxene granulate.

some of the anorthosites of Parry Sound regions of Greenville province (Davidson, 1984) and in some cases their multiple intrusive character ( Duchesne et al. 1985; Roy et al. 1986).

Geophysical investigations have been found to be very helpful in understanding the shape and size of anorthosite bodies, mass-heterogeneties within the pluton, the nature of feeder pipes or dykes if present and the presence or absence of underlying large mafic bodies complementary to anorthosites.

Kearey (1978) suggests that the nature of the gravity anomaly is governed not only by the rock type onto which it is intruded but also by the relative proportion of mafic to felsic constituents at depth. The negative gravity anomaly over Adirondacs massif has been analyzed by Simmons (1964) as indicating a tabular body of anorthosite 3-4.5 km. with two cylindrical feeder pipes about 6 km. diameter extending to about 10 km. depth. Positive gravity anomalies over Laramie anorthosite massif of Wyoming has been interpreted as a plate of 4 km thickness without feeders by Hodge, et.al.(1973) with a positive density contrast with the surrounding granite. Similarly positive gravity anomalies over Egersund anorthosite of Norway has been interpreted as a plate like mass 4 km thickness without feeder pipes (Smithson and Ramberg, 1979). Kearey (1978) proposed for Morin anorthosite, Quebec as a slab of 2-4 km thickness with several feeders. Similar geometrics has been proposed for some of the Ukrainian examples also (Moshkin and Dagelaiskaya, 1972; Bukharev et.al. 1973) on the basis of gravity data. These examples indicate tabular or lens

shaped or thin sheet like or pancake shape for anorthosite bodies with or without feeder pipes characterized by absence of large mafic or ultramafic units complementary to anorthosite required in the cumulate models of anorthosite genesis.

However in several cases the large mafic cumulates complementary to anorthosite massifs were observed. The positive gravity anomalies associated with the anorthosite intrusion of eastern Grenville province has been interpreted as due to large gabbro bodies underlying and extending to mid-crustal depths (Tanner ,1969; Thomas, 1974; Keary and Thomas, 1979). The interpretation of the gravity high observed over Bankura anorthosite has been interpreted as due to a high density mass of gabbroic composition with a maximum depth of 5 km underlying the anorthosite body of 200m thickness (Verma et.al., 1975). The positive gravity anomalies observed over the eastern part of the Duluth complex (Davidson, 1972) and over the San Gabriel anorthosite(Long and Grannel, 1971) suggests the presence of high density intrusive mass at depth. Aeromagnetic data over the San Gabriel anorthosite has been interpreted by Cummings and Regan (1976) concludes that the anorthosite of 3.4 km thick is underlain a gabbro-norite body.

Thomas (1990) describes four types of gravity signatures associated with anorthosites: prominent negative anomalies , interpreted as slab-like bodies 2-14 km thick with or without feeder pipes; prominent negative anomalies with

smaller positive anomalies, interpreted as anorthosite masses 4-19 km thick with subsidiary gabbroic or tractolitic intrusions; prominent positive anomalies associated mainly with gabbroic masses, interpreted as saucer or funnel shaped bodies representing the lower levels of chambers within which anorthosite had formed, but was subsequently removed; and extensive regional positive anomalies, interpreted as uplifted blocks of lower crust composed largely of mafic material complementary to anorthosites. Thus he concludes the presence of mafic cumulates complementary to massif-type anorthosites in some cases.

All these above investigations suggest that the shape and amplitude of the gravity signature, the geologic setting in which anorthosite has been emplaced and post-emplacement deformation are the main contributing factors in deciphering the structure and its tectono-magmatic evolution. Except the minor shearing observed at few places, the Perinthatta anorthosite has not been subjected to any major deformation or recrystalisation ( Nambiar et al., 1982 ; Nambiar et al., 1997 ). From the interpretation of the gravity field over the area, the Perinthatta anorthosite in plan has an irregular boundary, somewhat amoeboidal with cylindrical high-density masses beneath them. The four cylindrical bodies of 3 to 7 km. depth below the lens shaped anorthosite body could be either feeders or mafic/oxide rich anorthosite material sagged down during their crystallisation. It is possible that each such cylindrical mass is capped by small anorthositic lens which together formed individual units of the anorthosite pluton. This lends support to the last stage of the petrogenetic model

postulated by Ashwal(1993) (Fig. 7.6) for the evolution of Proterozoic massif type anorthosites which involves the rising of plagioclase rich mushes and coalescing in the upper crust to form the massifs.

## 7.6 Summary and Conclusions

Gravity surveys have been carried out over the Perinthatta anorthosite and the adjoining regions to decipher the structure, shape and extent of the pluton. The density measurements suggest that the anorthosite rocks have an average density of 2.77 gm/cc slightly higher than the average density of 2.76 gm/cc for the surrounding country rocks. The Bouguer anomaly map revels the absence of any conspicuous gravity anomaly corresponding to the plutons and thus precludes the existence of larger portions of the pluton in the immediate subsurface region. The residual gravity map obtained by regional-residual separation method shows a minor positive gravity field of irregular shape with localized highs of 6 – 12 mGal within and around the anorthosite body. Two-dimensional gravity interpretation of profiles across the pluton suggests subjacent nature and lensoid shape for the anorthosite which is underlain by small isolated cylindrical bodies ( $\simeq$ 2.5 km diameter) of higher density ( 2.9 gm/cc) extending 3 – 7 km downwards. These cylindrical bodies are inferred as either the mafic/oxide rich portions of the pluton sagged down during crystallization or the individual feeders of the plagioclase – rich mushes, which coalesced in the upper crust to give rise to the massif.

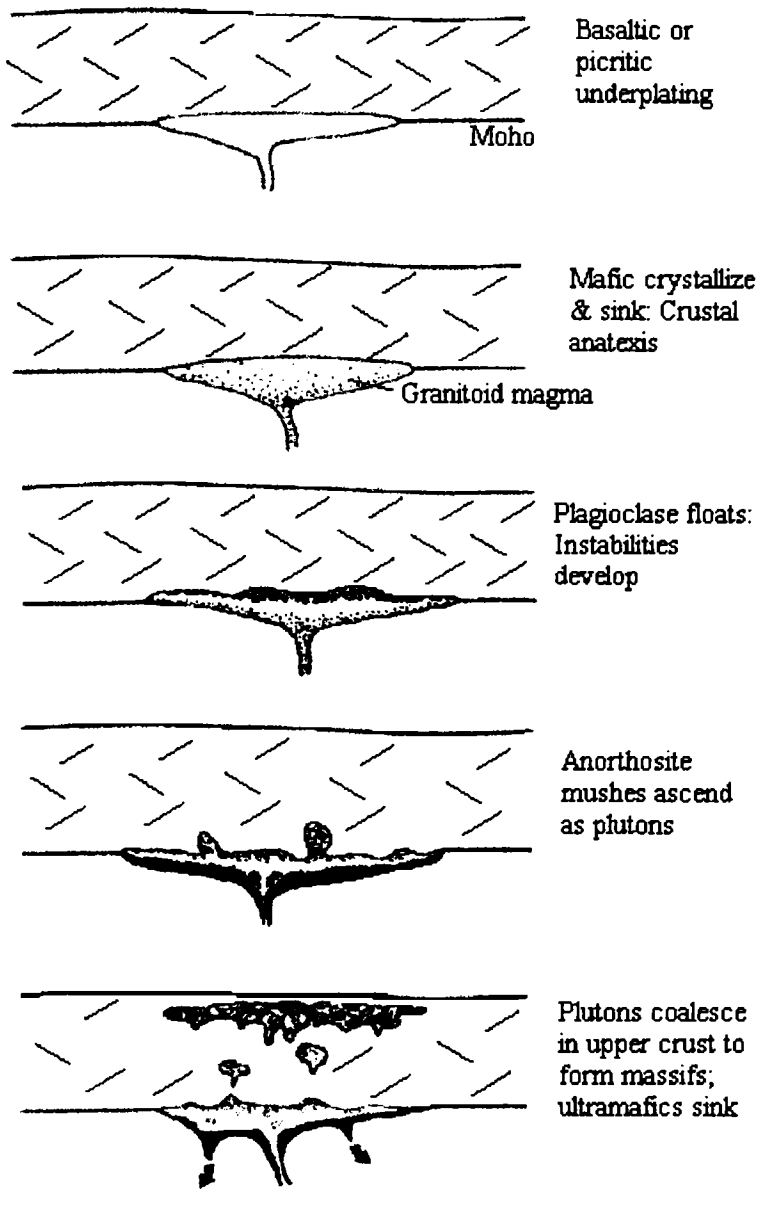


Fig. 7.6. Schematic diagram showing a plausible model of massif type anorthosite genesis (after Ashwal, 1993).

# *Chapter VIII*

# Interpretation of gravity field over the Kalpatta Granite

## 8.1 Introduction

The deep crustal section of southern India, comprising dominantly of granulite facies rocks, is punctured by a suite of alkali granites and syenites ranging in age from 550 – 765 Ma. Most of them lie on or close to major late-Proterozoic lineaments (Table 8.1). These intrusives indicate a long-lived magmatic activity in the time span from late Proterozoic to early Paleozoic, coinciding with pan-African events. Santosh and Masuda (1991) made a detailed mineralogical, geochemical and isotopic study of these alkali plutons and suggested magma derivation from deep crust or upper mantle. Study on oxygen and sulfur isotopic compositions of these plutons by them indicate source heterogeneities, varying degrees of fluid rock exchange and supracrustal interaction. Rajesh et al.(1996) suggested widespread occurrence of these alkali plutons along southern India due to Pan-African felsic magmatism and correlated them with those in other felsic magmatic provinces of eastern Gondwana.

Kalpatta granite is one among the felsic plutons of south India occurring along the southern part of the Bavali shear zone in northern Kerala (Fig. 8.1). Here, a brief evaluation of various studies related to the structure, form and emplacement mechanisms of granite plutons through geological and gravity studies has been made.

**Table 8.1 Summary of geologic and mineralogical characteristics of some alkaline plutons of southern India** (modified after Santosh and Masuda, 1991)

| Pluton | Related fault/ lineament | Country rock | General mineralogy | Age (ma) |
|---|---|---|---|---|
| Angadimoger | Mercara, Mangalore | Migmatitic gneiss | Quartz-K-feldspar-plagioclase hornblende-riebeckite-acmite-zircon-sphene | 638 |
| Ezhimala | Bavali | Migmatitic gneiss | Granite: Quartz-K-feldspar-plagioclase-biotite-sphere Gabbro: Plagioclase-augite-biotite-apatite-sphere | 678 |
| Peralimala | Bavali | Migmatitic gneiss | Quartz-K-feldspar-alkali amphibole-garnet-sphere-biotite | 750 |
| Kalpatta | Bavali | Migmatitic gneiss | Quartz-K-feldspar-plagioclase-biotite-apatite-sphere | 765 |
| Ambalavayal | Bavali | Migmatitic gneiss | Quartz-K-feldspar-plagioclase-riebeckite-hornblende-biotite-apatite-sphere | 595 |
| Vellingiri | Bhavani | Migmatitic gneiss | Quartz-K-feldspar-plagioclase-alkali amphibole-aegirine-garnet-spene-phlogopite | n.d. |
| Wadakkanchery | Idamalayer | Charnockite | Quartz-K-feldspar-plagioclase alkali amphibole-apatite-sphene | n.d. |
| Sholayar | Idamalayer | Migmatitic gneiss | Quartz-K-feldspar-plagioclase-augite-akkali amphibole-apatite-sphene | n.d. |
| Chenganno or | Achankovil | Charnockite | Quartz-K-feldspar-plagioclase-hornblende-biotite-sphene | 550 |
| Puttetti | Puttetti | Charnockite | Quartz-K-feldspar-plagioclase-plagioclase-augite-phlogopite-zircon-apatite | 580 |

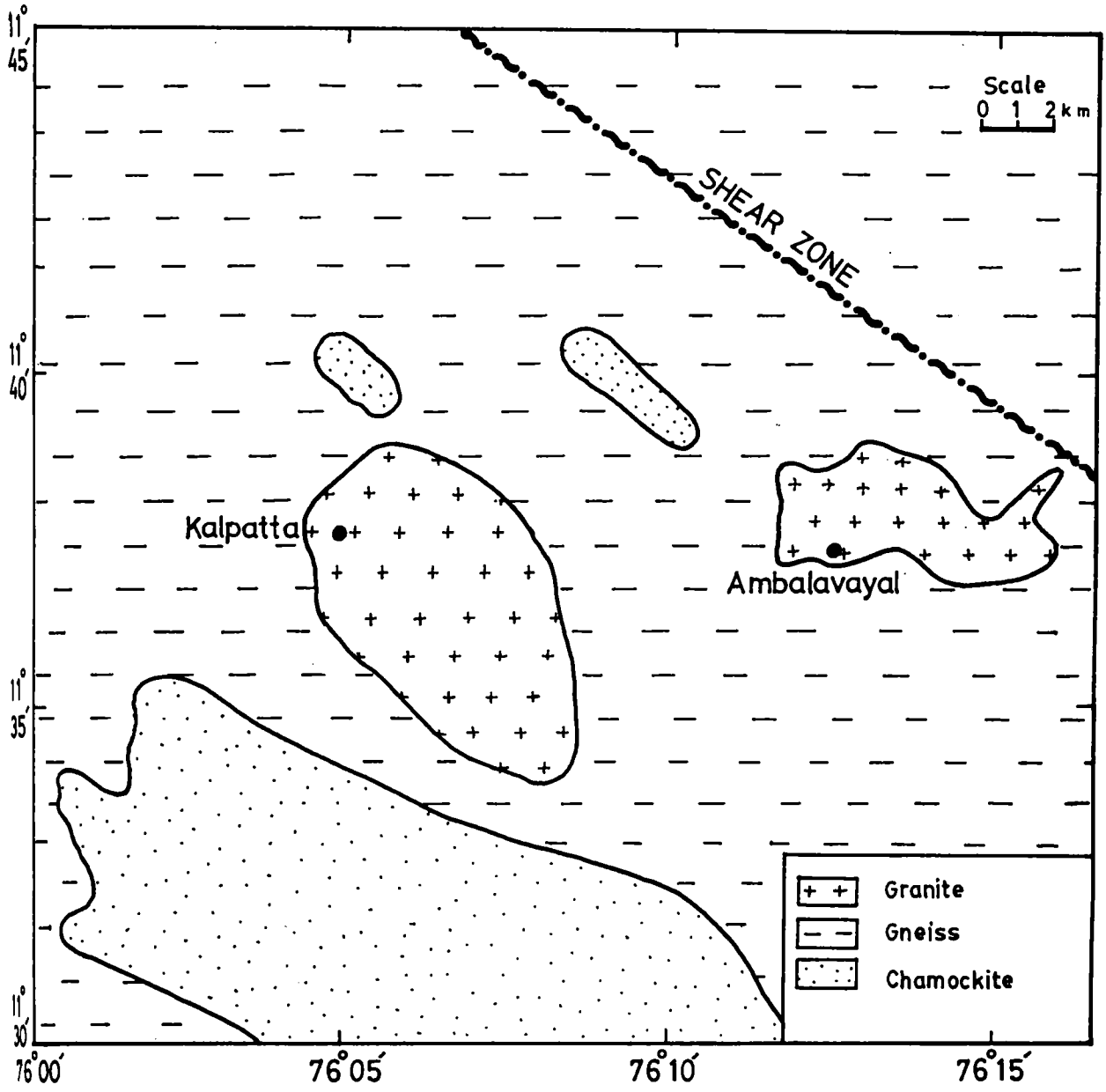


Fig. 8.1. Geological map of the region around Kalpatta granite (modified after GSI, 1995; Kumar et al. , 1998)

The granite is emplaced within the Precambrian gneisses and shows rather sharp contacts with the country rock at certain locations. Rocks of the Wynad schist complex lie towards the northeast of the pluton and are characterized by enclaves of schists/metapelites in a background of a hornblende/ biotite gneiss. Towards the southwestern side of the pluton, a large body of charnockite occurs interbanded with the gneiss. The formations in the area have a WNW-ESE regional structural trend. The structural foliation data of the area has been mapped by Kumar et al. (1998) and is given in Fig 8.2. The map shows a concentration of foliation plots in the NW part of the granite body, while further SE these are less in number indicating that the granite body is more massive. However, the foliation data do not clearly bring out if they are primary flow structures within the granite. In the NW part, the foliation attitudes are of high incidence and are often opposing to each other which would have been consistent with either folded structures or the superposition of more than one generation of foliations. This aspect is further discussed a little later in relation to 3-D shape of the granite body based on gravity modelling.

The Kalpatta pluton is an elliptical stock covering an area of almost 50 sq.km. and its overall character is suggestive of post-tectonic emplacement (Kumar et al.,1998). However, the character of the foliations does not rule out a late-tectonic emplacement. Nearest intrusive to the Kalpatta granite body is the Ambalavayal granite about 10 km east of Kalpatta . Mineralogical and textural

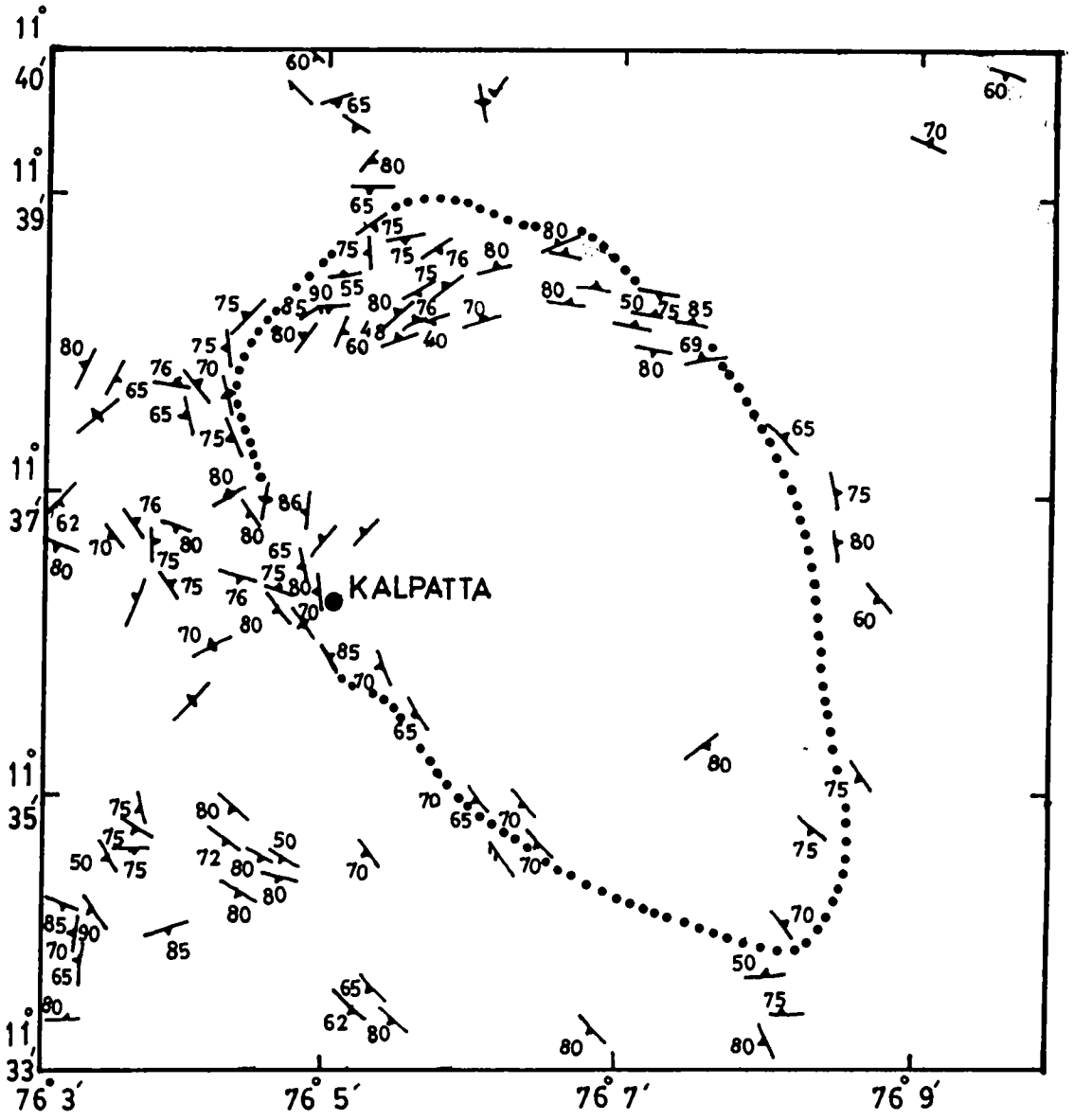


Fig. 8.2. Foliation map of the Kalpatta granite region (after Kumar et al. 1998). The dotted line indicate the outline of the granite body.

data suggest that both these plutons are different from each other as the Ambalavayal granite is foliated and has hornblende as the sole mafic mineral (Santosh and Masuda, 1991). The Kalpatta granite is assigned an age of 765 Ma based on U-Pb zircon dating (Odom, 1982), while K-Ar biotite dating gave an age of 512 ±20 Ma (Nair et.al., 1985). Geochemical investigations of the pluton suggest that the granites and their variants have mineralogical and geochemical characteristics indicative of a polyphased late magmatic crystallisation (Kumar et.al., 1998 ).

## 8.2 Form, structure and mechanism of emplacement of granite plutons: constraints from geological and gravity studies

Granites, the most abundant plutonic rock in the upper crust can occur in any form, but the two-dimensional outcrop shapes of the pluton usually range from circular to more common shapes of elliptical to almost linear. The level of erosion is almost reflected on the areal extent or two-dimensional shape of the granite body. Shapes and structures of the granite pluton generally depict the emplacement history and knowledge of post-emplacement deformation pattern.

Granites are usually associated with large negative Bouguer anomalies caused by their relatively low density contrast with the surrounding rocks. Gravity interpretation can provide valuable information regarding the subsurface geometry of granite pluton which in turn will help in understanding its tectonomagmatic evolution. In the present study, a detailed interpretation of the

Kalpatta granite pluton is attempted in order to study the structure and subsurface geometry and to infer its tectonic significance.

Shape is one of the expressions of ductility contrast between intrusion and envelope, so that smoothly concordant diapirs are expected to evolve towards angular discordant cauldrons as granite magmas stiffen on cooling and rising into a crust of decreasing ductility (Pitcher, 1979). In late-tectonic, high crustal, brittle fracture regimes, the contacts of granite plutons are polygonal, in detail linear and angular, controlled by pre-existing or intrusion produced fracture pattern (Pitcher, 1952; Bussel, 1976). If the ductility contrast is less pronounced, the country rocks are forcibly shouldered aside around smoothly arcuate contacts giving a shape as that of a steep sided, inward dipping cone. Hutchinson(1970) suggested that some tailed tadpole plutons represent an oblique section through such conical body. Some forcefully emplaced plutons would form as great sheets. They may coalesce into parallel sheets, which tongue and wedge their country rocks along their dominant grain as observed in Main Donegal granite (Pitcher and Berger, 1972). Bridgwater et al.(1974) observed mushroom shaped Rapakivi granites of the Proterozic in southern Greenland with inward-dipping floor.

A comprehensive compilation and interpretation of gravity anomalies over granite plutons world over have been made by Bott (1956) and Bott and Smithson (1967), among others. The most common gravity model obtained by

Bott (1956) for post-tectonic plutons is a steeply outward-dipping cone in which the density contrast disappears at depth greater than 10km. The potentiality of gravity surveys as petrological tools has been demonstrated by Bott and Smithson (1967). They demonstrate how gravity is useful for i) revealing the subsurface shape of plutons ii) determining the extent of gross density variations within granite plutons and iii) providing some evidence on the problems of emplacement and origin of granites. They quantitatively analyzed the gravity anomalies over granite plutons to infer shape, depth and various mechanisms of emplacement. They outlined a method to understand from gravity profiles and to determine whether the contact of the granite slopes inward, outward or is vertical with respect to the surrounding rock. Based on the derived models, Bott and Smithson (1967) suggested various emplacement mechanisms for granite plutons as given below:

***i)Emplacement by forcible intrusion*:** According to this hypothesis, granite emplacement takes place by magmatic intrusion removing the relative dense country rocks aside by force which implies that granite batholiths are floores close to the surface and are laceolithic in form.

***ii) Emplacement by stoping and cauldron subsidence*:** The blocks of country rocks may get separated along fractures and sink into granite magma accompanied by the uprise of granite body. This emplacement mechanism is known as stoping. If the replaced country rock sink as a single block, then it is called "cauldron subsidence".

***iii) Emplacement by granitisation*:** The pre-existing rocks can be transformed to granite by the action of fluids of appropriate composition arising from the depth. This process is known as granitisation.

Bott and Smithson (1967) concluded that a combination of stoping and forcible intrusion models explain satisfactorily several observed gravity anomalies. Hamilton and Myers (1967) interpreted the Sierra Nevada batholith and observed that it is less than 10 km thick and supports a model of accretion of many relatively silicic plutons raising and spreading out at a common shallow level in the crust. Young (1974) interpreted the gravity anomalies over the main Donegal granite and the model indicates a shallow plunging body like a prism. Leake (1978) suggested that the granite bodies could be very thin and may not preserve the shape that would have carried the intrusions upward through the crust. Qureshy et al. (1969) presented the results of gravity studies on some granite bodies of South India, which are associated with gravity lows ranging from –15 to –17 mGal. They inferred, extension of Closepet granite eastward beyond the boundary on the geological map, presence of a large granite body from Satyamangalam to Tammapatti Tamilnadu, a granite mass beneath Mananthavady and Gudalur region of northern Kerala. The gravity lows in Kodaikanal, Gudalur and Erode regions have been explained as due to the presence of three concealed granite batholiths at depth by Krishna Brahmam and Kanungo (1976). Subba Rao (1990) estimated the thickness of Singhbhum

granite batholith from gravity anomalies and the model gives rise to nearly 15 km thick granite body.

## 8.3 Bouguer Anomaly Map and its Interpretation

Based on 125 gravity observations in the area, a Bouguer anomaly map has been prepared with a contour interval of 2 mGal (Fig. 8.3 ). It can be seen from the anomaly map that a regional NW-SE gravity gradient zone on which a gravity low of the order of 8-10 mGal has been centered over the Kalpatta granite pluton. Though data were collected along all possible roads in the region, part of the area between Kalpatta and Ambalavayal shown in the map is less accessible due to thick reserved forest and non-availability of roads and hence data control is less here. A minor low of the order of 4-6 mGal is observed over the nearby Ambalavayal granite . The geometry of the contours as well as elliptical nature of the pluton, permit a detailed analysis of the gravity field over the Kalpatta granite.

For the purpose of regional – residual separation, 10 approximately N-S and 10 E-W profiles have been considered covering the pluton (given as N1 to N10 and E1 to E10 in Fig. 8.3). The separation was made using the graphical method of smoothing (Fig.8.4 (a) and (b)). Regionals for these profiles were fixed guided by the anomaly trends and based on the surface exposure of the pluton and by matching the regional anomaly at the intersecting points. The method is fairly reliable, particularly when sufficiently good geological information

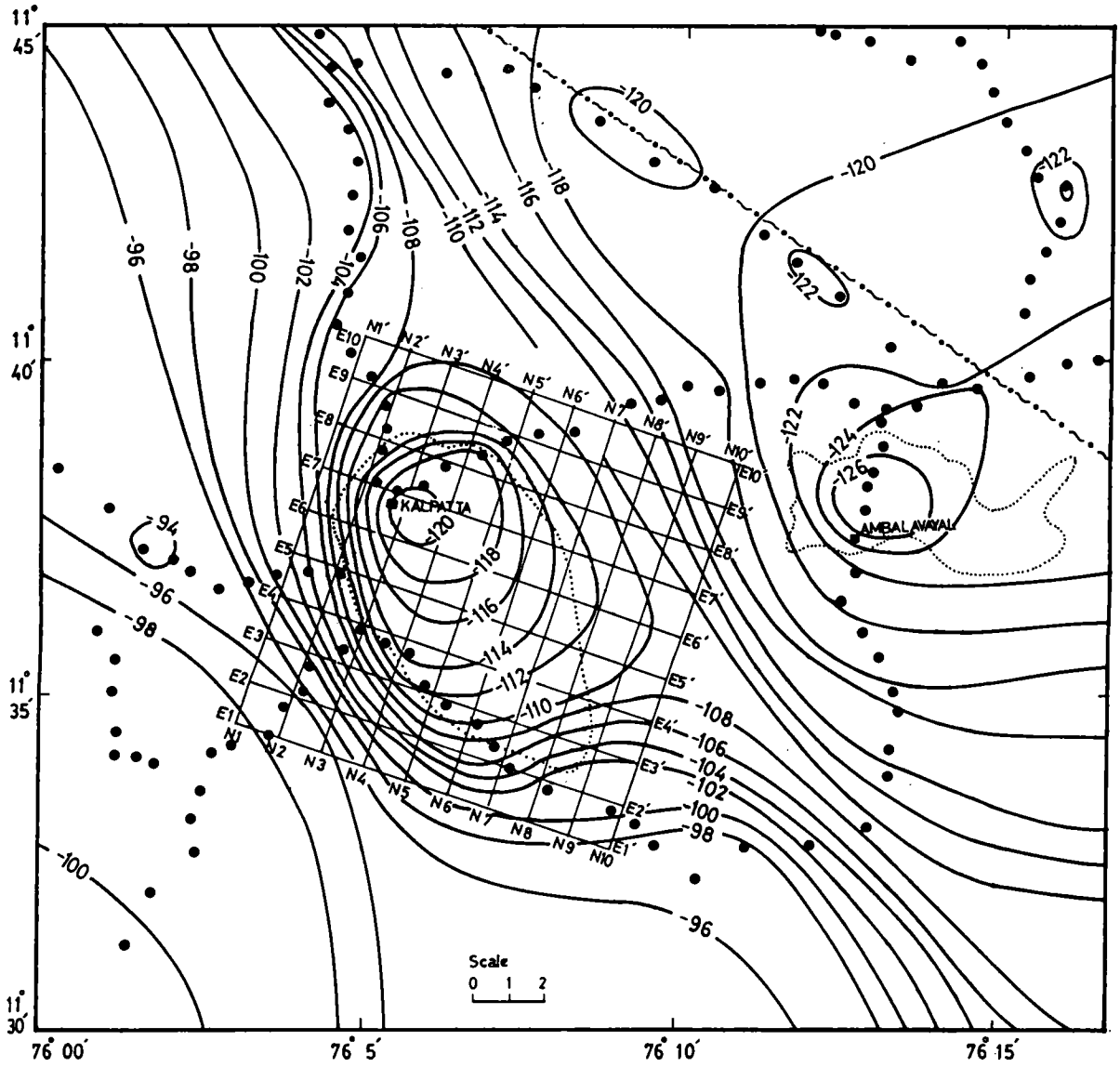


Fig. 8.3. Bouguer anomaly map of the Kalpatta granite and the adjoining regions (contour interval is 2 mGal). Solid circles indicate the locations of gravity observations. The small dotted lines indicate the surface exposure of the Kalpatta and Ambalavayal granite bodies. The location of the Bavali shear zone is also shown on the map. The location of the 10 approximately north oriented profiles (N1-N1' through N10-N10') and 10 east oriented profiles (E1-E1' through E10-E10') used for the preparation of residual anomaly map of the Kalpatta granite are shown.

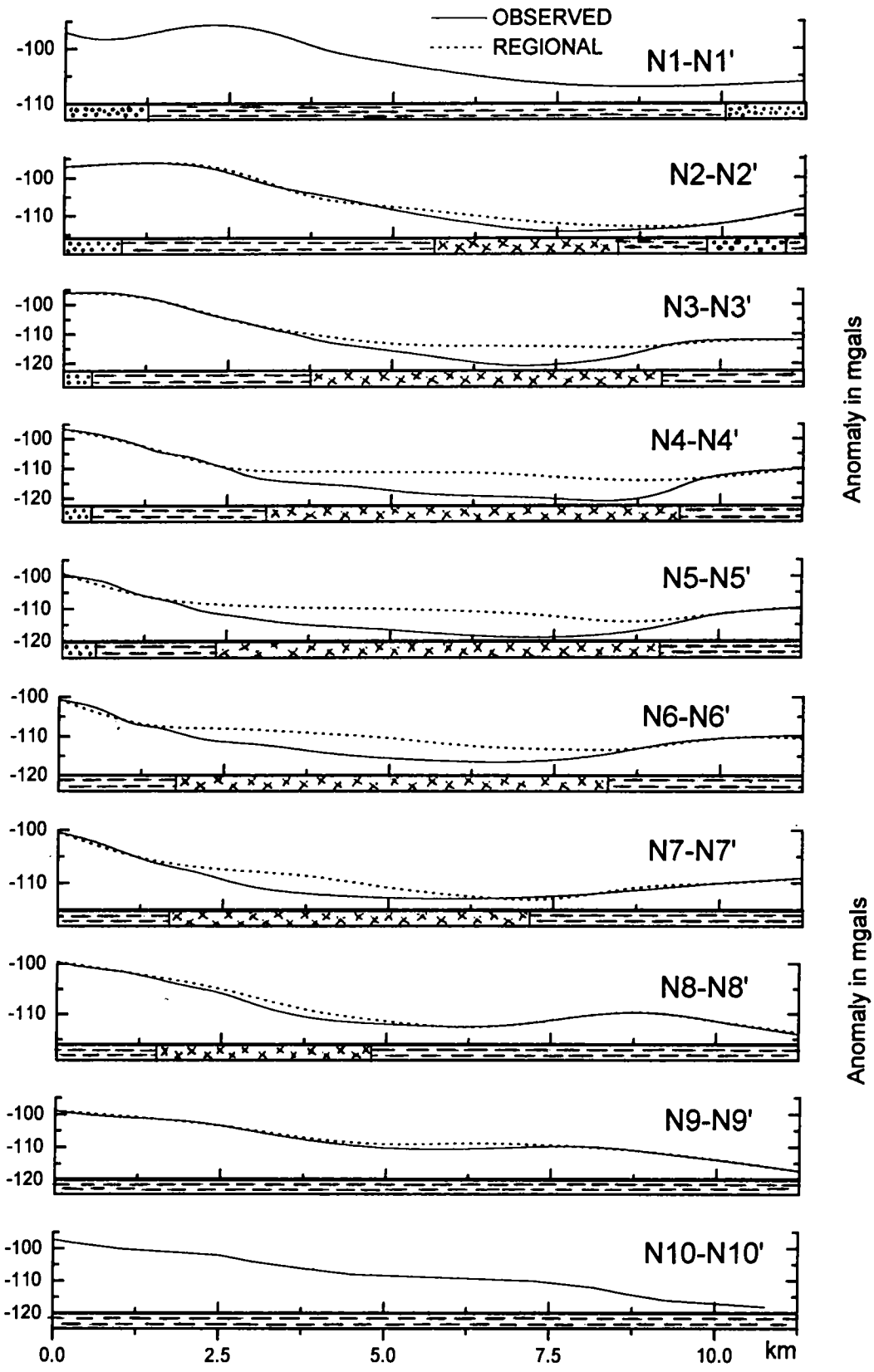


Fig 8.4(a).Ten north oriented profiles selected for regional- residual separation. Graphical smoothing method constrained by the surface geology was used to draw the regional. Symbols of rock types are same as those in Fig. 8.1.

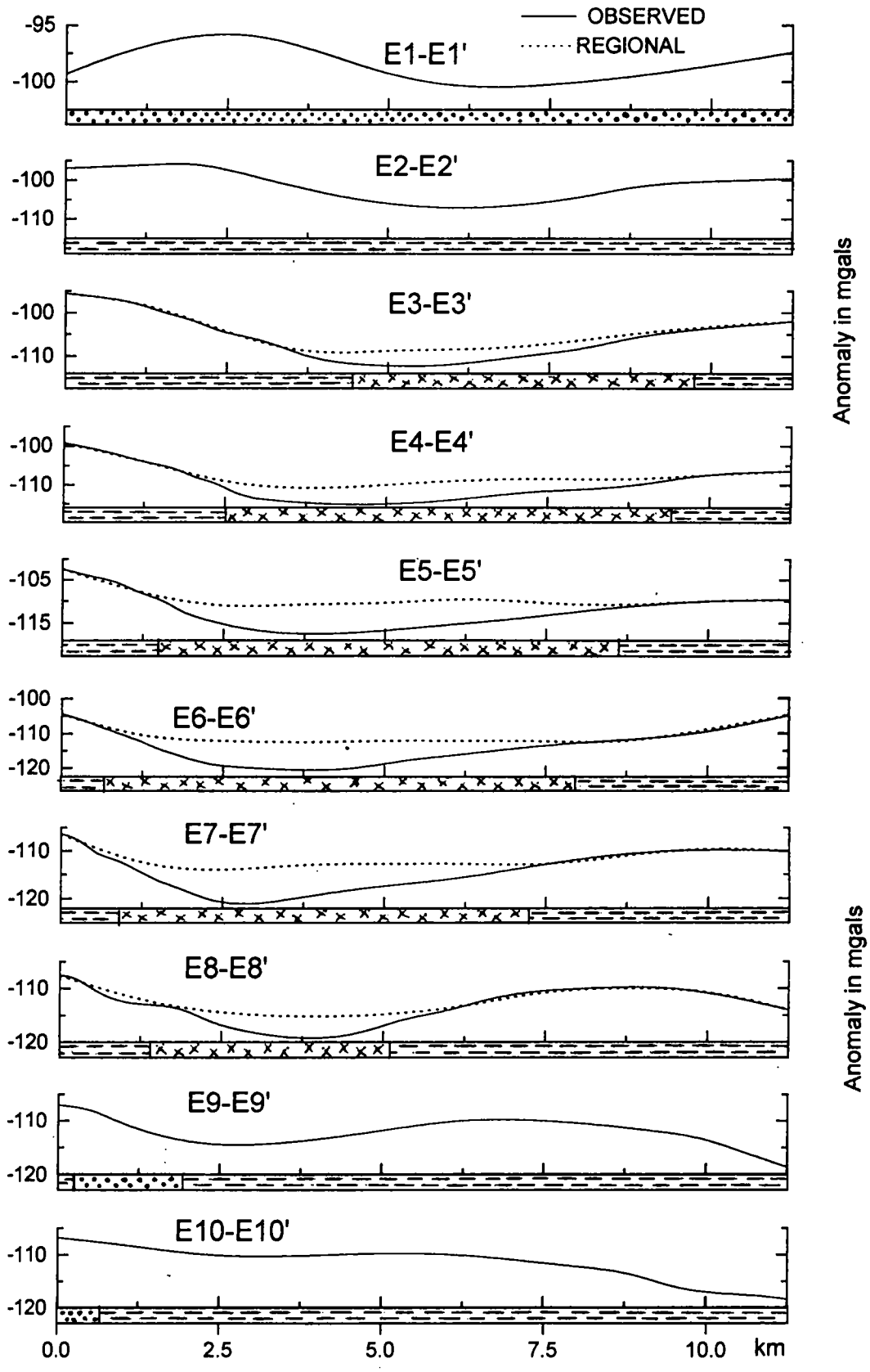


Fig 8.4(b). Ten east oriented profiles selected for regional- residual separation. Graphical smoothing method constrained by the surface geology was used to draw the regional. Symbols of rock types are same as those in Fig. 8.1.

is available. The residual anomalies so obtained have been utilized to prepare a residual anomaly map as shown in Fig. 8.5. The residual anomaly map shows a gravity low of 8 mGal and correlates well with the exposed geometry of the granite.

## 8.4 2-d Modelling

Three gravity profiles AA' , BB' and CC' across the pluton have been considered from the residual anomaly map in order to model the 2-d subsurface geometry in terms of shape, depth and subsurface extension of the Kalpatta granite body. The gravity modeling was carried out using SAKI program (Webring, 1985). A density contrast of –0.06 gm/cc was considered for this purpose based on the surface rock density estimates of 2.67 gm/cc for granites and 2.73 gm/cc for the surrounding gneisses (given in chapter III). Bott and Smithson (1967) suggested that in the case of no horizontal density variation in granite body, if the gravity anomaly at the surface contact falls less than half of the total amplitude of the anomaly, then the contacts of the pluton dip inward. The profiles AA' through CC' across the pluton (shown in Fig 8.5) shows a maximum anomaly of 6-7 mGals, while, the anomalies at the contact are around 2 mGal for all profiles. This reveals that the granitic body has inward dipping contacts. The interpreted 2-d models are shown in Fig 8.6 and the models indicate a steep inward dipping inclined canoe shaped plutonic body extending to a depth of 6 to 6.5 km.

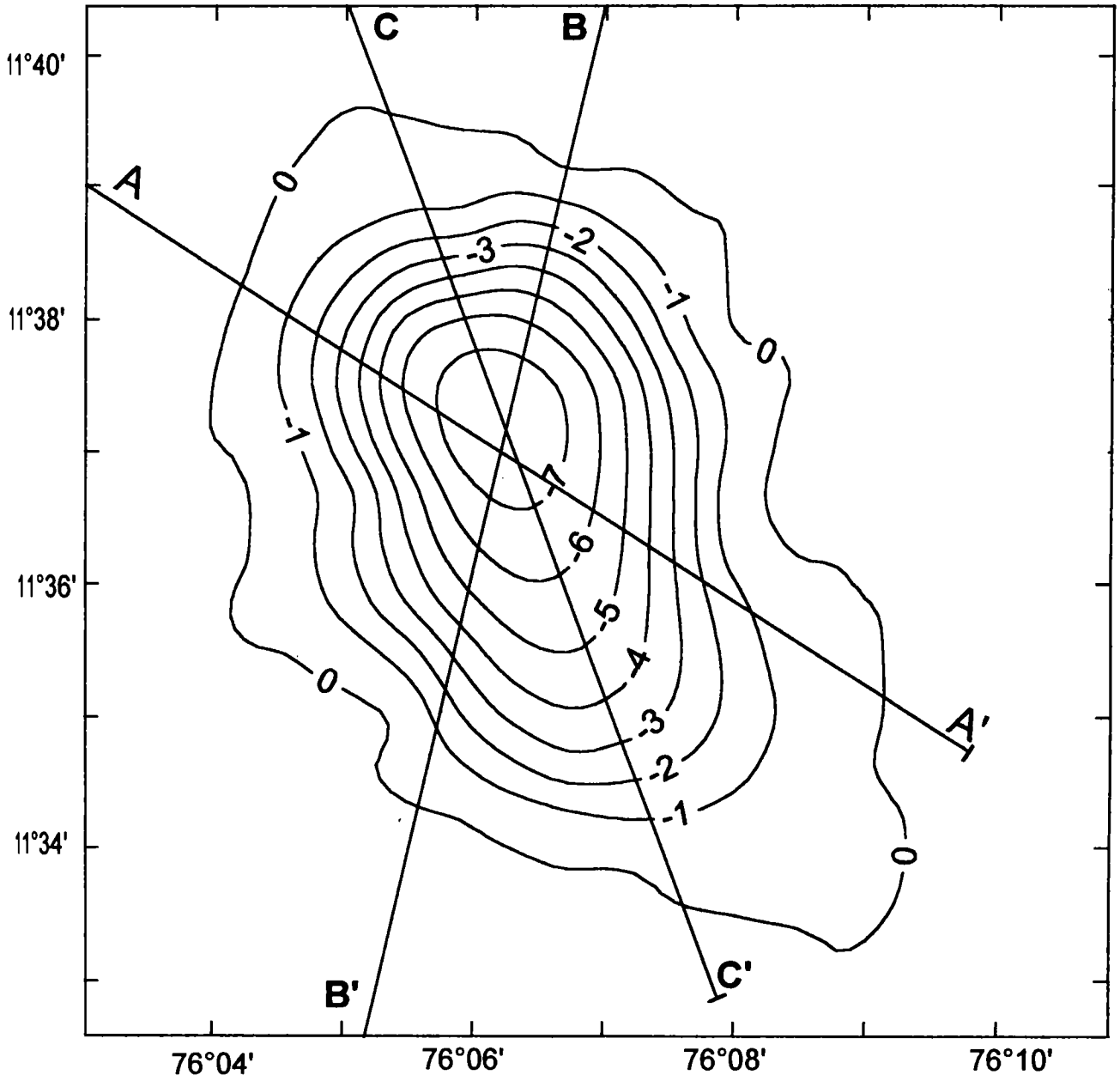


Fig. 8 5. Residual anomaly map of Kalpatta granite. The lines AA' to CC' indicate the profiles selected for 2-dimensional modelling.

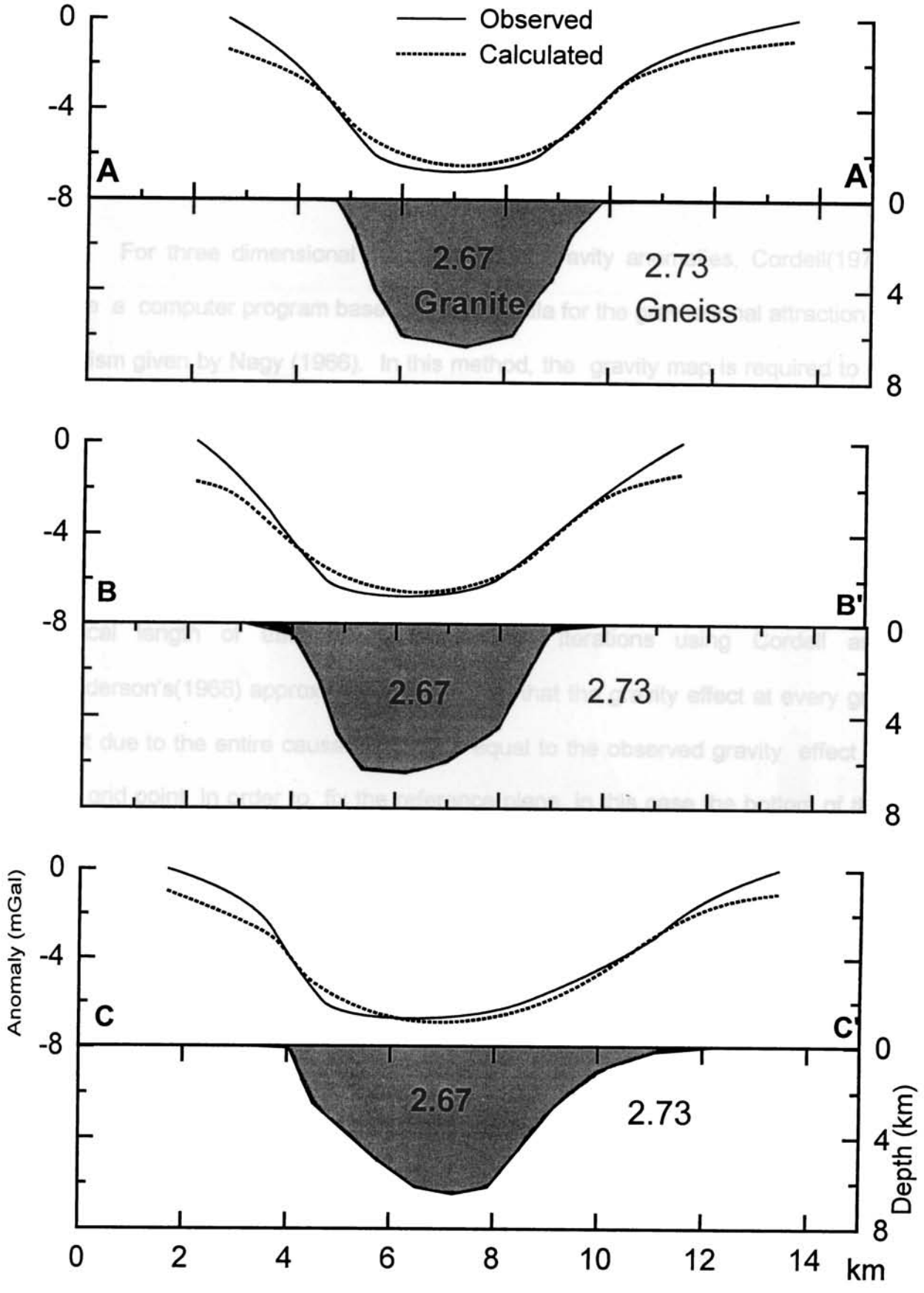


Fig 8.6. Two-dimensional gravity models of the Kalpatta granite body along profiles shown in Fig. 8.5.

## 8.5 3-d Modelling

For three dimensional interpretation of gravity anomalies, Cordell(1970) gave a computer program based on the formula for the gravitational attraction of a prism given by Nagy (1966). In this method, the gravity map is required to be digitized on a rectangular grid. The causative body is approximated by means of a bundle of vertical prism elements, each having a cross-section area of one square grid and a uniform density. The vertical position of each prism element is fixed with reference to a specified horizontal plane. The program calculates the vertical length of each prism element by iterations using Cordell and Henderson's(1968) approximate formula, so that the gravity effect at every grid point due to the entire causative body is equal to the observed gravity effect at that grid point. In order to fix the reference plane, in this case the bottom of the granite body, the maximum depth of 6.5 km obtained from the two-dimensional modeling of granite pluton has been used. The residual anomaly map is divided into 100 prism elements (10 X 10 grid points) with a grid width of 1.25 km. The results were obtained after 30 iterations with an RMS error of 0.9 mGal. The depth of the granite body obtained at each prism element has been used to prepare a 3-d depth map of the Kalpatta granite as shown in Fig. 8.7. As can be seen, the map correlates well with the surface exposure of the granite pluton.

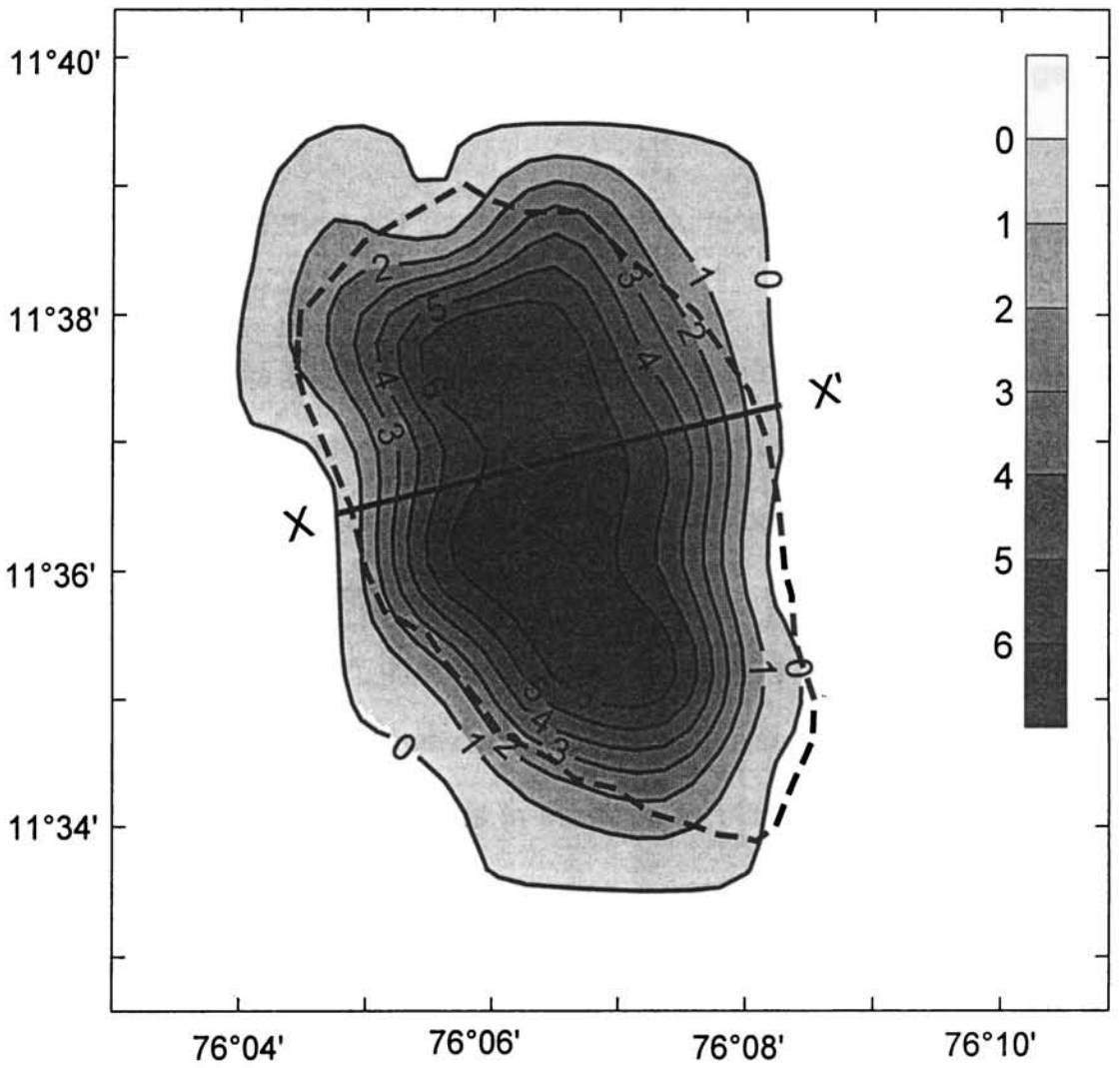


Fig. 8.7. Three-dimensional depth configuration of the Kalpatta granite body. The maximum depth obtained is about 6.5 km. The surface exposure of the granite body is shown as thick dashed line.

## 8.6 Discussion

The following are few significant aspects observed from this analysis:

- The granite is ellipsoidal somewhat pear shaped with horizontal dimensions of 6-11 km and the depth increasing towards center to about 6.5 km.
- It has a smooth oval shaped outcrop pattern as outlined on the geological map.
- The width of the body as seen on the surface, is wider in the NW which tapers to half its width towards SE.
- The contacts as deciphered from the 3-d depth section are inward dipping approximately around 70° (Fig. 8.8). The 3-d depth contour map suggests that overall shape of the body continues throughout its depth, but uniformly petering out at a depth of ~ 6.5 km.
- The steep foliation dips around the Kalpatta granite mass as mentioned earlier do often show outward dips. There is also a concentration of foliation attitudes. The outward dips in the foliation planes seemingly contradict the gravity model where the body dips inward. This contradiction may be explained in one of two ways.
  - The steep outward dips may reverse inward in depth.
  - The foliation dips are not primary and are unrelated from primary structure of the granite body.

A choice between these options calls for more detailed structural work.

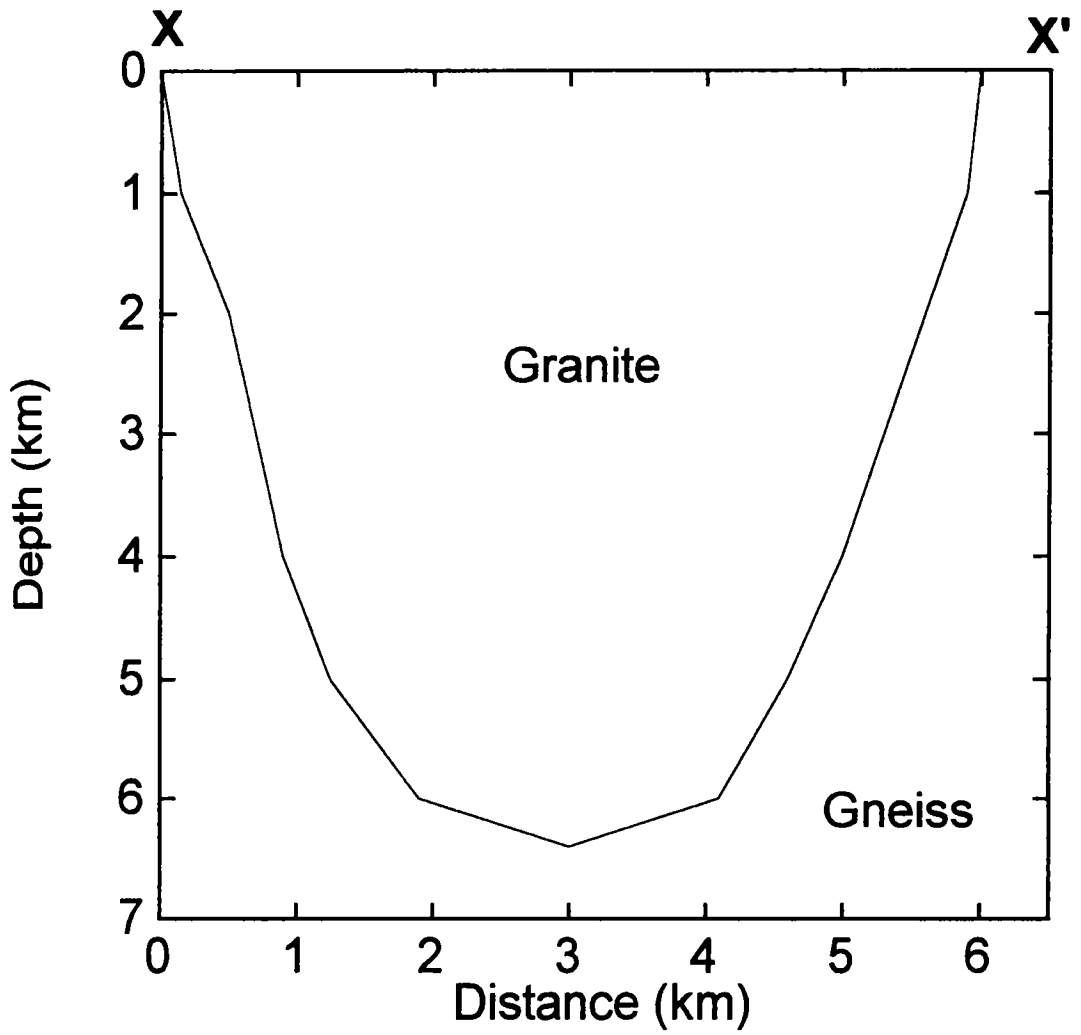


Fig. 8.8: Cross-section of the 3-D depth model along XX'
( Location shown in Fig. 8.7)

The most commonly inferred shape of permissive plutons are balloons or steep-sided inward dipping cones with circular or elliptical cross sections. Hutchinson (1970) inferred that oblique sections through such diapirs could be tailed tadpole plutons. The smooth oval shape is indicative of low ductility contrast, deeper level of emplacement and permissive nature of the intrusion. The NNW elongated outline of the pluton with a tapering towards SSE and the consistent downward extension of this shape on the 3-d depth model would imply an oblique crustal section with much deeper levels exposed in the southern part. In other words, the crustal block encompassing the pluton has suffered a NNW tilt during uplift after the emplacement of the Kalpatta granite. It can be further inferred from the models that there was no post intrusive shape modification and the NW tilting of the region has only influenced the present outcrop pattern of the granite body.

A regional northward tilting for the Indian peninsular shield has been speculated by many earlier workers (e.g., Pitchamuthu, 1965). The accreted crustal slabs along the amphibolite granulite terrain are steeply inclined northerly. Evidence for a northerly tilt also arises from steep metamorphic pressure gradients noticed in certain areas of the 'Transition Zone'. For example, across the Transition Zone, along Kabbal-Hanur area, the estimated metamorphic pressures of rocks increase southwards from 5.5 to 7.5 kb for a map distance of around 50 km (Hansen et.al., 1984), probably indicating a northward tilting of 3 km for 10 km subsequent to the metamorphism. The recognition of such

steeply tilted crustal blocks along or close to the transition zone will provide a clue for the evolution of the crust along the region. As the Kalpatta granite is located just south of the amphibolite-granulite facies transition zone, the northward tilting goes well with the available models of crustal evolution.

## 8.7 Summary and Conclusions

The gravity map of Kalpatta and adjoining areas shows a low of the order of 8 to 10 mGals centered over the Kalpatta granite and a minor low of the order of 4 to 6 mGals over the adjacent Ambalavayal granite. Regional-residual separation of the map reveals a gravity low of 8 mGals correlating well with the exposed geometry of the Kalpatta granite. The density measurements of the granite as well as the surrounding country rock give rise to a density of 2.67 gm/cc for granite and 2.73 gm/cc for gneiss giving rise to a density contrast of -0.06gm/cc for the granite body. Two-dimensional analysis of the granite pluton, geometry of the granite body as well as the elliptical nature of the contours enabled detailed 3-d analysis of the gravity field over the Kalpatta granite..

The Kalpatta granite has an elliptical shape with smooth arcuate contacts with an inward steep dipping surface increasing towards center to a maximum depth of 6.5 km. The shape of the surface exposure i.e., wider NW portion and narrow SE portion continues throughout its depth.

The smooth and arcuate contact of the body indicates low ductility contrast, permissive and deeper levels of emplacement. The elongated outline of the granite body could represent an oblique crustal section with much deeper levels exposed in the southern part due to northward regional tilting. Inward dipping contacts of the pluton are suggestive of diapiric or bubble model and that there was no post-intrusive shape modification.

# *Chapter IX*

## Summary

The southern Indian shield is regarded as a crustal unit made up essentially of Archean continental nuclei and Proterozoic mobile belts. The latter is represented by the wide-spread granulite terrain of the southern part of the shield. This southern Granulite terrain (SGT) is characterized by conspicuous structural features which have been interpreted as shear zones or deep crustal faults which mark the boundries of different crustal blocks. Among the various crustal units, the Bavali lineament and the Precambrian lower crustal segments adjacent to it provide a unique assemblage of several rock types and a variety of structural features. Geology of the area is obscured by the presence of thick cover of laterite/vegetation. Apart from the major rock types such as charnockite and gneiss, the region of Bavali shear zone is characterized by several major plutons of syenite, granite, anorthosite and gabbro. Previous geophysical information in this region is very scanty and data available is only of regional nature. The primary aim of the present study is to collect a good amount of gravity data, prepare gravity maps, analyze and interpret them in terms of the crustal structure and emplacement history of selected major plutons in the region of Bavali shear zone and Wynad schist belt of North Kerala. The study region covers an area of about 15,000 sq.km. falling between 11°15' N to 12° 30'N latitudes and 75°E to 76°30'E longitudes. A detailed geological map of the area compiled from the recent published maps (Fig. 2.2) enable one to divide it into three provinces, namely,

a) the northern charnockite province,

b) the southern charnockite province, and

c) the schist-gneiss province (Wynad Schist Belt) in between.

In order to aid the interpretation of gravity data, rock samples numbering around 200 in total representing all major geological units of the area were collected. Density and susceptibility determination of these rock samples were carried out. An attempt was made to correlate this data with the mineralogical data in order to understand the role of mineralogical composition on petrophysical properties. The average density estimated in this study (i.e., charnockite: 2.77; gneiss: 2.73; granulite: 2.75; granite: 2.67; gabbro: 2.99; anorthosite: 2.77; and dolerite: 3.02 gm/cc) has been utilized as the density values of the exposed geological units of the area for gravity interpretation. With the help of density vs magnetic susceptibility scatter plots, the D-MS fields for the rocks were identified and compared.

Due to the non-availability of reliable and permanent base stations in the study area, a good network of 36 new permanent base stations were established for the present purpose. The dynamic drift rate of the base stations shows that most of the drift values are below 0.006 mGal/ minute. The bases established in the present study also have a repeatability of 0.08 mGal, fairly accurate enough for conducting regional gravity surveys. Using the network of gravity bases, nearly 800 gravity observations were made in the regions of the Bavali shear zone and Wynad schist belt. The data measurements were made

at an average spacing of 1 km along all motorable roads. In certain critical areas cutting the geological structures, observations were made at a closer interval of 500m. Elevation data were collected from altimeter measurements, spot height and bench mark locations and from Survey of India topographic sheets.

Revised free-air and Bouguer anomaly maps of the region were prepared utilizing in addition to the data collected in the present study, the available NGRI data. The observed gravity field is explained in correlation with the surface geology. A qualitative analysis of the free-air and Bouguer anomaly maps vis-à-vis elevation map is made in order to obtain an idea on the trend and nature of anomalies and their relation to surface geology and elevation. The area north of Nileswaram, Virajpet and Sargur with an average elevation of 800m shows positive free-air anomalies. An average gradient of 4-5 mGal/km is observed on the free-air anomaly map coinciding with the western ghats. Bouguer anomaly map prepared in 5 mGal interval shows good correlation with the surface geology and the minor geological structures of the area and brings out several interesting points. The map shows an E-W trending gravity high gradient zone coinciding with the Bavali shear zone, a broad gravity high circumfering the northern charnockite province north of the shear zone and a major gravity low starting from Kannur and extending into the Wynad region south of the shear zone, coastal gravity high near Nileswaram and increase in gravity towards the coast. In order to understand the nature and wavelength of the gravity anomalies and the subsurface mass distribution, the average Bouguer and free-air

anomalies and their relationship with elevation has been studied for 1/8°x1/8° , 1/4°x1/4° and 1/2°x1/2° average values. The 1/8°x1/8° and 1/4°x1/4° average Bouguer anomaly maps indicate that the Bavali shear zone separates two distinct gravity fields with a gravity gradient following the shear. While the anomalies are positive on the northern side, the region south of the shear is characterized by large negative anomalies. The free-air anomalies show a positive correlation with elevation, while the Bouguer anomalies have a negative correlation. The regression relations for these data set have been obtained and compared with other parts of the Peninsular India. The low regression coefficient (-25 mGal/km) obtained from 1/2°x1/2° average anomaly-elevation regression suggests the presence of high density masses at depth.

The Bouguer anomaly map of the Bavali shear zone and the adjacent areas has been utilized to construct six gravity profiles across the shear zone. An estimate of the crustal thickness over the region was made utilizing the ¼ ° x ¼ ° averaged Bouguer anomaly map. The Moho contour map thus arrived at exhibits a crustal thickness in the region ranging from 38-39 km over a large part of the area, thickening to 40-41 km below Wynad Plateau, and a gradual thinning towards coast upto 34 km. Gravity modelling has been carried out taking these crustal thickness estimates and the two layer density configuration ie., 2.75 gm/cc for charnockites and 2.73 gm/cc for gneisses in the upper part of the crust, 2.85 gm/cc for the lower crust and a density of 3.3 gm/cc for the upper mantle. The gravity models indicate that the Bavali shear coincides with a steep plane

that separates two contrasting crustal densities extending beyond a depth of 30 km possibly down to Moho, justifying it to be a Mantle fault. However, in the Wynad Plateau region it has listric tendencies in the upper part of the crust. The models bring out the presence of large high density material of 2.98 gm/cc within the lower crust below northern charnockite province. An alternative model to this model is a 25 km of Moho rise which is considered unlikely. However, the crust below the Wynad Plateau is more homogeneous and distinctive due to the absence of high density masses.

The Perinthatta anorthosite is one among the series of mafic to felsic intrusives associated with the Bavali shear zone and Wynad schist belt. The anorthosite massif is emplaced within the high grade metamorphic rocks of northern Kerala. In order to obtain knowledge of the structure, shape and depth extent of this pluton, detailed gravity analysis has been carried out. The density measurements suggest a density of 2.77 gm/cc for anorthosite and 2.76 gm/cc for the surrounding country rock. The gravity anomaly map does not reveal any conspicuous positive gravity field associated with the anorthosite massif. However, residual map prepared after the regional separation shows a minor positive gravity field of irregular shape with localized highs of 6-12 mGal within and around anorthosite massif. The 2-D models across the pluton suggests subjacent nature and lensoid shape for anorthosite which is underlain by small isolated high density (2.90 gm/cc) cylindrical bodies extending 3-7 km downwards. These cylindrical bodies are inferred as either the mafic/ oxide rich

portions of the pluton sagged down during crystallization or the individual feeders of the plagioclase rich mushes which coalesced in the upper crust to give rise to the massif.

Granites are usually associated with large negative Bouguer anomalies caused by their relative low density with the surrounding rocks. The plutons in general exhibit circular to elliptical shapes with some degree of elongation along the structural grain of the rocks. Kalpatta granite is one among the felsic plutons occurring along the southern part of the Bavali shear zone. The pluton is an elliptical stock, emplaced within the Precambrian gneiss with sharp contacts. In order to obtain information on the form, structure and subsurface geometry of the pluton, a detailed 3-D interpretation of the gravity field has been made. The Bouguer anomaly map of the region shows a NW-SE gravity gradient zone with a gravity low of 8-10 mGal centered over the pluton. The residual anomaly shows a gravity low of 8 mGal and correlates well with the exposed geometry of the pluton. The granite has a density of 2.67 gm/cc giving rise to density contrast of – 0.06 gm/cc with the surrounding gneissic rocks. A 3-D depth map of the granite pluton has been prepared which reveals the following:

1) it has an overall ellipsoidal / somewhat pear shaped with a horizontal dimension of 6-11 km and the depth increasing towards the center to about 6.5 km.
2) it has arcuate contact dipping inward around 70° .

3) 3-D depth contour map suggests that overall shape of the granite body continues throughout its depth, but uniformly petering out at a depth of 6.5 km.

The smooth arcuate contact is indicative of low ductility contrast and a deeper level of emplacement. The elongated outline of the pluton represents an oblique crustal section with much deeper levels exposed in the southern part. Inward dipping contacts of the pluton is suggestive of a diapiric or bubble model and that there was no post intrusive shape modification.

The bearing of several features of the gravity field outlined above on processes of geological evolution of the region have been discussed. It is difficult to construct a generalized model of crustal evolution in terms of its varied manifestations using only the gravity data. However, the data constrains several aspects of crustal evolution and provides insights into some of the major events.

# Reference

**Anderson, A.T. and Morin, M. 1968.** Two types of massif anorthosite and their implications regarding the thermal history of the crust. In: Isachsen Y W (Ed) Origin of Anorthosite and Related Rocks. NY State Mus. Sci. Serv. Mem., v.18, pp.57-69.

**Aravamadhu, P.S. 1974.** Certain aspects of magnetic studies of charnockite at Waltair, India - Field investigations. Canadian jour. of Earth Sciences, v.11, no.4, pp.503-509.

**Ashwal, L.D. 1993.** Anorthosites, Springer-Verlag., 422p.

**Bak. J., Sorenson, K., Grocott. J., Korstgard, J.A., Nash and Waterson, J. 1975.** Tectonic implications of Precambrian belts in western greenland. Nature, v. 254, pp. 566-569.

**Bartlett, J.M., Harris, N.B.W., Hawkesworth, C.J. and Santosh, M. 1995.** New isotope constraints on the crustal evolution of South India and Pan-African grnulite metamorphism. Mem. Geol. Soc. India, No.34, pp. 391-397.

**Bhattacharyya, B.K. 1965.** Two-dimensional harmonic analysis as a tool for magnetic interpretation. Geophysics, vol.30, pp. 829 – 857.

**Bott, M.H.P. 1956.** A geophysical study of the granite problem. Q. J. Geol. Soc. London, v.112, pp. 45-62.

**Bott, M.H.P. and Smithson, S.B. 1967.** Gravity investigations of subsurface shape and mass distributions of granite batholith. Bull. Geol. Soc. Am., v.78, pp.859-878.

**Bridgewater, D., Sutton, J. and Watterson, J. 1974.** Crustal downfolding associated with igneous activity. Tectonophysics, 21, pp.57-77.

**Bukharev, V.P., Stekol'nikova, A.V. and Polyanskiy, V.D. 1973.** Tectonics and deep structure of anorthosite massifs in the northwest of the Ukranian Shield. Geotectonics, v.4, pp.207-210.

**Bussell, M.A. 1976.** Fracture control of high-level plutonic contacts in Coastal Batholith of Peru. Proc. Geol. Assoc. London, 87, pp. 237-246.

**Chacko, T, Ravindrakumar, G.R. and Newton, R.C. 1987.** Jour. Geol., v. 95, pp. 343-358.

**Chandrasekharam, D.** 1985. Structure and evolution of the western continental margin of India deduced from gravity, seismic, geomagnetic and geochronological studies. Phys. Earth. Planet. Inter., v.41, pp. 186-198.

**Chetty, T.R.K. 1996.** Proterozoic shear zones in the southern granulite terrain, India. Gondwana Research group Mem. 3, pp. 77-89.

**Christensen, N.I. and Mooney, W.D. 1995**. Seismic velocity structure and composition of continental crust – a global view. Jour. Geophys. Res., v.100, pp. 9761-9788.

**Cordell, Lindrith. 1970.** Iterative three-dimensional solution of gravity anomaly data. National information service, pp.196-970, U.S. Dept. Commerce.

**Cordell, Lindrith and Henderson, R.G. 1968.** Iterative three-dimensional solution of gravity anomaly data using a digital computer. Geophysics, v.33, no. 4, pp.596-601.

**Coward, M.P. and Park, R.G. 1987.** The role of mid-crustal shear zones in the early Proterozoic evolution of the Lewisian. Evolution of the Lewisian and comparable Precambrian high grade terranes. In: (Park, R.G. and Tarney, J. Eds.), Geol. Soc. Spl. Pub., No. 27, pp. 127-138.

**Crawford, A.R. 1969.** Reconnaissance Rb-Sr dating of the Precambrian rocks of Southern Peninsular India. Jour. Geol. Soc. India, v.10, pp.117-166.

**Cummings, D. and Regan, R.D. 1976.** Aeromagnetic survey of the San Gabriel Anorthosite Complex, southern California. Geol. Soc. America Bull., v.87, pp.675-680.

**Daly, M.C. 1986.** Crustal shear zones and thrust belts: their geometry and continuity in central Africa. Phil. Trans. Roy. Soc. London, A. 317, pp. 111-128.

**Davidson, D.M. Jr. 1972.** Eastern part of Duluth Complex, in Sims, P.K. and - Morey, G.B., eds., Geology of Minnesota; A centennial volume: Minnesota .Geol. Survey, pp.354-360.

**Davidson, A. 1984.** Tectonic boundaries within the Grenville Province of the Canadian Shield. Jour. Geodynamics, v.1, pp.433-444.

**Drury, S.A. and Holt, R.W. 1980**. The tectonic framework of the South Indian craton: a reconnaissance involving LANDSAT imagery. Tectonophysics, v.65, pp. T1-T15.

**Drury, S.A., Harris, N.B.W., Holt, R.W., Reeves-Smith, G.J. and Wightman, R.T. 1984.** Precambrian tectonics and crustal evolution in south India. Jour. Geology, v.92, pp.3-20.

**Durrheim, R. J. and Mooney, W.D. 1991.** Archaean and Proterozoic crustal evolution: evidence from crustal seismology. Geology, v.19, pp. 606-609.

**Duchesne, J.C., Maquil, R. and Demaiffe, D. 1985.** The Rogaland anorthosites: facts and speculations. In: Tobi AC, Touret JLR(eds) The deep Proterozoic crust in the North Atlantic provinces. NATO ASI, Ser C, 158. Reidel, Dordrecht, pp449-476.

**Fermor, L.L. 1936**. An attempt at the correlation of the ancient schistose formations of Peninsular India, Mem. Geol. Surv. India, v.70.

**Fountain, D.M** and Salisbury, M.H. 1981. Exposed cross-sections through the continental crust; implications for crustal structure, petrology and evolution. Earth. Planet. Sci. Lett., v.56, pp. 263-277.

**Friend, C.R.L., Nutman, A.P. and McGregor, A.R. 1988.** Late Archean terrane accretion in the Godthab region, southern west Greenland. Nature, v.335, pp. 535-538.

**Gopalakrishnan, K. 1994**. An overview of southern granulite terrain India -- Constraints in reconstruction of Precambrian assembly of Gondwanaland. Ninth International Gondwana symposium/Hyderabad/India. pp. 1003-1011.

**G.S.I.(Geological Survey of India). 1995.** Geological and mineral map of Kerala.

**Gulatee, B.L. 1956.** Gravity data in India. Survey of India, Tech. Paper. No. 10.

**Hamilton, W. and Myers, W.B. 1967**. The nature of Batholiths. Prof. Pap. U.S. geol. Surv., 554-C, 30p.

**Hansen, E.C., Newton, R.C. and Janardhan, A.S. 1984.** Fluid inclusions from rocks from the amphibolite-facies gneisses to charnockite progression in southern Karnataka, India: direct evidence concerning the fluids of granulite metamorphism. Jour. Metamorphic Geology, v.2, pp.249-264.

**Harinarayan and Subrahmanyam, C. 1986**. Precambrian tectonics of the south Indian shield inferred from geophysical data. Jour. Geol. v. 94, pp. 187-198.

**Harris, N.B.W., Holt, R.W. and Drury, S.A. 1982.** Geobarometry, geothermometry and later Archaean geotherms from granulite facies terrain of South India. Jour. Geology, v.90, pp.509-527.

**Henkel, H. 1970.** Density measurements on Precambrian basement rocks from the Uppsala region, Medd. Geodet. Inst. Ups. Uni., v.9.

**Henkel, H. 1976.** Studies of Density and Magnetic properties of rocks from northern Sweden. Pageoph., V.114, pp.235-249.

**Hodge, D.S., Owen, L.B. And Smithson, S.B. 1973.** Gravity interpretation of the Laramie Anorthosite Complex, Wyoming. Geol. Soc. Am. Bull., v.84, pp.1451-1464.

**Hutchinson, W.W. 1970.** Metamorphic framework and plutonic styles in the Prince Rupert region of the central Coast Mountains. British Columbia. Can. Jour. Earth Sci., v.7, pp.376-405.

**Ibrahim, A.E., Ebinger, C.J. and Fairhead, J.D. 1996**. Lithospheric extension northwest of central African shear zone in Sudan from potential field studies. Tectonophysics, v.255, pp. 79-97.

**Iyer, H.M., Gaur, V.K., Rai, S.S., Ramesh, D.S., Rao, C.V.R., Srinagesh, L.D. and Suryaprakasam, K. 1989.** High velociy anomaly beneath the Deccan volcanic province: evidence from seismic tomography. Proc. Indian Acad. Sci. (EPS), v.98,pp. 31-60.

**Kaila, K.L., Roy Chowdhury, K., Reddy, P.R., Krishna, V.G. Hari Narain, Subbotin, S.I., Sollogub, V.B., Chekunov, A.V., Kharetchko, G.E., Lazarenko, M.A. and Ilehenko, T.V. 1979**. Crustal structure along Kavali-Udupi profile in the Indian peninsular shield from deep seismic sounding. Jour. Geol. Soc. India, v. 20, pp. 307-33.

**Kaila, K.L. and Bhatia, S.C. 1981**. Gravity study along the Kavali-Udipi deep seismic sounding profiles in the Indian Peninsular shield : some inferences about the origin of anorthosites and the Eastern Ghat orogeny. Tectonophysics, v. 79, pp. 129-143.

**Kailasam, L.N. 1975.** Epeirogenic studies in India with reference to recent vertical tectonics. Tectonophysics, v.29, pp. 505-521.

**Katz,M.B. 1978**. Tectonic evolution of the Archaean Granulite facies belt of Sri Lanka and South India. Jour. Geol. Soc. India, v. 19, no. 5, pp. 185-205.

**Keary, P. 1978.** An interpretation of the gravity field of the Morin anorthosite complex, southwest Quebec. Geol. Soc. Am. Bull., v.89, pp. 467-475.

**Keary, P. and Thomas, M.D. 1979.** Interpretation of the gravity field of the Lac Fournier and Romaine River anorthosite massifs, eastern Grenville Province: significance to the origin of anorthosite. Jour. Geol. Soc. Lond., v.136, pp.725-736.

**Krishna Brahmam, N. 1993.** Gravity in relation to crustal structure, palaeosutures and seismicity of southern India. Geol. Soc. India. Memoir, v.25, pp. 165-201.

**Krishna Brabmam, N. and Kanungo, D.N. 1976.** Inference of granitic batholith by gravity studies in south India. Jour. Geol. Soc. India., v. 17, pp. 45-53.

**Kumar, S.N., Prasannakumar, V. and Nair, P.K.R. 1998.** Petrochemistry and petrogenesis of Kalpatta granite, South India. Current Science, v.74, no. 7, pp.613-619.

**Lambeck, K. 1983.** Structure and evolution of the intracratonic basins of central Australia. Geophys. JR Astron. Soc., pp. 843-886.

**Lambeck, K., Bergus, G. and Shaw, R.D. 1988.** Teleseismic travel time anomalies and deep crustal structure in central Australia. Geophys. J., v. 94,pp. 105-124.

**Lapointe, P., Chomyn, B.A., Morris, W.A. and Coles R.L. 1984.** Significance of magnetic susceptibility measurements from the Lac du Bonnet batholith, Manitoba, Canada. Geoexploration, v.22, pp.217-229.

**Leake, B. E. 1978.** Granite emplacement: the granites of Ireland and their origin. In: Bowers, D.R. and Leake, B. E. (eds.). Crustal evolution in northwestern Britain and adjacent regions. Spec. Iss. Geol. J. 10, pp. 221-248.

**Long, J.F. and Grannel, R.B. 1971.** A detailed gravity survey of the San Gabriel anorthosite body. Geol. Soc. America Abs. with Programs, v.3, pp.151-152.

**Mahadevan, T.M. 1993.** Transect studies -- an integrated approach to imaging the deep lithospheric structure and interpreting continental evolution. Mem. Geol. Soc. India, v. 25, pp. 1-34.

**Mahadevan, T.M. 1994.** Deep continental structure of India: a review. Geol. Soc. India. Mem. 28, 569p.

**Mahadevan, T.M. 1996.** Deep continental structure of northwestern and central Indian Peninsular shield- a review. Mem. Geol. Soc. India., v.31, pp. 1-35.

**Mahadevan, T.M. 1998.** A unitary model of evolution of the Precambrian Indian shield. Inter. Sympo. on charnockite and granulite facies rocks. Geol. Asson. Tamil Nadu, pp. 153-174.

**Manghnani, M.H. and Woolard, G.P. 1963.** Establishment of north-south gravimetric calibration line in India. Jour. Geophys. Res., v.68(23), pp. 6293-6301.

**Mallick, K. 1991**. Application of finite element method for separation of residual gravity anomaly and ore estimations: IMACS Internat. Symp. On Mathematical Modelling and Scientific Computation. pp. 1-12.

**Mallick, K and Sharma, G.S. 1997**. Computation of regional gravity anomaly - A novel approach. Proc. Indian Acad. Sci. (Earth and Planet. Sci.) vol. 106, pp. 55-59.

**Mallick, K and Vasanthi, A. 2000**. Delineation of subsurface extent of Perinthatta anorthosite, Kerala, India. Communicated to J. Geol. Soc. Inida.

**Martignole, J. and Schrijver, K. 1970.** Tectonic setting and evolution of the Morin anorthosite, Grenville Province, Quebec. Bull. Geol. Soc. Finland, v.42, pp.165-209.

**McCourt, S. and Vearncombe, J.R. 1992**. Shear zones of the Limpopo belt and Adjacent granitoid greenstone terraines: Implications for late Archaean collision tectonics in southern Africa. Precamb. Res., v.55, pp.553-570.

**Mishra, D.C. 1988**. Geophysical evidences for a thick crust south of Palghat-Tiruchi gap in the high-grade terraines of south India. Jour. Geol. Soc. India, v. 31, pp. 79-81.

**Mishra, D.C. 1989.** On deciphering the two scales of the regional and Bouguer anomaly of the Deccan traps and crust-mantle boundary. Jour. Geol. Soc. India, v. 33, pp. 48-54.

**Mishra, D.C. and Rao, M.B.S.V. 1993**. Thickening of crust under granulite province of south India and associated tectonics based on gravity-magnetic study. Mem. Geol. Soc. India, No. 25, pp. 203-219

**Moshkin, V.N. and Dagelaiskaya, I.N. 1972.** The Precambrian anorthosites of the USSR. Proc. 24$^{th}$ Int. Geol. Congr., Sect 2, pp.329-333.

**Mukhopadhyay, M. 1987.** Gravity field and its significance to the origin of the Bengal anorthosite. Jour. Geol. Soc. India, v.29, pp.489-499.

**Murthy, I.V.R. 1998.** Gravity and magnetic interpretation in exploration geophysics. Memoir 40, Geol. Soc. Inida, Bangalore.

**Naha, K and Srinivasan, R. 1996**. Nature of the Moyar and Bhavani shear zones, with a note on its implication on the tectonics of the southern Indian Precambrian shield. Proc. Indian Acad. Sci. (Earth Planet. Sci.)., v.105, No.2, pp. 173-189.

**Nagata, T. 1961**. Rock magnetism, Maruzen company Ltd., Tokyy.

**Nagy, D. 1966.** The gravitational attraction of a right rectangular prism. Geophysics, v.31, pp.362-371.

**Nair, M. M. 1990**. Structural trend line patterns and lineaments of the western Ghats, south of 13° latitude. Jour. Geol. Soc. India, v.35, pp. 99-105.

**Nair, M.M., Vidyadharan, K.T., Pawar, S.D., Sukumaran,P.V. and Murthy, Y.G.K. 1976.** The structural and stratigraphic relationship of the schistose rocks and associated igneous rocks of the Tellicherry – Manantoddy area, Cannanore district, Kerala. Ind. Mineralogist, v. 16, pp. 89-100.

**Nair, M.M. and Vidyadharan, K.T. 1982.** Rapakivi granite of Ezhimala complex and its significance. Jour. Geol. Soc. India, v.23, pp.46-51.

**Nair, N.G.K. and Santosh, M. and Thampi, P. K. 1983.** Geochemistry and petrogenesis of the alkali granite of Munnar, Kerala (India) and its bearing on rift-tectonics. Neues. Jahrb. Miner. Abh., v.148, pp.223-232.

**Nair, N.G.K. and Santosh, M. 1984.** Petrochemistry and Tectonic significance of the Peralimala alkali granite, Cannanore District, Kerala. Jour. Geol. Soc. India, v.25, pp.35-44.

**Nair, N.G.K., Soman, K., Santosh,M., Arkelyants, M.M. and Golubtev, V.N. 1985.** K-Ar ages of three granite plutons from the northern Kerala region. Jour. Geol. Soc. India, v.26, pp.676.

**Nambiar, A.R. 1987.** Mineralogy and geochemistry of Adakkathodu gabbro massif from the Bavali fault zone, north Kerala. Rec. Geol. Surv. India, pp.16-24.

**Nambiar, A.R., Vidyadharan , K.T. and Sukumaran, P.V. 1982.** Petrology of anorthosites of Kerala. Rec. Geol. Sury. India, v.114, pt.5, pp. 60-70.

**Nambiar,C.G. 1987.** Geochemistry and genesis of charnockites and associated rocks from northern Kerala. Unpublished Ph.D thesis, Indian Institute of Technology, Bombay, pp.191.

**Nambiar, C.G., Shreedhara, V. and Rao, B.B. 1985.** Certain geological and related aspects of Northern Kerala – an appraisal based on landsat data. Proc. Indian Geol. Cong., pp.85-94.

**Nambiar, C.G., Bhaskar Rao, B., Parthasarathy, R. and Fedkin, V.V. 1992.** Geochemistry and genesis of charnockites and associated gneisses from northern Kerala, India. In: High-Grade Metamorphics (Ed. A. Barto-Kyriakis), Theophrastue Pub. S.A., Greece, pp.187-215.

**Nambiar. C.G., Soney. K.P. and Radhakrishna. M. 1997.** Petrogenesis of the Perinthatta Anorthosite, northern Kerala, India., Jour. Geol. Soc. India., v.50, pp. 501-509.

**Nambiar, C.G., Radhakrishna, M., Soney Kurien, P. and John Kurian, P. 1999.** Final Technial Report on the DST project "Nature and evolution of lower crustal segments associated with Bavali lineament and Wynad schist belt (Unpublished).

**Naqvi, S.M. 1973**. Geological structure and aeromagnetic and gravity anomalies in the central part of the Chitradurga schist belt, Mysore, India. Geol. Soc. Amer. Bull., v.84, pp. 1721-1732.

**Naqvi, S.M. and Rogers, J.J.W. 1987**. Precambrian Geology of India, Oxford University Press. p.223.

**NGRI. 1978**. Isostatic gravity anomaly map of India. (Ref. No. NGRI/GPH-3) National Geophysical Research Institute, Hyderabad.

**Odom, A.L. 1982.** Isotopic age determination of rock and mineral samples from the Kerala Dist., India. U.N. Project Report (Case No.81-100840 Florida state Univ. (Unpubl.).

**Percival, J.A., Fountain, D.M. and Salisbury, M.H. 1990**. Exposed crustal cross-sections as windows on the lower crust. In: Fountain, D.M., Arculus, R.J. and Kay, R.W.(Eds.). Continental lower crust. Elsevier, Amsterdam, pp. 317-362.

**Pili, E., Ricard, Y., Lardeaux, J.M., and Sheppard, S.M.F. 1997**. Lithospheric shear zones and mantle-crust connections. Tectonophysics, v.280, pp. 15-29.

**Pitchamuthu, C.S. 1965**. Regional metamorphism and charnockitization in Mysore state, India. Indian Mineralogist 6, pp. 119-126.

**Pitcher, W.S. 1952.** The Rosses granite ring complex. County Donegal. Eire. Proc. Geol. Assoc. London, v.64, pp. 153-183.

**Pitcher, W.S. and Berger, A. R. 1972**. The geology of Donegal: a study of granite emplacement and unroofing. Wiley Interscience. London, 435p.

**Pitcher, W.S. 1979.** The nature, ascent and emplacement of granitic magmas. Jour. Geol. Soc. London, v.136, pp.627-662.

**Platou, S. 1968.** On the petrophysical properties of granitic rocks. Geol. Foren. Stockholm. Forh. 90.

**Plomerova, Babuska, V., Dorbath, C., Dorbath, L. and Lillie, R.J. 1993**. Deep lithospheric structure across the central African shear zone in Cameroon. Geophys. J. Int., v.115, pp. 381-390.

**Qureshy, M.N. 1963**. Gravity, elevation and isostasy in India. Nat. Geophy. Res. inst. Bull., v.1 (2), pp.99-106.

**Qureshy, M.N. 1964.** A regional gravity profile from Salem to the east coast of India. Bull. Geol. Soc. India, v.1, pp.6-10.

**Qureshy, M.N. 1970.** Relation of gravity to elevation, geology and tectonics in India. Proc. Second Symposium on Upper mantle project, NGRI, pp.1-20.

**Qureshy, M.N. 1971.** Relation of gravity to elevation and rejuvenation of blocks in India. Jour. Geophy. Res., v.76, pp.545-557.

**Qureshy, M.N. 1981**. Gravity anomalies, isostasy and crust – mantle relations in the Deccan traps and contiguous regions. India. Mem. Geol. Soc. India, v.3, pp. 184-197.

**Qureshy, M.N., Aravamadhu, P.S. and Bhatia, S.C. 1967.** Some regional gravity traverses through India. Proc. Symposium on Upper mantle project. Geophys. Research Board and NGRI, pp. 122-133.

**Qureshy, M.N. and Krishna Brahmam, N. 1969.** Gravity bases established in India by NGRI – Part I. Bull. NGRI, v.7, No.1, pp.31-49.

**Qureshi, M.N., Krishna Brahamam, N. and Aravamadhu, P.S. 1969.** Gravity surveys on some granitic bodies in south India. Jour. Indian Geoscience Assn., v.11, pp. 177-181.

**Qureshy, M.N., Krishna Brahmam, N., Naqvi, S.M., Aravamadhu, P.S., Grade, S.C., WEK Warsi, Bhatia, S.C., Subba Rao, D.V., Subrahmanyam, C., Rafi Ahmed and Venkatachalam, S. 1981.** Gravity data in India by National Geophysical Research Institute (Restricted publication) Part 1. Special report (gravity data).

**Radhakrishna, B.P. 1989. Jour.** Geol. Soc. India, v. 34, pp. 1-24.

**Radhakrishna, B.P. and Ramakrishnan, M. 1988.** Jour. Geol. Soc. India, v.32, pp. 263-278.

**Radhakrishna, B.P., Ramakrishnan, M. and Mahabaleswar, B. 1990.** Granulites of South India - Pichamuthu volume, Mem. Geol. Soc. India., v. 17, 502p.

**Radhakrishna, T. and Mathew, J. 1995.** Oxygen isotopes and mantle sources of the mafic dykes in the South Indian high-grade terrain. In: Dyke Swarms of peninsular India, Mem. 33, Geol. Soc. India. pp. 133-147.

**Radha Krishna, M., Murthy, B.V.S., Sunil, P.S., Arts, K.P., Krishna Mohan, S., Kurian, P.J. and Nambiar, C.G. 2000.** Gravity bases established by Cochin University of Science and Technology in southern Kerala. Jour. Geol. Soc. India. (under review).

**Radhakrishna, T., Poornachandra Rao, G.V.S., Mitchell, J.G. and Venkatesh, A.V. 1986.** Proterozoic basic dyke activity in Kerala along the western continental margin of India. Jour. Geol. Soc. India, v. 27, pp. 245-253.

**Radhakrishna, T. and Ramakrishnan, M. 1993.** Udipi-Kapili transect across south India, Mem. Geol. Soc. India, v. 25, pp. 45-61

**Radhakrishna Murthy, I.V. 1998.** Gravity and magnetic interpretation in exploration geophysics. Mem.Geol.Soc. India, v.40, pp.363.

**Rai, S.S., Srinagesh, D. and Gaur, V.K. 1993.** Granulite evolution in south India – A seismic tomographic perspective. Mem. Geol. Soc. India., v. 25, pp. 235-263.

**Raith, M., Rasse, P., Ackermand, D. and Lal, R.K. 1983.** Regional geothermobarometry in the granulite facies terrane of South India. Transactions of the Royal Society of Edinburgh: Earth Sciences, 73, pp. 221-244.

**Rajesh, H.M., Santosh, M. and Yoshida, M. 1996.** The felsic magmatic province in East Gondwana; implications for Pan-African tectonics. Jour. South East Asian Earth Sciences, v.14, pp. 275-291.

**Ramachandran, T.V. 1985.** Geological appraisal of absolute Total Intensity aeromagnetic data for parts of Kerala-Karnataka-Tamil Nadu and Correlation with Landsat and Bouguer gravity anomaly data. Indian Min., v.39, pp. 17-36.

**Ramachandran, T.V., Mishra, A. and Mishra, R.S. 1986.** Jour. Assoc. Expl. Geophys., v. 8, pp. 151-162.

**Ramachandran, C. 1992.** P-wave velocity in granulites from South India: implications for the continental crust. Geophysics, v.201, pp. 187-198.

**Ramachandran, C. 1990.** Metamorphism and magnetic susceptibilities in south Indian granulite terrain. Jour. Geol. Soc. India, v .35, pp.395-403.

**Ramachandran, C. and Bosu, L.R. 1991.** Densities of high grade metamorphic rocks from south Indian granulite terrain. Jour. Geol. Soc. India, v.37, pp.287-293.

**Ramakrishnan, M. 1988.** Tectonic evoluton of the Archean high grade terrain of Souh India. Jour. Geol. Soc. India, v.31, pp. 118-119.

**Ramakrishnan, M. 1993.** Tectonic evolution of the granulite terrain of South India. Mem. Geol. Soc. India, v. 25, pp. 35-44.

**Ramsay, I.G. 1980.** Shear zone geometry: review. J. struct. Geol., v. 2, pp. 83-99.

**Ravindrakumar, G.R. 1986.** The petrology and geochemistry of massif anorthosites and gabbros of the Bavali fault zone, north Kerala. Proc. Indian Acad. Sci. (Earth Planet. Sci.), v.95(1), pp.117-130.

**Ravindrakumar, G.R. and Sinha-Roy, S. 1985.** Field relations and geochemistry of Pernalimala synite pluton, north Kerala. Ind. Mineralogist, v.26, pp. 33-41.

**Reddi, A.G.B., Mathew, M.P., Singh, Baldau and Naidu, P.S. 1988.** Aeromagnetic evidence of crustal structure in the granulite terraine of Tamil Nadu-Kerala. Jour. Geol. Soc. India., v. 32, No.5, pp. 368-381.

**Reston, T.J. 1990.** Mantle shear zones and the evolution of the north Sea basin. Geology, v.18, pp.275-278.

**Roy, D.W., Woussen, G., Dimroth, E. and Chown, E.H. 1986.** The Central Grenville Province: A zone of protracted overlap between crustal and mantle processes. In: Moore J.M, Davidson A., Baer A.J (Eds) The Grenville Province . Geol. Assoc. Can. Spec. Pap., v.31, pp.51-60.

**Sacks, P.E., Nambiar, C.G. and Walters, L.J. 1997.** Dextral Pan-African shear along the southwestern edge of the Achankovil shear belt. Jour. Geol., v. 105, pp. 275-284.

**Sanker Narayan, P.V., Sarma, S.V.S. and Raju, C.V. 1963.** A Regional Gravity Study of Peninsular India South of Latitude 16°. In Proc. Of Seminar on "Geophysical Investigations in the Peninsular Shield", Eds. M.S. Krishnan and S. Balakrishana, Geology Dept., Osm. Univ., Hyderabad (May 27-31, 1963), pp.51-57.

**Santosh, M. 1986.** Geochemistry of coexisting hornblende and biotite from the Ambalavayal granite, Kerala. Proc. Indian Acad. Sci., v.95, pp.91-102.

**Santosh, M. and Masuda, H. 1991.** Reconnaissance oxygen and sulfur isotopic mapping of Pan-African alkali granites and syenites in the southern Indian shield. Geochemical Journal, v.25, pp.173-185.

**Santosh, M. and Nair, N.G.K. 1986.** Petrogensis of the Angadimogar syenite, Kerala and its taphrogenic affiliation. Jour. Geol. Soc. India, v.27, pp. 494-507.

**Santosh, M., Iyer, S.S., Vasconcellos, M.B.A. and Enzweiler, J. 1989.** Late Precambrain alkaline plutons in southwest India: geochronologic and rare earth element constraints on Pan-African magmatism. Lithos, v.24, pp.65-79.

**Santosh. M., Nair. N.G.K., Pande. K. and Gopalan. K. 1986.** Rb-Sr Geochronolgy of the Ambalavayal granite, Kerala. Jour. Geol. Soc. India, v.27, pp.309-312.

**Shazina, N and Grushinsky, N.P., (1971).** Gravity prospecting, Translated from Russian by A.K.Chatterjee, Mir Publishers, Moscow, 1972, 491 p.

**Singh, H.N., Panchanathan, P.V. and Unnikrishnan, K.R. 1985.** Gravity bases established by the Centre for Earth Science Studies in and around Palghat gap region, South India- Part I. Jour. Geol. Soc. India, v.26, pp.704-711.

**Simmons, G. 1964.** Gravity survey and geological interpretation, northern New York: Geol. Soc.Am. Bull., v 75, pp.81-98.

**Sinha-Roy, S. and Ravindra Kumar, G.R. 1986.** Geochemistry of the gabbro-tenalite-trondhjemite-granite suite of the Ezhimala pluton, north Kerala. Jour. Geol. Soc. India, v.27, pp.325-337.

**Smithson, S.B., and Ramberg, I.B. 1979.** Gravity interpretation of the Egersund anorthosite complex, Norway: its petrological and geothermal significance. Geol. Soc. Am. Bull. 90: pp.199-201.

**Soney, K.P. 2000.** Geochemistry and petrogenesis of Perinthatta anorthosite, northern Kerala. Unpublished Ph.D. Thesis, Submitted to Cochin University of Science & Technology, Cochin.

**Spector, A. and Grant, F.S. 1970.** Statistical models for interpreting aeromagnetic data. Geophysics, vol. 35, pp.293-302.

**Spooner, C.M. and Fairbairn, H.W. 1970.** Strontium 87/Stronitium 86 initial ratios in Pyroxene granulite terrains. Jour. Geol. Soc. India, v.75, pp. 6706-6713.

**Subba Rao, D.V. 1988.** Density structure of the Indian continental lithosphere-Gravity modelling, NGRI technical report 34.

**Subba Rao, P.B.V. 1990.** Building a model for the Precambrian crustal growth of the singhbhum-orissa iron ore craton on the basis of the gravity data. Unpublished Ph.D thesis submitted to Indian School of Mines, Dhanbad November, 1998.

**Subrahmanyam, C. 1978.** On the relation of gravity anomalies to geotectonics of the Precambrian terrains of the Southern Indian Shield. Jour. Geol. Soc. India, v.19, pp.241-263.

**Subrahmanyam, C. 1983.** An overview of gravity anomalies, Precambrian metamorphic terrains and their boundary relationships in the Southern India Shield. Geol. Soc. India, Memoir 4, pp.553-566.

**Subrahmanyam, C. and Verma, R.K. 1980.** The nature and free-air, Bouguer and isostatic anomalies in southern peninsular India. Tectonophysics, v 69, pp. 147-162.

**Subrahmanyam, C. and Verma, R.K. 1981.** Densities and magnetic susceptibilities of Precambrian rocks of different metamorphic grade (Southern Indian shield). Jour. Geophysics, v 49, pp.101-107.

**Subrabmanyam, C. and Verma, R.K. 1982**. A gravity interpretation of the Dharwar greenstone gneiss granite terrain in the southern Indian shield and its geological implication. Tectonophysics, v. 84, pp. 225-245.

**Tanner, J.G. 1969.** A geophysical interpretation of structural boundaries in the eastern Canadian Shield. Ph.D. Thesis, Univ. Durham, pp.194.

**Tapponier, P, Molnar, P. 1977.** Active faulting and tectonics in China. Jour. Geophys. Research, v.82, pp. 2905-2930.

**Thakur, N.K. and Nagrajan, N. 1992.** Geotectonic remobilization of the lower crustal segment of southern Peninsular India. Phys. Earth Planet. Int., v. 73, pp. 153-162.

**Thomas, M.D. 1990.** Deep structure of Middle Proterozoic anorthositic intrusions in the eastern Canadian Shield: insights from gravity modeling. In: Gower CF, Rivers T, Ryan B (Eds) Mid-Proterozoic Laurentia-Baltica, Geol. Assoc. Can. Spec. Pap., v.38, pp. 353-372.

**Thomas, M.D. 1974.** The correlation of gravity and geology in southeastern Quebec and southern Labrador: Canada Dept. Energy, Mines and resources Earth Physics Br. Gravity Map Ser., nos. 64-67 and 96-98.

**Treitel, S, Clement, W.G. and Kaul, R.K. 1971.** The spectral determination of depths to burried magnetic basement rocks. Geophys. J.R. Astron. Soc., vol. 24, pp.415-428.

**Varadarajan, K. and Balakrishnan, M.K. 1980.** Kerala Coast – A landsat's view. Proc. Sym. On geology and geomorphology of Kerala, spl. Publ. No. 5. Geol. Surv. India, pp. 67-68.

**Varaprasada Rao, S.M., Satyanarayana Murty, B.V. and Bhimasankaram, V.L.S. 1978.** Petro-physical properties (Density and magnetic-susceptibility) and lithological composition of some dolerite dykes of Andhra Pradesh, India. Jour. Geophysics, v.44, pp.353-356.

**Venkatasubramanian, V.S. 1975.** Studies in the geochronology of the Mysore craton. Geophy. Res. Bull., v.13, pp. 239-246.

**Verma, R.K. and Mukhopadhyay, M. 1976.** Tectonic significance of Anomaly-elevation relationships in North Eastern India. Tectonophysics, v.34, pp. 117-133.

**Verma, R.K., Ghosh, D., Roy, S.K. and Ghosh, A. 1975.** Gravity survey over Bankura anorthosite complex, West Bengal. Jour. Geol. Soc. India, v.16, pp.361-369.

**Verma, R.K., Mukhopadhyay, M., Rao, C.M. and Sarma, A.U.S. 1984.** Relationships of free-air and Bouguer anomalies to elevation in Peninsular India and the Himalaya. Geophy. Res. Bull., v.22 (no.4), pp. 159-172.

**Vidyadharan, K.T., Sukumaran, P.V and Nair, M.M. 1977.** A note on the occurrence of anorthosite near Perinthatta, Taliparamba taluk, Cannanore district, Kerala. Jour. Geol. Soc. India, v. 18, pp.519-520.

**Vissers, R.L.M., Drury, M.R., Hoogerduijn Strating, E.H., Vanderval, D. 1991.** Shear zones in the upper mantle: a case study in the Alpine type lherzolite massif. Geology, v.90, pp. 990-993.

**Vissers, R.L.M., Drury, M.R., Hoogerduijn Strating, E.H., Spiers, C.J., Vanderval, D. 1995.** Mantle shear zones and their effect on lithospheric strength during continental breakup. Tectonophysics, v.249, pp. 155-171.

**Webring, M. 1985**. Semi-automatic Marquardt inversion of gravity and magnetic profiles. U.S. Geological Survey Open-file Report OF-122.

**Woollard, G.P. 1969.** Regional variations in gravity. Geophysical Monograph No.13, Am. Geophy. Union, pp.320-340.

**Woollard, G.P. 1970.** Regional variations in gravity. Nature of solid earth, Ed. E.Robertson, pp.463-505.

**Woollard, G.P. 1959.** Crustal structure from gravity and seismic measurements. Jour. Geophy. Res., v.69 (10), pp.1524-1544.

**Woollard, G.P., Manghnani, M.H. and Mathur, S.P. 1969.** Gravity measurements in India, Part-2. HIG Publication 69-17, (Contract DACA 71-67-C-0080) Hawaii (USA), pp.51.

**Worzel, J.L. and Shurbet, G.L. 1955**. Gravity interpretation from standard oceanic and continental crustal sections. Geol. Soc. Amer. Spec. pap. 62, pp. 87-100.

**Young, D.G.G. 1974**. The Donegal granite – a gravity analysis. Proc. R. Irish Acad., v. 74B, pp. 63-73.

## APPENDIX - I

**Program to process the raw gravity data in 'c' language**

```
#include <stdio.h>
#include <io.h>
#include <math.h>
#include <conio.h>
#include <dos.h>
main()
{
        float lalon(int,int,int);
        int round(float);
        int help(void);
        int stop(void);
        int error(char *);
        char fle[20];
        double lat,CNSA,CNSB;
        int i=0,j,k,hour[100],mi[100],min[100],n=0,t,x;
        int l1[100],l2[100],l3[100],lo1[100],lo2[100],lo3[100],el[100];
        float gr[100],g[100],cr[100],cf,crd[100],ds[100],dm[100];
        float g1,g2;
        int FLAG,IFL,td[100];
        float tem[100],lo[100],la[100];
        float gn[100],cec[100],ba[100],fa[100];
        char dfle[10],ofle[10],q;
        FILE *fp,*gp,*hp,*pt;
        help();
        FLAG = 1;
        IFL =  1;
while(FLAG)
{
        textbackground(WHITE);
        textcolor(BLACK);
        gotoxy(1,6);
        insline();

for(;;)
        {
        gotoxy(1,6);
        clreol();
        cprintf("Enter name of data file:  ");
```

```
        scanf("%s",dfle);
        fp = fopen(dfle,"r");

        if(!fp)
                {
                printf("\n The File  '%s'  does not exist or the path is not correct.
\n",dfle);
                        while(IFL)
                        {
                        gotoxy(1,15);
                        printf(" Try again ? [y/n] :");

                gotoxy(21,15);
                  q=getche();
                        textbackground(BLUE);
                        textcolor(BLUE);
                        gotoxy(21,15);
                        delline();
                        gotoxy(2,18);
                        clreol();
                        textcolor(BLACK);
                        textbackground(WHITE);
                        if(q!='y'&&q!='n')
                                        {
                                        sound(500);
                                        gotoxy(2,14);
                                        cprintf("answer with 'y' or 'n' only");
                                        delay(50);
                                nosound();
                                        IFL = 1;
                                        }
                        else            IFL = 0;
                        }
                if(q=='n')
                        {
                        stop();
                        exit(0);
                        }
                else if(q=='y')
                        {
                        IFL = 1;
                        }
                }
```

```
else if(fp)break;
}
textbackground(BLUE);
textcolor(7);
clrscr();
j=fscanf(fp,"%s",fle);

        if(j!=1)
                {
                error(dfle);
                stop();
                exit(0);
                }

j=fscanf(fp," %f %f",&g1,&g2);

        if(j!=2)
                {
                error(dfle);
                stop();
                exit(0);
                }
j=10;
i=0;
while(j==10)
{
i++;
j=fscanf(fp,"%d %d %d %d %d %d %d %d %d
%f",&lo1[i],&lo2[i],&lo3[i],&l1[i],&l2[i],&l3[i],&hour[i],&mi[i],&el[i],&gr[i]);
}
n=i-1;
if(i<2)
        {
        error(dfle);
        stop();
        exit(0);
        }
for(i=1;i<=n;i++)
        {
        min[i]=hour[i]*60+mi[i];
        }

hp=fopen("a:\\data\\bgrb.dat","a");
```

```
if(!hp)
        {
        printf("\nThe output file 'bgrb.dat' cannot be created !\n");
        printf("gTOOLb terminates....");
        exit(0);
        }
pt=fopen("a:\\data\\bgrb.plt","a");
if(!pt)
        {
        printf("\nThe output file 'bgrb.plt' cannot be created\n");
        printf("gTOOLb terminates");
        exit(0);
        }
fprintf(hp,"%s\n",fle);
fprintf(pt,"%s\n",fle);
cf=(((gr[1]-gr[n])-((g1-g2)/0.24))/(min[n]-min[1]));
printf("<%s>",fle);
printf("\nLatitude    Longitude   F.Anomaly     B.Anomaly\n");
for(k=1;k<=n;k++)
        {
        td[k]= min[k]-min[1];
        cr[k]  = cf*td[k];
        crd[k] = gr[k]+cr[k];
        ds[k]  = crd[1]-crd[k];
        dm[k]  = ds[k]*0.24;
        g[k]   = g1-dm[k];
        la[k]=lalon(l1[k],l2[k],l3[k]);
        lo[k]=lalon(lo1[k],lo2[k],lo3[k]);
        lat = (double)la[k] * M_PI/180.0;
        CNSA = 0.0052884*sin(lat)*sin(lat);
        CNSB = 0.0000059*sin(2*lat)*sin(2*lat);
        gn[k]=(float)978049.0*(1.0 + CNSA - CNSB);
        fa[k]=g[k]-gn[k]+0.09406*el[k];
        cec[k]=0.05994*el[k];
        ba[k]=g[k]-gn[k]+ cec[k];
        printf("%2dø %2d' %2d%c   %2dø %2d' %2d%c  %6.2f
%6.2f\n",l1[k],l2[k],l3[k],34,lo1[k],lo2[k],lo3[k],34,fa[k],ba[k]);
        fprintf(pt," %2dø %2d' %2d%c   %2dø %2d' %2d%c  %8.2f
%8.2f\n",l1[k],l2[k],l3[k],34,lo1[k],lo2[k],lo3[k],34,fa[k],ba[k]);
        fprintf(hp," %f %f %f %f\n",la[k],lo[k],fa[k],ba[k]);
        }
```

```
        fcloseall();
        printf("\n\n  Do you have any other file to process ? [y/n] :");
        q=getche();
        if(q=='y')      {clrscr();FLAG=1;}
        else            FLAG=0;
}

        stop();
        printf("\n\n  press any key to return to DOS.....");
                        getch();
                        fcloseall();
                        textcolor(WHITE);
                        textbackground(BLACK);
                        highvideo();
                        lowvideo();
                        clrscr();
        }
int round(float e)
        {
        int a1;
        float a2;
        a2=e-(int)e;
        if(a2>=0.5)
        a1=(int)e+1;
        else
        a1=(int)e;
        return(a1);
        }

float lalon(int cl1,int cl2,int cl3)
        {
        float cl;
        cl=cl1+cl2/60.0+cl3/3600.0;
        return(cl);
        }

int help(void)
        {
        int i;
        clrscr();
        textbackground(WHITE);
        textcolor(BLACK);
        gotoxy(1,1);
```

```
        insline();
        insline();
        gotoxy(1,1);
        cprintf("              gTOOL  - A Programme For Gravity Reduction");
        gotoxy(1,2);
        cprintf("          Developed by P. John Kurian &  C. Manoj , March 1998");
        textbackground(BLUE);
        textcolor(7);
        for(i=3;i<25;++i)
                {
                gotoxy(1,i);
                insline();
                }
        gotoxy(30,4);
        cprintf("ABOUT gTOOL\n");
        gotoxy(5,5);
        cprintf("The programme performs drift corrections, absolute gravity value
");
        gotoxy(5,6);
        cprintf("calculations, and outputs Bouguer Anomaly values");
        gotoxy(1,8);
        cprintf("     The input data file should contain");
        gotoxy(1,9);
        cprintf(" (1) Name of the traverse (Without any space in between)");
        gotoxy(1,10);
        cprintf(" (2) Absolute gravity values of base stations at start and end of the
traverse");
        gotoxy(1,11);
        cprintf(" (3) Data should then be entered in the ordrer follows..");
        gotoxy(1,12);
        cprintf("    lat(deg min sec) long(deg min sec) time(hour min) elevation(in
m., rounded) ");
        gotoxy(1,13);
        cprintf("    and gravimeter reading");
        gotoxy(1,15);
        cprintf("  The processed data is written in two files - BGR.DAT and
BGR.PLT");
        gotoxy(1,17);
        cprintf("  BGR.DAT contains lat, long and Bouguer anomaly. The
geographical cordinates");
        gotoxy(1,18);
        cprintf("  are given in decimal format to be used with any plotting package
like surfer");
```

```
        gotoxy(1,20);
        cprintf("  BGR.PLT contains the same data. The geographical cordinates
are given in");
        gotoxy(1,21);
        cprintf("  degree minute second format");
        gotoxy(1,23);
        cprintf("  The two output files are appended when subsequent calls are
made");
        gotoxy(1,25);
      textbackground(WHITE);
        textcolor(BLACK);
        insline();
        cprintf("              press any key to continue....");
        getch();
        textbackground(BLUE);
        textcolor(7);
        clrscr();
        return(0);
        }

int stop(void)
        {

                printf("\n\n  press any key to return to DOS.....");
                        getch();
                        fcloseall();
                        textcolor(WHITE);
                        textbackground(BLACK);
                        highvideo();
                        lowvideo();
                        clrscr();
                        return(0);
        }
int error(char *dfile)
        {

        printf("The file does not have any data/not in the prescribed format");
        printf("\nPlease ensure the data file %s is in the correct format",dfile);
        printf("\n\n For any clarification, see the opening messages of gTool");

        return(0);
        }
```